CONFERENCE BOOK



GLOBE 2ND INTERNATIONAL CONFERENCE ON ENGINEERING, ARCHITECTURE, MATHEMATICS and APPLIED SCIENCES
OCTOBER 1 - 6, 2026
BARSELONA

ISBN: 978-625-8795-56-1
Published by : Academy Global Publishing Hose

GLOBE CONGRESS

GLOBE 2ND INTERNATIONAL CONFERENCE ON ENGINEERING, ARCHITECTURE, MATHEMATICS and APPLIED SCIENCES
OCTOBER 1 - 6, 2026
BARSELONA

Edited By
ASSOC. PROF. DR. MEHMET FIRAT BARAN

Issued: 28.10.2026
ISBN: 978-625-8795-56-1

ASSOCIATION & ACADEMIC INCENTIVES :
In the conference 6 papers have been presented by Turkish participants and 15 papers by international participants.
Members of the organizing committees of the conference perform their duties with an "official assignment letter"

The Contents Of This Book Are Solely Those Of The Authors.
Bu Kitabın içeriğinin tüm sorumluluğu yazarlarına aittir.

Web: www.globekongre.org Contact: globekongre@gmail.com

CONFERENCE ID

GLOBE 2ND INTERNATIONAL CONFERENCE ON ENGINEERING, ARCHITECTURE, MATHEMATICS AND APPLIED SCIENCES

DATE – PLACE
OCTOBER 1 - 6, 2026
BARSELONA

ORGANIIZATION
ACADEMY GLOBAL CONFERENCES & JOURNALS

EVALUATION PROCESS
All applications have undergone a double-blind peer review process.

PARTICIPATING COUNTRIES
Turkey – Malaysia – Bangladesh – Uzbekistan – Qatar – Hungary – Bulgaria- Tajikistan
-

PRESENTATION
Oral presentation

No part of this book may be reprinted or reproduced or utilized in any form or by any electronic, mechanical or any other means, now known or hereafter invented, including photocopying and recording, or in any form of information storage or retrieval systems, without permission from the publishers.
Academy Global–2026©

CONGRESS ORGANIZING BOARD

Prof. Dr. Hülya Çiçek - Gaziantep Universitesi

Prof. Dr. Ali Bilgili - Ankara Üniversitesi

Prof. Dr. Naile Bilgili - Gazi Üniversitesi

Prof. Dr. Başak Hanedan - Atatürk Üniversitesi

Prof. Dr. Hajar Huseynova - Azerbaijan Devlet Pedagoji Üniversitesi

Prof. Dr. Dwi Sulisworo - Ahmad Dahlan University

Prof. Zain Musa - Royal Academy of Cambodia

Prof. Dr. Sameer Jain - NICMAR University

Prof Yakup Babayev - Azerbaijan Devlet Pedagoji Üniversitesi

Prof. Dr. Suyatno - Ahmad Dahlan University

Prof. Dr. Al-Rashiff H. Mastul -Mindanao State University

Prof. Dr. Alhisan U. Jemsy - Mindanao State University

Prof. Dr. Elif Akpınar Külekçi - Atatürk Üniversitesi

Prof. Dr. Mehtap Kavurmacı - Atatürk Üniversitesi

Prof. Dr. Belkıs Özkara - Afyon Kocatepe Üniversitesi

Prof. Dr. Mavlonova Ugiloy Khamdamovna - Zarmed University

Assoc. Prof. Dr. Aysel Arslan - Sivas Cumhuriyet Üniversitesi

Assoc. Prof. Dr. Yeliz Çakır Sahilli - Munzur Üniversitesi

Assoc. Prof. Dr. Sıddık BAKIR - Ataturk Universitesi

Assoc. Prof. Dr. Berna Koçak - Munzur Üniversitesi

Assoc. Prof. Dr. Irade Kerimova - Azerbaycan Devlet Pedagoji Üniversitesi

Assoc. Prof. Dr. Dhesi Ari Astuti - Ahmad Dahlan University

Assoc. Prof. Dr. Mehmet Fırat Baran - Batman Üniversitesi

Assoc. Prof. Dr. Abdulkadir Aydın - Dicle Üniversitesi

Assoc. Prof. Dody Hartanto - Ahmad Dahlan University

Assoc. Prof. Dr. Rungchacadaporn - Ahmad Dahlan University

Assoc. Prof. Nazile Abdullazade - Azerbaijan Devlet Pedagoji Üniversitesi

Assoc Prof. Dr. Feran Aşur - Van Yüzüncü Yıl Üniversitesi

Assoc Prof. Dr. Erkan EFİLTİ - Kırgızistan-Türkiye Manas University

Assoc. Prof. Dr. Dini Yuniarti - Ahmad Dahlan University

Assoc. Prof. Ivaylo Staykov - New Bulgarian Üniversitesi

Assoc. Prof. Dr. Abbas Ghaffari - Tebriz Universitesi

Assoc. Prof. Dr. Yasemin Taş - Gazi Üniversitesi

Assoc. Prof. Dr. Yeganə Qəhrəmanova - Azerbaijan Devlet Pedagoji Üniversitesi

Assoc. Prof. Dr. Bülent Işık - Karamanoğlu Mehmet Bey Üniversitesi

Assoc. Prof. Dr. Nurkan Yılmaz - İnönü Üniversitesi

Assoc. Prof. Dr. Həmzə Əliyev- Azerbaijan Devlet Pedagoji Üniversitesi

Assoc. Prof. Dr. Sevra Fırıncıoğulları

Assist. Prof. Ihwan Ghazali - Technic University of Malaysia

Assist. Prof. Dr. Abışov Elşad Şərəfxan oğlu- Azerbaijan Devlet Pedagoji Üniversitesi

Assist. Prof. Dr. Mahrukh Dovlatzade - Azerbaijan Devlet Pedagoji Üniversitesi

Assist. Prof. Dr. Naci Büyükkaracığan- Selçuk Üniversitesi

Assist. Prof. Dr. Songül Atak - Dicle Üniversitesi

Lecturer Mehmet Nuri Ödük - Selçuk Üniversitesi

Dr. Fatih İ. Kurşunmaden - Selçuk Üniversitesi

Assist. Prof. Dr. Mehdi Meskini Heydarlou –

Dr. Dadash Mehravari - Tebriz Universitesi

Dr. Aynurə Əliyeva - Azerbaijan Devlet Pedagoji Üniversitesi

Dr. Gültekin Gürçay

Dr. Amaneh Manafidizajı

Scientific & Review Committee

Prof. Dr. Hülya Çiçek – Turkiye

Prof. Dr. Emine Koca – Turkiye

Prof. Dr. Fatma Koç – Turkiye

Prof. Dr. Valide Paşayeva - Türkiye

Prof. Dr. Ali Bilgili - Turkiye

Prof. Dr. Naile Bilgili - Turkiye

Prof. Dr. Başak Hanedan – Turkiye

Prof. Dr. Aysel Güven - Turkiye

Prof Dr. Bülent Kurtişoğlu – Turkiye

Prof. Dr. Hajar Huseynova – Azerbaijan

Prof. Dr. Dwi Sulisworo – Indonesia

Prof. Dr. Natalia Latygina – Ukraina

Prof. Dr. Yunir Abdrahimov – Russia

Prof. Muntazir Mehdi – Pakistan

Prof. Dr. T.Venkat Narayana Rao – India

Prof. Dr. İzzet Gümüş – Turkiye

Prof. Dr. Mustafa Bayram – Turkiye

Prof. Dr. Saim Zeki Bostan – Turkiye

Prof. Dr. Hyeonjin Lee – China

Prof. Yakup Babayev - Azerbaijan

Prof. Dr. Suyatno – Indonesia

Prof. Dr. Zain Musa – Cambodia

Prof. Dr. Sameer Jain – India

Prof. Mehdi Mohammadzade – Iran

Prof. Dr. Ika Maryani – Indonesia

Prof. Dr. Guler Yenice – Turkiye

Prof. Dr. Elif Akpınar Külekçi – Turkiye

Prof. Dr. Mavlonova Ugiloy Khamdamovna – Uzbekistan

Prof. Dr. Mehtap Kavurmacı – Türkiye

Prof. Dr. Belkıs Özkara – Türkiye

Prof. Dr. Al-Rashiff Hamjilani Mastul – Philipinnes

Prof. Dr. Alhisan U. Jemsy – Philippines

Assoc. Prof. Dr. Aysel Arslan - Turkiye

Assoc. Prof. Dr. Sıddık Bakır – Turkiye

Assoc. Prof. Dr. Meryem Öztürk - Turkiye

Assoc. Prof. Dr. Yeliz Çakır Sahilli - Turkiye

Assoc. Prof. Dr. Berna Koçak - Turkiye

Assoc. Prof. Dr. Dhesi Ari Astuti – Indonesia

Assoc. Prof. Dr. Abdulkadir Aydın - Turkiye

Assoc Prof. Dr. Feran Aşur – Turkiye

Assoc. Prof. Dr. Yasemin Taş – Turkiye

Assoc. Prof. Dr. Bülent Işık - Turkiye

Assoc. Prof. Dr. Nurkan Yılmaz - Turkiye

Assoc. Prof. Dr. Sevra Fırıncıoğulları - Turkiye

Assoc. Prof. Dr. Abdulsemet Aydın – Turkiye

Assoc. Prof. Dr. Mehmet Fırat Baran - Turkiye

Assoc. Prof. Dr. Dilorom Hamroeva - Ozbekistan

Assoc. Prof. Dr. Abbas Ghaffari – Iran

Assoc. Prof. Ivaylo Staykov - Bulgaria

Assoc. Prof. Dr. Dini Yuniarti – Indonesia

Assoc. Prof. Dr. Ümit Ayata – Turkiye

Assoc. Prof. Dr. Həmzə Əliyev - Azerbaijan

Assoc. Prof. Dr. Okan Sarıgöz – Turkiye

Assoc. Prof. Dr. Eda Bozkurt – Turkiye

Assoc. Prof. Dr. Ahmet Topal – Turkiye

Assoc. Prof. Dr. Abdulkadir Kırbaş – Turkiye

Assoc. Prof. Dr. Mesut Bulut – Turkiye

Assoc. Prof. Dr. Fahriye Emgili – Turkiye

Assoc. Prof. Dr. Sandeep Gupta – India

Assoc. Prof. Dr. Veysel Parlak – Turkiye

Assoc. Prof. Dr. Mahmut İslamoğlu – Turkiye

Assoc. Prof. Dr. Nazile Abdullazade – Azerbaijan

Assoc. Prof. Dr. Irade Kerimova - Azerbaijan

Assoc. Prof. Dr. Yeganə Qəhrəmanova – Azerbaijan

Assoc. Prof. Dr. Ali Vandshoari – İran

Assoc. Prof. Dr. Dinara Fardeeva – Rusya

Assoc. Prof. Dr. Göksel Ulay – Turkiye

Assoc. Prof. Dr. Erkan Efilti - Kirgizhstan

Assist. Prof. K. R. Padma – India

Assist. Prof. Dr. Omid Afghan - Afghanistan

Assist. Prof. Dr. Maha Hamdan Alanazi - Saudi Arabia

Assist. Prof. Dr. Dzhakipbek Altaevich Altayev - Kazakhstan

Assist. Prof. Dr. Amina Salihi Bayero – Nigeria

Assist. Prof. Dr. Ahmad Sharif Fakheer - Jordania

Assist. Prof. Dr. Dody Hartanto - Indonesia

Assist. Prof. Dr. Ihwan Ghazali - Malaysia

Assist. Prof. Dr. Mehdi Meskini Heyladou – Iran

Assist. Prof. Dr. Bazarhan İmangalieva - Kazakhstan

Assist. Prof. Dr. Keles Nurmaşulı Jaylıbay - Kazakhstan

Assist. Prof. Dr. Mamatkuli Juraev – Ozbekistan

Assist. Prof. Dr. Kalemkas Kalibaeva – Kazakhstan

Assist. Prof. Dr. Bouaraour Kamel – Algeria

Assist. Prof. Dr. Alia R. Masalimova - Kazakhstan

Assist. Prof. Dr. Amanbay Moldibaev - Kazakhstan

Assist. Prof. Dr. Ayslu B. Sarsekenova - Kazakhstan

Assist. Prof. Dr. Bhumika Sharma - India

Assist. Prof. Dr. Gulşat Şugaeva – Kazakhstan

Assist. Prof. Dr. K.A. Tleubergenova - Kazakhstan

Assist. Prof. Dr. Cholpon Toktosunova – Kirgizia

Assist. Prof. Dr. Hoang Anh Tuan – Vietnam

Assist. Prof. Dr. Songül Atak - Türkiye

Assist. Prof. Dr. Botagul Turgunbaeva - Kazakhstan

Assist. Prof. Dr. Dinarakhan Tursunalieva - Kirgizia

Assist. Prof. Dr. Yang Zitong – China

Assist. Prof. Dr. Gulmira Abndirasulova – Kazakhstan

Assist. Prof. Dr. Imran Latif Saifi – South Africa

Assist. Prof. Dr. Murat Genç – Turkiye

Assist. Prof. Dr. Monisa Qadiri – India

Assist. Prof. Dr. Vaiva Balciuniene – Lithuania

Assist. Prof. Dr. Meltem Avan – Turkiye

Assist. Prof. Dr. Abışov Elşad Şərəfxan oğlu - Azerbaijan

Assist. Prof. Dr. Mahrukh Dovlatzade – Azerbaijan

Assist. Prof. Dr. Naci Büyükkaracığan – Turkiye

Assist. Prof. Dr. Raihan Yusoph – Philippines

Dr. Que-Nhu Duong - Vietnam

Dr. Fatih İ. Kurşunmaden – Turkiye

Dr. Mehmet Nuri Ödük – Turkiye

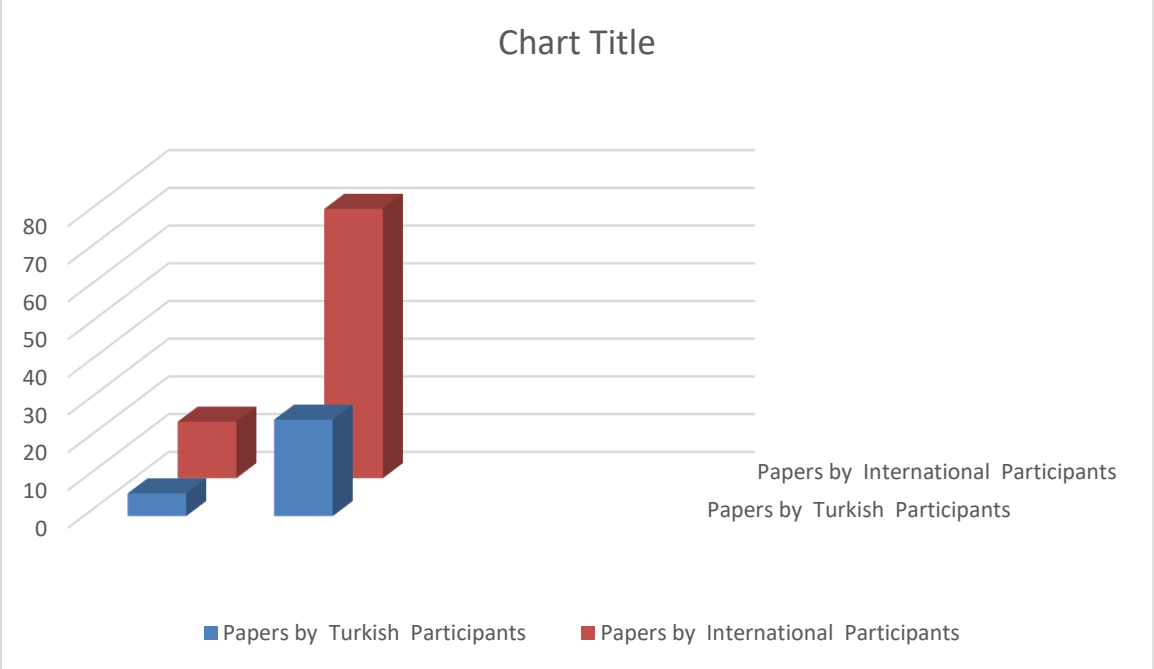
Dr. Ayşe Baran - Turkiye

Dr. Aynurə Əliyeva - Azerbaijan

Dr. Sonali Malhotra – India

Dr. Amaneh Manafidizaji – Iran

	Number of paper	*%*
Papers by Turkish Participants	6	28,57
Papers by International Participants (7 Countries)	15	71,43



GLOBE 2ND INTERNATIONAL CONFERENCE ON ENGINEERING, ARCHITECTURE, MATHEMATICS AND APPLIED SCIENCES
OCTOBER 1 - 6, 2026
BARSELONA

NO : **AC- 2G - 2026. 367B– 3876**
Konu : Akademik Teşvik Uygunluk Belgesi 20/10/2026

İLGİLİ MAKAMA

Academy Global Conferences tarafından düzenlenen **GLOBE 2ND INTERNATIONAL CONFERENCE ON ENGINEERING, ARCHITECTURE, MATHEMATICS and APPLIED SCIENCES** kongresi 1- 6 Ekim 2026 tarihlerinde Barselona'da 8 farklı ülkeden akademisyenin katılımıyla gerçekleştirilmiştir. Kongre kapsamında sunulan 21 bildirinin 6's Türkiye'den, 15'i ise farklı 7 ülkeden katılan akademisyenler tarafından sunulmuştur. Kongre, 16 Ocak 2020 Akademik Teşvik Ödeneği Yönetmeliğine getirilen "Tebliğlerin sunulduğu yurt içinde veya yurt dışındaki etkinliğin uluslararası olarak nitelendirilebilmesi için Türkiye dışında en az beş farklı ülkeden sözlü tebliğ sunan konuşmacının katılım sağlaması ve tebliğlerin yarıdan fazlasının Türkiye dışından katılımcılar tarafından sunulması esastır." değişikliğine uygun olarak düzenlenmiştir.

Bilgilerinize arz ederiz

Saygılarımızla

Prof. Dr. Elif Akpınar Külekçi

T.C.
ATATÜRK ÜNİVERSİTESİ REKTÖRLÜĞÜ
Personel Daire Başkanlığı

Sayı : E-16710634-03-903.07.02-2300384284 01.12.2023
Konu : Doç.Dr.Elif AKPINAR KÜLEKÇİ'nin Görevlendirilmesi

MİMARLIK VE TASARIM FAKÜLTESİ DEKANLIĞINA

İlgi : 29.11.2023 tarihli ve E-53120705-000-2300381989 sayılı belge.

Fakülteniz Peyzaj Mimarlığı Bölümü öğretim üyelerinden Doç.Dr.Elif AKPINAR KÜLEKÇİ'nin, Yükseköğretim Genel Kurulunun 15.06.2023 tarihli, 10 sayılı oturumunda alınan 2023.10.183 sayılı kararı gereğince Doçentlik Başvuru Şartlarında bulunan ve doçent olacak adaylardan istenen "Diğer uluslararası/ ulusal bilimsel toplantının düzenleme komitesinde resmi olarak görevlendirilmiş üniversite akademisyen temsilcisi bulunması zorunludur." maddesi gereğince, Academy Global Conference & Journals tarafından yapılan kongrelerin düzenleme kurullarında yolluksuz ve gündeliksiz olarak görevlendirilmesi Rektörlüğümüzce uygun görülmüştür.

Bilgilerini ve gereğini rica ederim.

Prof.Dr. Ömer ÇOMAKLI
Rektör

Bu belge, güvenli elektronik imza ile imzalanmıştır.
Doğrulama Kodu: 87c7a395-d4b6-4f7a-abc6-5dee8674e3d1 Doğrulama Adresi: https://www.turkiye.gov.tr/ataturk-universitesi-ebys

Atatürk Üniversitesi Rektörlüğü 25240 Erzurum
Tel: +90 442 2311023
Elektronik Ağ: www.atauni.edu.tr
Kep Adresi: atauni@hs01.kep.tr
Bilgi: Mehmet KOÇ
Faks: +90 442 2361014
E-Posta: personel@atauni.edu.tr

GLOBE 2ND INTERNATIONAL CONFERENCE ON SOCIAL SCIENCES
GLOBE 2ND INTERNATIONAL CONFERENCE ON ENGINEERING, ARCHITECTURE, MATHEMATICS and APPLIED SCIENCES
GLOBE 2ND INTERNATIONAL CONFERENCE ON HEALTH and SPORT SCIENCES

October 1 - 6, 2026
BARSELONA

Kongre Bağlantı Linki :

Join Zoom Meeting

https://us06web.zoom.us/j/88571518350?pwd=fOYazCWBmbAiWrHygjKSjkbbSvotfd.1

Meeting ID: 885 7151 8350

Passcode: 202224



ÖNEMLİ AÇIKLAMA (Lütfen okuyunuz)

- ZOOM bağlantısı için yukarıda verilen bağlantıyı veya yine yukarıda verilen giriş bilgilerini kullanabilirsiniz.
- **Oturum içerisinde en KIDEMLİ olan moderator olarak seçilir. Moderatörün oturum düzenini gözetmesi, akademisyen adaylarını yönlendirmesi beklenmektedir.**
- Oturuma bağlanmadan önce Salon numaranızı adınızın önüne aşağıdaki gibi ekleyiniz. Bu sayede kongre açılışında beklemeden oturumlarınıza gönderilebileceksiniz. Ör. 5 Ahmet Ahmetoglu
- **Sunum süresi 10 dakikadır. Bu sürenin aşılmamasını moderatörler temin edecektir.**
- Sunum sonrası 5 dakikayı geçmeyen soru-cevap, tartışma süresi verilmektedir.
- **Sunumlar TÜRKÇE veya İNGİLİZCE yapılabilmektedir.**
- Kameralar, oturum süresince toplam % 70 oranında açık olmak zorundadır.
- **Sunum yapan katılımcının kamerası açık olmak zorundadır.**
- Sunum yapmak zorunludur. **Herhangi bir nedenle sunum yapmamış olan katılımcıya sertifika verilmesi ve çalışmasının yayınlanması sözkonusu olamaz.**
- Katılımcı, kendi oturumda, oturum bitene kadar bulunmak zorundadır.
- Katılımcıların kendi oturumları dışındaki oturumlara katılma zorunluluğu yoktur.
- ZOOM platformunun kapasite sınırı nedeniyle, DİNLEYİCİ, sadece kapasite izin verdiği sürece kabul edilebilmektedir.
- **SADECE ÇALIŞMADA YAZAR OLARAK GEÇEN KİŞİLER SUNUM YAPABİLİR !**

IMPORTANT, PLEASE READ CAREFULLY

- To be able to make a meeting online, login via https://zoom.us/join site, enter ID instead of "Meeting ID
- or Personal Link Name" and solidify the session.
- The Zoom application is free and no need to create an account.
- The Zoom application can be used without registration.
- The application works on tablets, phones and PCs.
- Speakers must be connected to the session **10 minutes before** the presentation time.
- All congress participants can connect live and listen to all sessions.
- During the session, your camera should be turned on **at least %70** of session period
- Moderator is responsible for the presentation and scientific discussion (question-answer) section of the session.

TECHNICAL INFORMATION

- Make sure your computer has a microphone and is working.
- You should be able to use screen sharing feature in Zoom.
- Attendance certificates will be sent to you as pdf at the end of the congress.
- Moderator is responsible for the presentation and scientific discussion (question-answer) section of the session.
- Before you login to Zoom please indicate your name surname and hall number,

GLOBE 2ND INTERNATIONAL CONFERENCE ON HEALTH and SPORT SCIENCES October 1 - 6, 2026 BARSELONA Meeting ID: 885 7151 8350 Passcode: 202224				
2 Ekim / October 2, 2026 / 11:00 – 13:00 Time zone in Turkey (GMT+3)				
Salon	Moderator		Bildiri No ve Başlığı / Paper ID and Title	Authors
HALL / SALON 8	**Doç. Dr. Alper Yusuf Köroğlu**	1	ARTIFICIAL INTELLIGENCE IN MIDWIFERY EDUCATION AND THE HOLISTIC NATURE OF MIDWIFERY: A SCOPING REVIEW	İmran Aslan Filiz Okumuş
		2	TÜRKİYE'DE DOĞURGANLIĞIN ÇEYREK ASIRLIK DÖNÜŞÜMÜ (2001–2025): TÜİK VERİLERİYLE KARŞILAŞTIRMALI BİR ANALİZ	İmran Aslan Filiz Okumuş
		3	SLEEPY BODIES, DECLINING MOVEMENT: EXAMINING THE RELATIONSHIP BETWEEN DAYTIME SLEEPINESS AND PHYSICAL ACTIVITY IN ADOLESCENTS	Öğr. Gör. Dr., Bekir Tokay Prof. Dr., Mustafa Akıl
		4	DOES ACADEMIC ACHIEVEMENT REDUCE EMOTIONAL EATING? THE PROTECTIVE ROLE OF PHYSICAL ACTIVITY IN ADOLESCENTS	Prof. Dr., Mustafa Akıl Öğr. Gör. Dr., Bekir Tokay
		5	ERKEN ÇOCUKLUK DÖNEMİNDE DİJİTAL İÇERİK TÜKETİMİ: PASİF İZLEMEDEN İNTERAKTİF DENEYİME KARŞILAŞTIRMALI BİR DERLEME	Doç. Dr. Alper Yusuf Köroğlu
		6	ERKEN ÇOCUKLUK DÖNEMİNDE GELİŞİMSEL TAKİP: GELENEKSEL KLİNİK ÖLÇEKLERDEN DİJİTAL EBEVEYN BİLDİRİM PLATFORMLARINA KARŞILAŞTIRMALI BİR İNCELEME	Doç. Dr. Alper Yusuf Köroğlu
		7	CONE-BEAM COMPUTED TOMOGRAPHY IN ORTHODONTICS AND PEDIATRIC DENTISTRY: CURRENT INDICATIONS, DIAGNOSTIC CONTRIBUTIONS, AND RADIATION SAFETY	Öğr. Üyesi Gizem Yazdan Özen Dr. Öğr. Üyesi Ali Kağan Özen Dt. Nesli Damla Deniz
		8	THE EFFECTS OF PILATES ON DYSMENORRHEA PAIN	Ebe /Yüksek Lisans Öğrencisi İremsu Kırpık O . Dr.Öğretim Üyesi Hilal Özbek
		9	A STUDY ON THE EVALUATION OF PACKAGED BABY BISCUITS	Assist. Prof. Dr. Çiler ÖZENİR

GLOBE 2ND INTERNATIONAL CONFERENCE ON ENGINEERING, ARCHITECTURE, MATHEMATICS and APPLIED SCIENCES October 1 - 6, 2026 BARSELONA Meeting ID: 885 7151 8350 Passcode: 202224				
2 Ekim / October 2, 2026 / 11:00 – 13:00 Time zone in Turkey (GMT+3)				
Salon	Moderator		Bildiri No ve Başlığı / Paper ID and Title	Authors
HALL / SALON 9	**Assist. Prof. Dr. Hayriye Güçkır Çakır**	1	A SECOND-ORDER HYBRID TECHNIQUE FOR THE NUMERICAL TREATMENT OF SECOND-ORDER FREDHOLM INTEGRO-DIFFERENTIAL EQUATIONS	Assist. Prof. Dr. Hayriye Güçkır Çakır Assist. Prof. Dr. Fırat Çakır
		2	NUMERICAL SOLUTION OF NONLINEAR SECOND-ORDER FREDHOLM INTEGRO-DIFFERENTIAL EQUATIONS WITH A BOUNDARY LAYER USING A SECOND-ORDER COMPUTATIONAL SCHEME	Assist. Prof. Dr. Hayriye Güçkır Çakır Assist. Prof. Dr. Fırat Çakır
		3	COULD WIDE-BUNDLE GEOMETRY PROVIDE GAMA ATTENUATION PARAMETERS AS ACCURATE AS THOSE FROM NARROW-BUNDLE GEOMETRY?	CANSU YILMAZ ZEYNEP ER CÜNEYT ÇELİKTAŞ
		4	THE EFFECT OF IMAGE ENHANCEMENT TECHNIQUES ON DEEP LEARNING-BASED CLASSIFICATION PERFORMANCE IN BRAIN TUMOR MRI IMAGES	Assistant Professor Olcay PALTA Professor Doctor Hanifi GÜLDEMIR Professor Doctor Musa ÇIBUK
		5	EXPLAINABLE ARTIFICIAL INTELLIGENCE IN BRAIN TUMOR MRI CLASSIFICATION: A COMPARATIVE ANALYSIS BASED ON GRAD-CAM AND GRAD-CAM++	*Assistant Professor Olcay PALTA Professor Doctor Musa ÇIBUK Professor Doctor Hanifi GÜLDEMIR
		6	THE ENVIRONMENTAL IMPACT OF INPUT USE IN AGRICULTURAL ENTERPRISES ENGAGED IN CROP PRODUCTION	Kardelen UĞUR Zuhal KARAKAYACI

GLOBE 2ND INTERNATIONAL CONFERENCE ON ENGINEERING, ARCHITECTURE, MATHEMATICS and APPLIED SCIENCES October 1 - 6, 2026 BARSELONA Meeting ID: 885 7151 8350 Passcode: 202224				
2 Ekim / October 2, 2026 / 11:30 – 13:30 Time zone in Turkey (GMT+3)				
Salon	Moderator		Bildiri No ve Başlığı / Paper ID and Title	Authors
HALL / SALON 10	**Prof. Dr. Péter Molnár**	1	IMPACTS OF OPEN-PIT COPPER AND GOLD MINING ON SOIL HEAVY METAL ACCUMULATION AND NATURAL FOREST VEGETATION IN THE ALMALYK MINING REGION OF UZBEKISTAN	Prof. Dr. Bakhtiyor Rakhimov Dilnoza Karimova Sherzod Tursunov
		2	CARBON SEQUESTRATION POTENTIAL AND ECOSYSTEM SERVICES OF AVICENNIA MARINA MANGROVE FORESTS ALONG THE QATARI COASTLINE: A FIELD-BASED AND SATELLITE MONITORING STUDY	Assoc. Prof. Dr. Jassim Al-Hajri Aisha Al-Muhannadi Mohammed Al-Kaabi
		3	LIMESTONE AND GABBRO QUARRYING IN ARID ENVIRONMENTS OF QATAR: DUST EMISSIONS, DESERT VEGETATION LOSS AND POST-MINING LAND REHABILITATION APPROACHES	Dr. Khalid Al-Mannai Maryam Al-Kuwari Prof. Dr. Abdulrahman Al-Sulaiti Noora Al-Marri Assist. Prof. Dr. Hamad Al-Naimi
		4	RIVERBED SAND AND STONE MINING IN THE SYLHET REGION OF BANGLADESH: EFFECTS ON RIPARIAN FOREST ECOSYSTEMS, RIVERBANK EROSION AND LOCAL LIVELIHOODS	Asst. Prof. Dr. Kamrul Hasan Talukder
		5	MANGROVE FOREST DEGRADATION IN THE SUNDARBANS: A GIS-BASED ANALYSIS OF SALINITY INTRUSION, ILLEGAL LOGGING AND COMMUNITY-BASED CONSERVATION STRATEGIES IN BANGLADESH	Prof. Dr. Abul Kalam Chowdhury Sabrina Haque Md. Imran Hossain Dr. Rumana Sultana
		6	ASSESSING THE ENVIRONMENTAL AND SOCIOECONOMIC CONSEQUENCES OF THE BARAPUKURIA UNDERGROUND COAL MINE ON SURROUNDING AGRICULTURAL LAND, GROUNDWATER LEVELS AND FOREST RESOURCES IN NORTHWESTERN BANGLADESH	Md. Rafiqul Islam Dr. Nusrat Jahan Tanvir Ahmed Assoc. Prof. Dr. Shahida Akter Mahmudul Hasan Farzana Rahman
		7	CLIMATE CHANGE, DROUGHT STRESS AND TIMBER PRODUCTION IN HUNGARIAN BEECH AND OAK FORESTS: IMPLICATIONS FOR SUSTAINABLE FOREST MANAGEMENT POLICIES UNDER EUROPEAN UNION REGULATIONS	Prof. Dr. Péter Molnár Anikó Farkas

GLOBE 2ND INTERNATIONAL CONFERENCE ON ENGINEERING, ARCHITECTURE, MATHEMATICS and APPLIED SCIENCES October 1 - 6, 2026 BARSELONA Meeting ID: 885 7151 8350 Passcode: 202224				
2 Ekim / October 2, 2026 / 11:30 – 13:30 Time zone in Turkey (GMT+3)				
Salon	Moderator		Bildiri No ve Başlığı / Paper ID and Title	Authors
HALL / SALON 11	**Prof. Dr. Péter Molnár**	1	SYNTHESIS AND CHARACTERIZATION OF ZEOLITE-BASED ADSORBENTS FROM NATURAL CLINOPTILOLITE FOR THE REMOVAL OF HEAVY METAL IONS FROM INDUSTRIAL WASTEWATER	Prof. Dr. Ivan Georgiev Petrov
		2	EFFECT OF SOL-GEL PROCESSING PARAMETERS ON THE MICROSTRUCTURE, PHASE COMPOSITION AND PHOTOCATALYTIC ACTIVITY OF NITROGEN-DOPED TITANIUM DIOXIDE THIN FILMS	Assoc. Prof. Dr. Maria Dimitrova Stoyan Kolev Dr. Elena Todorova Nikolay Ivanov Desislava Angelova
		3	INVESTIGATION OF THE THERMODYNAMIC PROPERTIES AND CORROSION BEHAVIOR OF ALUMINIUM–ZINC ALLOYS MODIFIED WITH RARE-EARTH ELEMENTS IN NEUTRAL CHLORIDE MEDIA	Prof. Dr. Rustam Nazarov Farrukh Saidov Dilnoza Rahimova
		4	PHYSICOCHEMICAL PROCESSING OF LOCAL KAOLIN CLAYS FOR THE PRODUCTION OF ALUMINA-CONTAINING COAGULANTS BY ACID LEACHING AND THERMAL ACTIVATION	Assist. Prof. Dr. Firuz Qodirov Shahlo Mirzoeva
		5	GREEN SYNTHESIS OF SILVER NANOPARTICLES USING JUTE LEAF EXTRACT AND THEIR INCORPORATION INTO CHITOSAN-BASED FILMS FOR ANTIBACTERIAL FOOD PACKAGING APPLICATIONS	Prof. Dr. Mohammad Rafiqul Islam Nusrat Jahan Dr. Tanvir Ahmed Sadia Afrin Md. Kamrul Hasan Farhana Akter
		6	CATALYTIC PYROLYSIS OF WASTE POLYETHYLENE AND POLYPROPYLENE OVER MODIFIED HZSM-5 CATALYSTS FOR LIQUID FUEL PRODUCTION: KINETIC AND PRODUCT DISTRIBUTION ANALYSIS	Assoc. Prof. Dr. Shahidul Alam Rumana Chowdhury Md. Arifur Rahman Dr. Tahmina Sultana
		7	DEVELOPMENT OF RICE HUSK ASH-DERIVED MESOPOROUS SILICA AS A LOW-COST SUPPORT FOR NICKEL CATALYSTS IN THE HYDROGENATION OF VEGETABLE OILS	Mahmudul Hasan Chowdhury
		8	OPTIMIZATION OF BIODIESEL PRODUCTION FROM WASTE PALM COOKING OIL USING CALCIUM OXIDE CATALYST DERIVED FROM EGGSHELL WASTE VIA RESPONSE SURFACE METHODOLOGY	Prof. Dr. Nor Azlina Abdullah Lim Wei Keat Dr. Muhammad Hafiz Ramli Siti Aisyah Kamaruddin Rajesh Kumar Subramaniam

GLOBE 2ND INTERNATIONAL CONFERENCE ON HEALTH and SPORT SCIENCES October 1 - 6, 2026 BARSELONA Meeting ID: 885 7151 8350 Passcode: 202224				
2 Ekim / October 2, 2026 / 11:30 – 13:30 Time zone in Turkey (GMT+3)				
Salon	Moderator		Bildiri No ve Başlığı / Paper ID and Title	Authors
HALL / SALON 12	**Assoc. Prof. Dr. Katalin Horváth**	1	EFFECTS OF A 12-WEEK HIGH-INTENSITY INTERVAL TRAINING PROGRAM ON CARDIOMETABOLIC RISK MARKERS AND AEROBIC CAPACITY IN SEDENTARY UNIVERSITY STUDENTS	Prof. Dr. Zoltán Kovács Eszter Nagy Dr. Bence Tóth
		2	THE RELATIONSHIP BETWEEN REGULAR RECREATIONAL SWIMMING, BODY COMPOSITION AND PERCEIVED QUALITY OF LIFE AMONG MIDDLE-AGED WOMEN: A CROSS-SECTIONAL STUDY	Assoc. Prof. Dr. Katalin Horváth
		3	ASSESSMENT OF PHYSICAL ACTIVITY LEVELS, SLEEP QUALITY AND ACADEMIC STRESS IN ADOLESCENTS: EVIDENCE FROM SECONDARY SCHOOLS IN TIRANA	Prof. Dr. Arben Hoxha Elona Shehu Assist. Prof. Dr. Klodian Dervishi Ermira Kola Dr. Besnik Leka
		4	INJURY PREVALENCE, RISK FACTORS AND RETURN-TO-PLAY TIMELINES IN ALBANIAN PROFESSIONAL FOOTBALL PLAYERS DURING A COMPETITIVE SEASON	Dr. Erion Mema Anila Gjoka
		5	THE IMPACT OF A STRUCTURED MULTICOMPONENT EXERCISE INTERVENTION ON BALANCE, MUSCLE STRENGTH AND FALL RISK IN OLDER ADULTS LIVING IN NURSING HOMES	Prof. Dr. Goran Stojanovski Assoc. Prof. Dr. Marija Petrovska Aleksandar Nikolovski Ivana Trajkovska Assist. Prof. Dr. Dejan Georgievski Elena Dimitrova
		6	NUTRITIONAL HABITS, HYDRATION STATUS AND ENERGY AVAILABILITY IN YOUNG ELITE ATHLETES: IMPLICATIONS FOR PERFORMANCE AND LONG-TERM HEALTH	Assist. Prof. Dr. Biljana Ristovska Stefan Jovanovski Dr. Vesna Angelovska Nikola Kostovski
		7	PHYSICAL EXERCISE AS AN ADJUNCT THERAPY FOR ANXIETY AND DEPRESSIVE SYMPTOMS IN YOUNG ADULTS: A SYSTEMATIC REVIEW OF RANDOMIZED CONTROLLED TRIALS	Dr. Tamara Velkovska
		8	PREVALENCE OF OVERWEIGHT AND OBESITY AND ITS ASSOCIATION WITH SCREEN TIME AND PHYSICAL INACTIVITY AMONG PRIMARY SCHOOL CHILDREN IN KAZAKHSTAN	Prof. Dr. Nurlan Abenov Aigerim Sadykova Assoc. Prof. Dr. Yerlan Zhakupov Dana Kassymova Arman Tokhtarov

GLOBE 2ND INTERNATIONAL CONFERENCE ON HEALTH and SPORT SCIENCES October 1 - 6, 2026 BARSELONA Meeting ID: 885 7151 8350 Passcode: 202224				
2 Ekim / October 2, 2026 / 11:30 – 13:30 Time zone in Turkey (GMT+3)				
Salon	Moderator		Bildiri No ve Başlığı / Paper ID and Title	Authors
HALL / SALON 13	**Dr. Mariana Castro Vieira**	1	PREVALENCE AND RISK FACTORS OF HYPERTENSION AMONG ADULTS IN RURAL MOUNTAIN COMMUNITIES: A CROSS-SECTIONAL POPULATION-BASED STUDY IN WESTERN GEORGIA	Prof. Dr. Giorgi Beridze Nino Kapanadze Dr. Tamar Lomidze
		2	ANTIBIOTIC PRESCRIBING PATTERNS AND AWARENESS OF ANTIMICROBIAL RESISTANCE AMONG PRIMARY CARE PHYSICIANS IN TBILISI: A MIXED-METHODS EVALUATION	Assoc. Prof. Dr. Levan Tsiklauri
		3	EVALUATION OF MATERNAL AND NEONATAL HEALTH OUTCOMES FOLLOWING THE IMPLEMENTATION OF REGIONAL PERINATAL CARE CENTERS IN THE REPUBLIC OF MOLDOVA: A TEN-YEAR RETROSPECTIVE COHORT ANALYSIS	Prof. Dr. Ion Rusu Elena Ciobanu Assist. Prof. Dr. Victor Munteanu Ana Moraru Dr. Sergiu Lungu
		4	IMPACT OF THE FAMILY HEALTH STRATEGY ON HOSPITALIZATIONS FOR PRIMARY CARE-SENSITIVE CONDITIONS IN NORTHEASTERN BRAZIL: A LONGITUDINAL ECOLOGICAL STUDY OF MUNICIPAL DATA	Prof. Dr. João Pereira da Silva Ana Carolina Souza Dr. Rafael Oliveira Costa Beatriz Mendes Almeida Assoc. Prof. Dr. Lucas Ferreira Rocha Camila Ribeiro Santos
		5	LONG-TERM NEUROLOGICAL AND DEVELOPMENTAL OUTCOMES IN CHILDREN WITH CONGENITAL ZIKA SYNDROME: A FIVE-YEAR FOLLOW-UP OF A MULTICENTER COHORT IN PERNAMBUCO	Dr. Juliana Barbosa Teixeira Mateus Cardoso Pinto Assoc. Prof. Dr. Fernanda Lima Carvalho Gabriel Araújo Nunes
		6	ASSOCIATION BETWEEN ULTRA-PROCESSED FOOD CONSUMPTION AND METABOLIC SYNDROME AMONG UNIVERSITY STUDENTS IN SÃO PAULO: A CROSS-SECTIONAL ANALYSIS USING DIETARY RECALL DATA	Dr. Mariana Castro Vieira
		7	BARRIERS TO ACCESS AND UTILIZATION OF MENTAL HEALTH SERVICES AMONG ADOLESCENTS IN METRO MANILA: A QUALITATIVE STUDY OF STUDENTS, PARENTS AND SCHOOL COUNSELORS	Prof. Dr. Maria Cristina Santos Jose Miguel Reyes Assist. Prof. Dr. Angelica Dela Cruz Paolo Villanueva Kristine Joy Mendoza

GLOBE 2ND INTERNATIONAL CONFERENCE ON SOCIAL SCIENCES October 1 - 6, 2026 BARSELONA Meeting ID: 885 7151 8350 Passcode: 202224				
2 Ekim / October 2, 2026 / 15:00 – 17:00 Time zone in Turkey (GMT+3)				
Salon	Moderator		Bildiri No ve Başlığı / Paper ID and Title	Authors
HALL / SALON 8	**Assoc. Prof. Dr. Semra TETİK**	1	EVALUATION OF ORGANIZATIONAL COMMITMENT AMONG BLUE-COLLAR EMPLOYEES IN TERMS OF DEMOGRAPHIC FACTORS	Assoc. Prof. Dr. Semra TETİK
		2	THE RELATIONSHIPS BETWEEN CAREER STRESS, EMOTIONAL INTELLIGENCE, SELF-EFFICACY, AND PSYCHOLOGICAL RESILIENCE: A CASE OF VOCATIONAL SCHOOL STUDENTS	Assoc. Prof. Dr. Semra TETİK
		3	EXPORT RESTRICTIONS AND CRITICAL RAW MATERIAL TRADE IN A GLOBAL PRODUCT-LEVEL PANEL	Arş. Gör., Bilal Orhan Prof. Dr., Muhammed Benli
		4	INCUMBENT ADVANTAGE AND EXPORT REALLOCATION IN AI-ENABLING GOODS TRADE	Arş. Gör., Bilal Orhan Prof. Dr., Muhammed Benli
		5	SAĞLIK HİZMETLERİ KALİTESİNİN ÖLÇÜLMESİNDE SERVQUAL SKORLARININ DEĞERLENDİRİLMESİ: YÜKSEK ÖĞRETİM KURUMU (YÖK) TEZ VERİ TABANI ÜZERİNDE YAPILMIŞ BİR ARAŞTIRMA	Doç.Dr .İzzet Aydemir Prof.Dr. İmran Aslan
		6	TÜRKİYE'DE TRAFİK KAZALARINA BAĞLI YAŞAM YILI KAYBININ TÜİK VE KÜRESEL HASTALIK YÜKÜ VERİLERİYLE İNCELENMESİ	Prof.Dr. İmran Aslan Doç.Dr .İzzet Aydemir
		7	SAĞLIK HİZMETLERİNDE DİL AYRIMCILIĞI	Dr. Öğretim Üyesi Dilan Mızrak
		8	FİNANSAL OKURYAZARLIK DÜZEYİNİN KAMU KAYNAKLI EKONOMİK DESTEKLERE ETKİSİ: AYDIN İLİ ÖRNEĞİ	Dr. Öğr. Üyesi Emine Ebru BOZÇELİK
		9		

No:3

GLOBE 2ND INTERNATIONAL CONFERENCE ON SOCIAL SCIENCES October 1 - 6, 2026 BARSELONA Meeting ID: 885 7151 8350 Passcode: 202224				
2 Ekim / October 2, 2026 / 15:00 – 17:00 Time zone in Turkey (GMT+3)				
Salon	Moderator		Bildiri No ve Başlığı / Paper ID and Title	Authors
HALL / SALON 9	**Doç.Dr. Hilal Süreyya Yılmaz**	1	NOLAN SİNEMASINDA ZAMAN: MEMENTO, INTERSTELLAR VE TENET ÜZERİNE KARŞILAŞTIRMALI BİR ANALİZ	Doç.Dr. Hilal Süreyya Yılmaz
		2	TÜKETİM TOPLUMUNDA ÖZNE: *THE SUBSTANCE VE NOMADLAND* FİLMLERINDE METALAŞMA VE DİRENİŞ	Doç.Dr. Hilal Süreyya Yılmaz
		3	THE LIFE, INSTRUMENTAL COMPOSITIONS, AND ANALYSIS OF THE HÜSEYNÎ SAZ SEMÂÎSİ OF KEMÂNÎ AYDIN NAFİZ ORAN	Doç. Dr. Ahmet Hakan BAŞ Dr. Dilek YÜZLÜER
		4	A NEW FIELD IN THE MEDIA SECTOR: SYNTHETIC JOURNALISM	Assoc. Prof. Dr. Hakan YUKSEL
		5	THE CHANGING AND TRANSFORMING PHENOMENON OF VISUAL NARRATIVE IN INTERNET MEDIA	Assoc. Prof. Dr. Hakan YUKSEL

GLOBE 2ND INTERNATIONAL CONFERENCE ON SOCIAL SCIENCES October 1 - 6, 2026 BARSELONA Meeting ID: 885 7151 8350 Passcode: 202224				
2 Ekim / October 2, 2026 / 15:00 – 17:00 Time zone in Turkey (GMT+3)				
Salon	Moderator		Bildiri No ve Başlığı / Paper ID and Title	Authors
HALL / SALON 10	**Doç. Dr. SEVRA FIRINCIOĞULLARI**	1	POLITENESS AS A LINGUISTIC AND PRAGMATIC CATEGORY IN ENGLISH AND UZBEK DISCOURSE	Prof. Mavlonova Ugiloy Khamdamovna
		2	A LOOK AT WOMEN'S WORKING CONDITIONS IN THE BRITISH ARISTOCRACY, BASED ON ANNE BRONTE'S NOVEL "AGNES GREY"	Doç. Dr. SEVRA FIRINCIOĞULLARI
		3	SİBER PSİKOLOJİNİN ÖNEMİ, ALINACAK ÖNLEMLER ve GELİŞTİRİLECEK YÖNLER	Öğr.Gör.Burcu GÜLDÜREN FİDANCI
		4	REASSESSING DEISM THROUGH MĀTURĪDĪ THEOLOGY: REASON, REVELATION AND HUMAN RESPONSIBILITY	Doctoral Lecturer, ASLI MENEKŞE

GLOBE 2ND INTERNATIONAL CONFERENCE ON SOCIAL SCIENCES October 1 - 6, 2026 BARSELONA Meeting ID: 885 7151 8350 Passcode: 202224				
2 Ekim / October 2, 2026 / 15:30 – 17:30 Time zone in Turkey (GMT+3)				
Salon	Moderator		Bildiri No ve Başlığı / Paper ID and Title	Authors
HALL / SALON 11	**Dr. Teresa Aquino**	1	REVITALIZATION OF TRADITIONAL BATIK ART THROUGH CONTEMPORARY DESIGN PRACTICES IN INDONESIA	Prof. Dr. Agus Santoso Rina Prameswari
		2	CULTURAL SYMBOLISM IN BALINESE PAINTING AND ITS TRANSFORMATION IN MODERN VISUAL ARTS	Dr. Made Wirawan Ketut Sari
		3	CONTEMPORARY FILIPINO STREET ART AS A MEDIUM OF POLITICAL EXPRESSION AND SOCIAL COMMENTARY	Carlos Dela Cruz Assoc. Prof. Dr. Miguel Reyes Ayu Lestari
		4	PRESERVATION OF INDIGENOUS ART FORMS IN PHILIPPINE RURAL COMMUNITIES THROUGH DIGITAL ARCHIVING	Dr. Liza Fernandez Ana Santos Roberto Villanueva
		5	THE ROLE OF FILIPINO CINEMA IN SHAPING NATIONAL IDENTITY IN THE 21ST CENTURY	Prof. Dr. Juan Bautista Elena Garcia Marco Lopez
		6	VISUAL NARRATIVES IN FILIPINO CONTEMPORARY PHOTOGRAPHY AND URBAN TRANSFORMATION	Dr. Teresa Aquino Assoc. Prof. Dr. Paolo Mendoza
		7	TRADITIONAL WEAVING TECHNIQUES AND THEIR INTEGRATION INTO MODERN FILIPINO FASHION DESIGN	Assoc. Prof. Dr. Regina Salazar Isabel Cruz Daniel Torres Maria Velasco
		8	AFRICAN MASK ART AND ITS INFLUENCE ON CONTEMPORARY SENEGALESE SCULPTURE	Prof. Dr. Mamadou Diop Aissatou Ndiaye

GLOBE 2ND INTERNATIONAL CONFERENCE ON SOCIAL SCIENCES October 1 - 6, 2026 BARSELONA Meeting ID: 885 7151 8350 Passcode: 202224				
2 Ekim / October 2, 2026 / 15:30 – 17:30 Time zone in Turkey (GMT+3)				
Salon	Moderator		Bildiri No ve Başlığı / Paper ID and Title	Authors
HALL / SALON 12	**Assoc. Prof. Dr. Katalin Horváth**	1	DIGITAL TRANSFORMATION AND PRODUCTIVITY GROWTH IN CENTRAL EUROPEAN SMALL AND MEDIUM-SIZED ENTERPRISES: EVIDENCE FROM HUNGARIAN MANUFACTURING FIRMS BETWEEN 2010 AND 2024	Prof. Dr. László Kovács Eszter Szabó Dr. Gábor Tóth
		2	INFLATION EXPECTATIONS, MONETARY POLICY CREDIBILITY AND HOUSEHOLD CONSUMPTION BEHAVIOUR IN HUNGARY DURING THE POST-PANDEMIC PRICE SHOCK	Assoc. Prof. Dr. Katalin Horváth
		3	THE ROLE OF REMITTANCES IN POVERTY REDUCTION AND HOUSEHOLD INVESTMENT DECISIONS IN ALBANIA: A REGIONAL ANALYSIS OF RURAL AND URBAN AREAS	Prof. Dr. Arben Hoxha Elira Dervishi Assist. Prof. Dr. Klodian Shehu Ermira Leka
		4	TOURISM-LED GROWTH HYPOTHESIS AND ITS SUSTAINABILITY IN THE WESTERN BALKANS: AN ECONOMETRIC ASSESSMENT OF THE ALBANIAN COASTAL ECONOMY	Dr. Blerina Kola Ardit Muça
		5	FOREIGN DIRECT INVESTMENT, INSTITUTIONAL QUALITY AND EXPORT DIVERSIFICATION IN NORTH MACEDONIA: IMPLICATIONS FOR EUROPEAN UNION ACCESSION	Prof. Dr. Aleksandar Stojanovski Marija Petrovska Assoc. Prof. Dr. Nikola Trajkovski Elena Georgievska Dr. Besim Ademi
		6	YOUTH UNEMPLOYMENT, SKILLS MISMATCH AND LABOUR MIGRATION FROM NORTH MACEDONIA TO THE EUROPEAN UNION: CAUSES, CONSEQUENCES AND POLICY RESPONSES	Ivana Dimitrova
		7	FISCAL DECENTRALIZATION AND REGIONAL ECONOMIC DISPARITIES IN NORTH MACEDONIA: A PANEL DATA ANALYSIS OF MUNICIPAL REVENUES AND PUBLIC SPENDING EFFICIENCY	Assist. Prof. Dr. Dragan Nikolovski Snezhana Ristovska Prof. Dr. Vesna Angelovska Goran Jovanovski Dr. Ardita Rexhepi Filip Velkovski

GLOBE 2ND INTERNATIONAL CONFERENCE ON SOCIAL SCIENCES October 1 - 6, 2026 BARSELONA Meeting ID: 885 7151 8350 Passcode: 202224				
2 Ekim / October 2, 2026 / 15:30 – 17:30 Time zone in Turkey (GMT+3)				
Salon	Moderator		Bildiri No ve Başlığı / Paper ID and Title	Authors
HALL / SALON 13	**Assoc. Prof. Dr. Noor Sabah Al-Obaidi**	1	PSYCHOLOGICAL DISTRESS, POST-TRAUMATIC STRESS SYMPTOMS AND ACCESS TO MENTAL HEALTH SERVICES AMONG INTERNALLY DISPLACED ADULTS IN POST-CONFLICT REGIONS OF NORTHERN IRAQ: A CROSS-SECTIONAL STUDY	Prof. Dr. Ahmed Kadhim Al-Saadi Zainab Hussein Jaber Dr. Mustafa Abdulameer Al-Khafaji Assoc. Prof. Dr. Noor Sabah Al-Obaidi
		2	PREVALENCE AND PSYCHOSOCIAL PREDICTORS OF DEPRESSIVE SYMPTOMS AMONG OLDER ADULTS RECEIVING PRIMARY HEALTH CARE IN KARAGANDA REGION: IMPLICATIONS FOR GERIATRIC MENTAL HEALTH SERVICE PLANNING	Assoc. Prof. Dr. Gulnara Ospanova Askar Temirbekov Madina Kassymova
		3	PATIENT SATISFACTION, THERAPEUTIC ALLIANCE AND TREATMENT ADHERENCE IN OUTPATIENT PSYCHIATRIC SERVICES OF ALMATY AND ASTANA: A MULTICENTER EVALUATION OF SERVICE QUALITY IN KAZAKHSTAN	Aigerim Bekova Prof. Dr. Yerlan Serikbayev Dana Zhumabekova Dr. Nurlan Abdikarimov Assel Tulegenova
		4	DIGITAL MENTAL HEALTH INTERVENTIONS AND TELEPSYCHOLOGY USE AMONG ADOLESCENTS IN URBAN AND RURAL AREAS OF EAST JAVA: ACCEPTABILITY, ENGAGEMENT AND PERCEIVED EFFECTIVENESS	Assist. Prof. Dr. Nur Aini Wulandari
		5	THE RELATIONSHIP BETWEEN SOCIAL SUPPORT, RELIGIOUS COPING AND QUALITY OF LIFE AMONG CAREGIVERS OF PATIENTS WITH SCHIZOPHRENIA IN YOGYAKARTA AND CENTRAL JAVA, INDONESIA	Prof. Dr. Dewi Lestari Putri Agus Wibowo Dr. Rina Kartikasari Muhammad Fajar Hidayat Indah Permata Sari Andi Prasetyo
		6	HEALTH LITERACY, MENTAL HEALTH HELP-SEEKING ATTITUDES AND STIGMA TOWARD PSYCHIATRIC SERVICES AMONG UNIVERSITY STUDENTS IN ISFAHAN AND SHIRAZ: A STRUCTURAL EQUATION MODELING APPROACH	Prof. Dr. Ali Asghar Mohammadi Dr. Leila Hosseini Fard Sara Jafari Amir Hossein Sadeghi Narges Bahrami
		7	THE EFFECTIVENESS OF GROUP-BASED ACCEPTANCE AND COMMITMENT THERAPY ON DEPRESSION, ANXIETY AND PSYCHOLOGICAL FLEXIBILITY IN WOMEN WITH TYPE 2 DIABETES ATTENDING PRIMARY HEALTH CARE CENTERS IN TEHRAN: A RANDOMIZED CONTROLLED TRIAL	Mohammad Reza Karimi Assist. Prof. Dr. Fatemeh Moradi Hossein Ahmadi Nejad Maryam Rezaei Tabar

GLOBE 2ND INTERNATIONAL CONFERENCE ON ENGINEERING, ARCHITECTURE, MATHEMATICS and APPLIED SCIENCES
October 1 - 6, 2026 – BARSELONA
ISBN NR.: 978-625-8795-56-1

Contents

A SECOND-ORDER HYBRID TECHNIQUE FOR THE NUMERICAL TREATMENT OF SECOND-ORDER FREDHOLM INTEGRO-DIFFERENTIAL EQUATIONS 1

NUMERICAL SOLUTION OF NONLINEAR SECOND-ORDER FREDHOLM INTEGRO-DIFFERENTIAL EQUATIONS WITH A BOUNDARY LAYER USING A SECOND-ORDER COMPUTATIONAL SCHEME 2

COULD WIDE-BUNDLE GEOMETRY PROVIDE GAMA ATTENUATION PARAMETERS AS ACCURATE AS THOSE FROM NARROW-BUNDLE GEOMETRY? 3

THE EFFECT OF IMAGE ENHANCEMENT TECHNIQUES ON DEEP LEARNING-BASED CLASSIFICATION PERFORMANCE IN BRAIN TUMOR MRI IMAGES 19

EXPLAINABLE ARTIFICIAL INTELLIGENCE IN BRAIN TUMOR MRI CLASSIFICATION: A COMPARATIVE ANALYSIS BASED ON GRAD-CAM AND GRAD-CAM++ 33

THE ENVIRONMENTAL IMPACT OF INPUT USE IN AGRICULTURAL ENTERPRISES ENGAGED IN CROP PRODUCTION 46

IMPACTS OF OPEN-PIT COPPER AND GOLD MINING ON SOIL HEAVY METAL ACCUMULATION AND NATURAL FOREST VEGETATION IN THE ALMALYK MINING REGION OF UZBEKISTAN 60

CARBON SEQUESTRATION POTENTIAL AND ECOSYSTEM SERVICES OF AVICENNIA MARINA MANGROVE FORESTS ALONG THE QATARI COASTLINE: A FIELD-BASED AND SATELLITE MONITORING STUDY 61

LIMESTONE AND GABBRO QUARRYING IN ARID ENVIRONMENTS OF QATAR: DUST EMISSIONS, DESERT VEGETATION LOSS AND POST-MINING LAND REHABILITATION APPROACHES 62

RIVERBED SAND AND STONE MINING IN THE SYLHET REGION OF BANGLADESH: EFFECTS ON RIPARIAN FOREST ECOSYSTEMS, RIVERBANK EROSION AND LOCAL LIVELIHOODS 63

MANGROVE FOREST DEGRADATION IN THE SUNDARBANS: A GIS-BASED ANALYSIS OF SALINITY INTRUSION, ILLEGAL LOGGING AND COMMUNITY-BASED CONSERVATION STRATEGIES IN BANGLADESH 64

ASSESSING THE ENVIRONMENTAL AND SOCIOECONOMIC CONSEQUENCES OF THE BARAPUKURIA UNDERGROUND COAL MINE ON SURROUNDING AGRICULTURAL LAND, GROUNDWATER LEVELS AND FOREST RESOURCES IN NORTHWESTERN BANGLADESH 66

CLIMATE CHANGE, DROUGHT STRESS AND TIMBER PRODUCTION IN HUNGARIAN BEECH AND OAK FORESTS: IMPLICATIONS FOR SUSTAINABLE FOREST MANAGEMENT POLICIES UNDER EUROPEAN UNION REGULATIONS 67

SYNTHESIS AND CHARACTERIZATION OF ZEOLITE-BASED ADSORBENTS FROM NATURAL CLINOPTILOLITE FOR THE REMOVAL OF HEAVY METAL IONS FROM INDUSTRIAL WASTEWATER 68

EFFECT OF SOL-GEL PROCESSING PARAMETERS ON THE MICROSTRUCTURE, PHASE COMPOSITION AND PHOTOCATALYTIC ACTIVITY OF NITROGEN-DOPED TITANIUM DIOXIDE THIN FILMS 69

INVESTIGATION OF THE THERMODYNAMIC PROPERTIES AND CORROSION BEHAVIOR OF ALUMINIUM–ZINC ALLOYS MODIFIED WITH RARE-EARTH ELEMENTS IN NEUTRAL CHLORIDE MEDIA 70

PHYSICOCHEMICAL PROCESSING OF LOCAL KAOLIN CLAYS FOR THE PRODUCTION OF ALUMINA-CONTAINING COAGULANTS BY ACID LEACHING AND THERMAL ACTIVATION 71

ISBN NR.: 978-625-8795-56-1

GREEN SYNTHESIS OF SILVER NANOPARTICLES USING JUTE LEAF EXTRACT AND THEIR INCORPORATION INTO CHITOSAN-BASED FILMS FOR ANTIBACTERIAL FOOD PACKAGING APPLICATIONS 72

CATALYTIC PYROLYSIS OF WASTE POLYETHYLENE AND POLYPROPYLENE OVER MODIFIED HZSM-5 CATALYSTS FOR LIQUID FUEL PRODUCTION: KINETIC AND PRODUCT DISTRIBUTION ANALYSIS 74

DEVELOPMENT OF RICE HUSK ASH-DERIVED MESOPOROUS SILICA AS A LOW-COST SUPPORT FOR NICKEL CATALYSTS IN THE HYDROGENATION OF VEGETABLE OILS..... 76

OPTIMIZATION OF BIODIESEL PRODUCTION FROM WASTE PALM COOKING OIL USING CALCIUM OXIDE CATALYST DERIVED FROM EGGSHELL WASTE VIA RESPONSE SURFACE METHODOLOGY..... 77

GLOBE 2ND INTERNATIONAL CONFERENCE ON ENGINEERING, ARCHITECTURE, MATHEMATICS and APPLIED SCIENCES
October 1 - 6, 2026 – BARSELONA
ISBN NR.: 978-625-8795-56-1

A SECOND-ORDER HYBRID TECHNIQUE FOR THE NUMERICAL TREATMENT OF SECOND-ORDER FREDHOLM INTEGRO-DIFFERENTIAL EQUATIONS

Assist. Prof. Dr. Hayriye Güçkır Çakır
Faculty of Engineering and Architecture, Batman University, Batman, Turkiye
hayriyeguckir.cakir@batman.edu.tr -0000-0002-1570-1534

Assist. Prof. Dr. Fırat Çakır
Faculty of Engineering and Architecture, Batman University, Batman, Turkiye
firat.cakir@batman.edu.tr - 0000 0001 5555 4244

ABSTRACT

Solving second-order linear Fredholm integro-differential equations (FIDEs) accurately remains a meaningful challenge in numerical mathematics. In this work, we introduce a new hybrid approach that brings together a first-order finite difference scheme and Richardson extrapolation. The first-order finite difference scheme is constructed using the integral identity approach with basis functions, while the integral terms are handled via interpolatory quadrature rules with remainder terms. Further, we incorporate Richardson extrapolation into the first-order numerical method, effectively raising the order of convergence to second-order. We also conduct rigorous error estimates and convergence analysis of the proposed method. The factorization technique is employed to establish the algorithm. In addition, we validate the theoretical findings through numerical examples.

Anahtar Kelimeler : FIDE; Difference scheme; Error estimates; Richardson Extrapolation.

GLOBE 2ND INTERNATIONAL CONFERENCE ON ENGINEERING, ARCHITECTURE, MATHEMATICS and APPLIED SCIENCES
October 1 - 6, 2026 – BARSELONA
ISBN NR.: 978-625-8795-56-1

NUMERICAL SOLUTION OF NONLINEAR SECOND-ORDER FREDHOLM INTEGRO-DIFFERENTIAL EQUATIONS WITH A BOUNDARY LAYER USING A SECOND-ORDER COMPUTATIONAL SCHEME

Assist. Prof. Dr. Hayriye Güçkır Çakır
Faculty of Engineering and Architecture, Batman University, Batman, Turkiye
hayriyeguckir.cakir@batman.edu.tr -0000-0002-1570-1534

Assist. Prof. Dr. Fırat Çakır
Faculty of Engineering and Architecture, Batman University, Batman, Turkiye
firat.cakir@batman.edu.tr - 0000 0001 5555 4244

ABSTRACT

Many phenomena in science and engineering involve intricate relationships between causes and their resulting effects. A particularly striking instance of this arises in singularly perturbed problems — a class of problems characterized by the presence of a small positive parameter multiplying the highest-order derivative term, where even a slight perturbation produces disproportionately large effects in the form of sharp boundary or interior layers where the solution changes rapidly over a very narrow region. Standard numerical methods often fall short in capturing these rapid variations accurately, making the development of specialized numerical techniques essential. This paper aims to develop a new second-order numerical approach for a class of second-order nonlinear singularly perturbed Fredholm integro-differential equations. To this end, the problem is first approximated using a non-standard finite difference scheme constructed on a Bakhvalov-type mesh. The first-order scheme is built upon an integral identity with basis functions, and the integral terms are treated through appropriate quadrature rules. The first-order method is then combined with Richardson extrapolation, giving rise to a new second-order method for the problem under consideration. A thorough error analysis and convergence investigation of the proposed methods are carried out, and the theoretical results are supported and illustrated through representative numerical examples along with the corresponding numerical results.

Anahtar Kelimeler : FIDE; Singular Perturbation; Difference scheme; Bakhvalov-type mesh; Error estimates; Richardson Extrapolation.

GLOBE 2ND INTERNATIONAL CONFERENCE ON ENGINEERING, ARCHITECTURE, MATHEMATICS and APPLIED SCIENCES
October 1 - 6, 2026 – BARSELONA
ISBN NR.: 978-625-8795-56-1

COULD WIDE-BUNDLE GEOMETRY PROVIDE GAMA ATTENUATION PARAMETERS AS ACCURATE AS THOSE FROM NARROW-BUNDLE GEOMETRY?

CANSU YILMAZ
Ege University, 04230000284@ogrenci.ege.edu.tr – 0009-0009-7692-1758

ZEYNEP ER
Ege University, 04220000249@ogrenci.ege.edu.tr – 0009-0005-4625-641X

CÜNEYT ÇELİKTAŞ
Ege University, cuneyt.celiktas@ege.edu.tr – 0000-0001-8608-066X

ABSTRACT

A significant part of gamma transmission studies utilizes NaI(Tl)-based inorganic spectrometers or compact scintillation systems, along with narrow-beam geometries that limit photon scattering. It is observed that gamma transmission studies carried out with Cs-137 sources mostly focus on directly measuring the pure attenuation of the primary photon beam passing through the absorber, and for this reason, narrow-beam geometries with collimators on the source or detector side are preferred. In the present study, a wide-beam geometry was designed in which secondary scatter is naturally included in the measurement. In the study, a closed, disk-shaped Cs-137 radioactive source with a nominal activity of 5 μCi and a BC-400-type plastic scintillator measuring $5 \times 5 \times 0.5$ cm^3 were used, and the attenuation behaviour of gamma photons within pure lead and pure aluminium absorber plates was investigated. The half-value thickness (HVL), tenth-value thickness (TVL), and mean free path (MFP) shielding parameters were derived not from the theoretical narrow-beam linear attenuation coefficient, but from the effective linear attenuation coefficient (μ_{eff}) determined in the experimental wide-beam geometry. Furthermore, the mass attenuation coefficients determined experimentally were compared with NIST XCOM reference values. The transmission characteristics of Pb and Al absorbers against gamma photons with an energy of approximately 662 keV were experimentally investigated in this study, and it was determined that Pb exhibits a more pronounced attenuation tendency compared to Al. The findings highlight the need for future studies to compare narrow- and wide-beam measurement geometries using different gamma-ray energies and absorber materials, as well as to investigate in greater depth the effects of the detector system proposed here on attenuation coefficients.

Keywords: Photomultiplier tube **(**PMT), Cs-137, Absorption, BC-400, Gamma attenuation.

ISBN NR.: 978-625-8795-56-1

1. INTRODUCTION

The energy loss of uncharged high-energy gamma rays within matter occurs through discrete, instantaneous interactions, in contrast to the continuous deceleration behaviour observed in charged particles. When gamma photons are directed into an absorbing material, a portion of the photons is separated from the initial beam as a result of photoelectric absorption and scattering interactions within the material. As the thickness of the absorbing material increases, the number of primary photons that manage to reach the detector without undergoing any interaction decreases, and as a result, a clear decrease in the measured radiation intensity is observed. This fundamental approach is widely accepted in the literature as a standard method for experimentally investigating the attenuation behaviour of gamma rays in different materials [1].

Under ideal narrow-beam conditions, a single-energy gamma beam undergoes an intensity loss as it passes through a homogeneous absorbing medium and exhibits exponential attenuation behaviour. The decrease in photon intensity in the primary beam as a function of the thickness of the absorbing material is described by the Beer-Lambert law [2, 3]. However, in the wide-beam geometry used in laboratory conditions, the process deviates from the ideal case. A portion of the photons undergoing Compton scattering within the absorber manage to reach the detector after changing direction. Consequently, the radiation intensity measured by the instrument includes not only the primary photons that reach the target without undergoing any interaction, but also the secondary photons generated by the scattered photons and the contribution from pile-up. Based on these experimental findings, the attenuation coefficient obtained under wide-beam conditions should be distinguished from the theoretical narrow-beam coefficient and treated as the effective linear attenuation coefficient (μ_{eff}) accepted in the literature [2, 4].

The linear attenuation coefficient, used as a physical parameter, expresses the attenuation in the intensity of a photon beam of a specific energy per unit path length travelled within an absorbing medium; in other words, it represents the probability of the photons in the beam interacting. This coefficient is directly dependent on the material's atomic composition, density and the energy of the incident photon. A high value for this coefficient indicates that the material is capable of effectively stopping gamma photons over very short distances and attenuates the beam more significantly [1, 2].

As the linear attenuation coefficient is defined as a parameter dependent on the material's physical density, it is not reasonable to compare the radiation attenuation behaviour of absorbing materials with different densities based solely on this value. To overcome this limitation and eliminate the dependence on physical density, the mass attenuation coefficient (μ_ρ), which is calculated in the literature by dividing the linear attenuation coefficient by the material's volumetric density and has the unit cm^2/g, is preferred. This parameter expresses

ISBN NR.: 978-625-8795-56-1

photon attenuation behaviour per unit mass rather than per unit volume. It thus enables a far more consistent comparison of materials with different atomic structures [2, 3].

The fundamental criterion for the transmission of gamma photons is to measure the loss in intensity that the radiation undergoes as it passes through absorbers of different thicknesses and to compare the resulting attenuation coefficient with theoretical data. This method has been successfully applied in the literature. The gamma attenuation coefficients of aluminium alloys and composites (Al/B_4C) were calculated using scintillation detectors, and it was demonstrated by comparison that the results were consistent with XCOM data [3, 5]. Furthermore, the linear attenuation coefficients and pile-up characteristics of lead and aluminium metals at this energy level have been investigated [4]. The attenuation capacities of the same shielding materials at the 662 keV energy level were tested under collimated narrow-beam conditions. The experimental results obtained were supported by MCNP simulations [1]. Furthermore, the gamma attenuation coefficients of Al, Fe and Pb absorber materials at an energy level of 662 keV were also determined in an experimental setup featuring collimated narrow-beam geometries [1, 5]. The radiation tolerance of PEN and PET-type plastics, which possess excellent scintillation properties, at high radiation doses was tested using the same type of radioisotope and photomultiplier tube (PMT) as those used in this study [6].

It is observed that a significant part of gamma transmission studies utilises NaI(Tl)-based inorganic spectrometers or compact scintillation systems, as well as narrow-beam geometries that limit photon scattering. In gamma transmission studies conducted with Cs-137 sources, the primary objective is usually to measure as directly as possible the pure attenuation of the primary photon beam passing through the absorber. For this reason, in many experimental studies in the literature, narrow-beam geometries with collimators on either the source or detector side are preferred to prevent the contribution of secondary photons scattered within the absorber material from reaching the detector. However, photons representing wide-beam conditions do not travel in an ideal, narrow line. Based on this physical reality, this study did not use a collimator but instead employed a wide-beam geometry in which secondary scattering is naturally included in the measurement. Furthermore, there are few studies in which a measurement system consisting of a plastic scintillator, a light guide and a PMT has been used to compare the transmission properties of Pb and Al within the same system under a wide-beam geometry without a collimator. In this study, effective attenuation parameters for lead and aluminium, corresponding to real-world shielding conditions, were analysed using a system consisting of a plastic scintillator, a light guide and a PMT. As the transmission values measured in this study include not only directly transmitted photons but also, to the extent permitted by the experimental geometry, the contributions of scattered photons, it is more accurate to interpret the calculated coefficients as effective linear attenuation coefficients specific to the experimental conditions.

ISBN NR.: 978-625-8795-56-1

2. EXPERIMENTAL STUDIES

2.1. Experimental Setup and Materials Used

In this study, a closed, disc-shaped Cs-137 radioactive source with a nominal activity of 5 μCi was used, utilising the wide-beam gamma-ray transmission method. The reason for selecting the Cs-137 radioisotope is that it emits a single, distinct gamma photon at a specific energy (662 keV) and is used in the literature as a standard energy calibration source [1, 3]. Within the scope of this study, the attenuation behaviour of 662 keV gamma photons emitted from the Cs-137 source within pure lead and pure aluminium absorber plates was investigated. To ensure the geometric consistency of the measurement conditions in the wide-beam transmission geometry of the setup, the centre of the Cs-137 source, the centre of the absorber plates and the centre of the active surface of the scintillation detector have been positioned on a single axis. The distance between the absorber's radiation-exposed front surface and the source has been kept constant at 4 cm for all measurements.

In the coefficient calculations, the densities of the materials were taken as 11.34 g/cm^3 (Pb) and 2.70 g/cm^3 (Al), respectively. The surface areas of the absorber plates used were located to completely cover the detector window and ensure that the radiation from the source reached the detector after passing through the absorber material. Absorber thickness was increased by 0.1 cm for each material, and ten layers of each material were placed between the source and the detector. Three measurements were taken for each thickness, and the averages of these measurements were recorded as the results.

In the detector system, a BC-400-type plastic scintillator measuring 5 × 5 × 0.5 cm^3 was used to detect gamma rays. Generally, in a scintillator, the energy transferred as a result of the interaction of incoming gamma photons with the material causes the formation of scintillation light in the visible spectrum. These weak light sparks generated in the scintillator are transmitted to the Hamamatsu R7525HA-1 photomultiplier tube via an optical guide and converted into electrical signals within the tube. To ensure that the scintillation light produced in the scintillator is transmitted to the photomultiplier tube with minimal loss, an EJ-560 model optical pad was placed between the tube and the light guide. The selection of this photomultiplier tube also considered the optical performance studies reported in the literature. During characterisation tests examining the optical performance of plastic scintillators, a Hamamatsu R7525 series photomultiplier tube was used, and it was demonstrated that this tube's quantum efficiency reaches a maximum peak at a wavelength of approximately 420 nm [7]. Measurements carried out using various radioactive isotope sources, including Cs-137, confirm that the plastic scintillator–PMT system, when integrated, provides a reliable and safe detection approach for gamma-ray counting applications. In this respect, the detector configuration used here differs from the NaI(Tl) detector configuration commonly found in the literature. This is one of the factors that sets this study apart from the literature.

ISBN NR.: 978-625-8795-56-1

A detailed view of the optical connection between the photomultiplier tube and the light guide used in the measurements is shown in Figure 1, whilst the physical setup of the system comprising the BC-400 scintillator, light guide and photomultiplier tube is shown in Figure 2.



Figure 1: A detailed view of the connection between the Hamamatsu R7525HA-1 photomultiplier tube and the light guide via the optical pad.

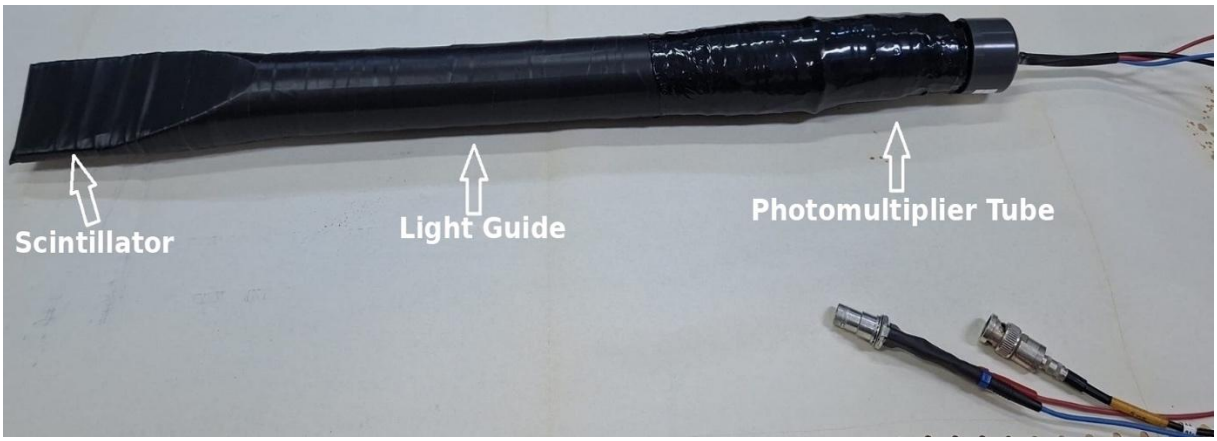


Figure 2: An overview of the detector system comprising the BC-400 plastic scintillator and Hamamatsu R7525HA-1 photomultiplier tube components, integrated via a light guide.

During signal processing, the raw signals obtained from the detector were shaped and amplified using an Ortec Model 485 unit. To control any fluctuations in signal quality at the amplifier output, the system was regularly monitored throughout the measurement using a GW

ISBN NR.: 978-625-8795-56-1

Instek GDS-2204 digital oscilloscope. During the data collection process, the signals received from the amplifier were also recorded using an Ortec Model 775 counter. The duration of each measurement taken during the experiment was controlled using an Ortec Model 719 timer. In this study, the pulses generated in the detector during the measurements were not separated into distinct groups according to their energy levels, nor was any specific filtering applied to select only pulses corresponding to a particular energy band. Instead, the system recorded the total counts generated by the pulses detectable in the detector system over the specified measurement period. The study focuses on the physical investigation of the attenuation profiles of gamma rays in lead and aluminium as the absorber thickness is gradually increased, examining the response as a function of thickness. With this setup, measurements carried out at different absorber thicknesses were compared under the same detector, the same electronic system and the same measurement conditions. A schematic diagram of the detector and the electronic signal processing circuit used is shown in Figure 3.

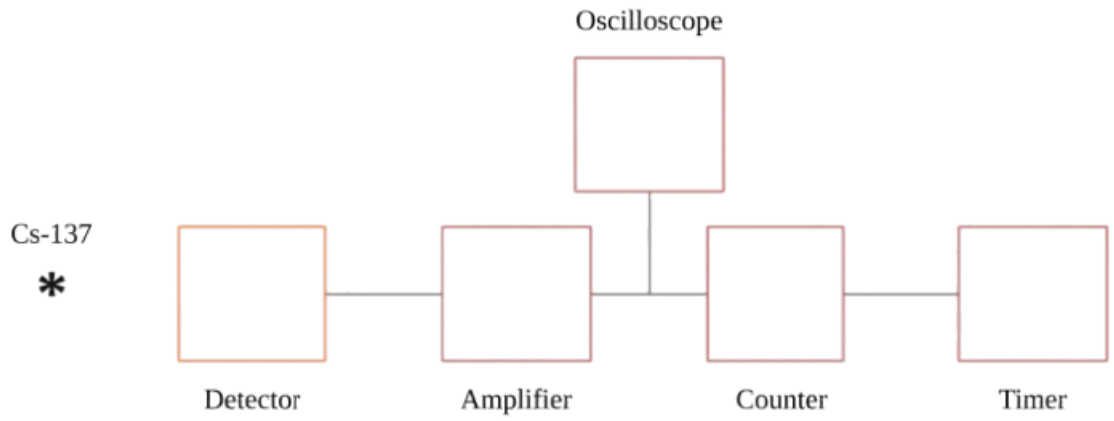


Figure 3: A schematic diagram of the detector and electronic signal processing circuit used in the experiment.

In the design of the experimental setup, no collimator component was used to restrict the gamma radiation between the source and the detector to a narrow region. Therefore, the measurements were carried out using a wide-beam geometry. Due to the absence of a collimator, it was not possible to prevent photons that had scattered and changed direction within the absorbing material from reaching the detector. Some of these scattered photons may reach the detector's active volume, generating a signal in the system and contributing to the total count measured. As a result, the transmission value recorded in the system under wide-beam geometry includes not only the contribution of primary photons passing through the material without undergoing any interaction, but also that of scattered photons. For this reason, the linear attenuation coefficient determined from the experimental data obtained in this study has been defined as the effective linear attenuation coefficient μ_{eff}, which includes all the effects of the counting system and the wide-beam geometry used.

ISBN NR.: 978-625-8795-56-1

2.2. Measurement Procedure

For both absorber materials, the starting point for the measurement stages was selected as the x=0 condition, where no material is present between the source and the detector. Following the recording of this initial count, the lead and aluminium plates were placed in the system in separate, independent measurement series. Transmission measurements were then carried out whilst increasing the total absorber material thickness in regular increments of 0.1 cm until a thickness of 1.0 cm was reached. As the target thicknesses were reached, standard lead absorber plates, each 0.1 cm thick, were gradually stacked on top of one another. To ensure the reliability of the data and minimise errors, care was taken to ensure that the absorber plates completely covered the detector's active surface, and that the alignment of the source, absorber and detector was checked to maintain the measurement geometry as closely as possible.

During the data collection process, the duration of each measurement was set at 60 seconds for each increase in the absorber thickness of the setup. Three independent count measurements were carried out at the same thickness step. The primary reason for repeating measurements at the same thickness is the statistical nature of radioactive decay. However, even when the same experimental conditions are applied, the successive count values recorded by the detector may differ from one another. Therefore, rather than using a single measurement value, three different count values were recorded for each thickness increment; by recording the average of these three counts, the aim was to obtain more reliable data from the relevant measurements. Counts were taken every 60 seconds until the total thicknesses of both absorbent materials reached 1.0 cm. This enabled the comparison of count values obtained for different materials and absorbent thicknesses under the same conditions. For each absorber, the change in count rate in relation to the increase in thickness was examined at the same time intervals.

Following a procedure independent of the transmission measurements, the Cs-137 source was completely removed from the experimental setup, and six separate background measurements were taken over the same period whilst maintaining the same operating conditions for the detector and the electronic system. Rather than relying on a single background measurement, six repeated measurements were taken with the aim of limiting the effect of statistical fluctuations that might arise in background counts over time and of increasing the accuracy of the reference value. The reference background count was determined by taking the arithmetic mean of the six background counts obtained. During the data analysis stage, this value was subtracted from the average total count values obtained for each absorber thickness to determine the net count values. Thus, by applying this background subtraction process, the measurement system was isolated from environmental influences in the absence of a Cs-137 source, and corrections were made for the attenuation characteristics with respect to Cs-137 photons.

Throughout the transmission measurements carried out for lead and aluminium, all environmental and system parameters that could cause variations in the experimental results

ISBN NR.: 978-625-8795-56-1

were kept constant; only the type of absorbing material and the thickness of the absorber were kept constant as independent variables. Throughout the data collection period, the same Cs-137 source, the same BC-400 plastic scintillator, light guide, PMT detector system and the same electronic signal processing chain were used. Whilst the absorber thickness was varied, the 4 cm distance between the source and the front face of the absorber material—the surface first exposed to radiation—was maintained during the measurement stages. In this way, an attempt was made to eliminate any errors arising from the system that might affect the relationship between the attenuation behaviour observed in subsequent data analyses and the type of absorber material and total absorber thickness.

2.3. Data Analysis and Determination of the Effective Linear Attenuation Coefficient

As the first step in the analysis of the experimental data, the arithmetic mean N_{avg} of the total count values obtained from three replicate and independent measurements carried out for each absorber thickness step was calculated. The average background count B_{avg} was determined by taking the arithmetic mean of the total counts obtained from the recorded background measurements. The background count B_{avg} taken as a reference from the average total counts recorded for each increase in absorber thickness, was excluded. From this, the net count value for the corrected background, to be used directly in the attenuation analysis, can be found using equation (1):

$$N_{net}(x) = N_{avg}(x) - B_{avg} \quad (1)$$

In this equation, the variable $N_{net}(x)$ defines the net count value obtained by subtracting the average background count from the average total count for an absorber of thickness x. The background correction process has also been applied to the counts obtained under the initial condition where no absorber material is present in the environment (x=0); thus, the initial net count value to be used as a reference throughout the analysis is denoted as $N_{net}(0)$.

As a result of the quantitative analysis of the change observed in the net count data with an increase in the thickness of the absorbing material, the Beer–Lambert law, which describes the exponential attenuation behaviour of gamma photons within matter, was taken as the basis. In this study, as the counts were taken at standard 60-second intervals, the net count values recorded by the system can be treated solely as physical quantities proportional to the radiation intensity. By isolating the time parameter, the Beer–Lambert law was fitted to the measured experimental count data as follows:

$$N_{net}(x) = N_{net}(0)e^{-\mu x} \quad (2)$$

The parameter Nnet(0) represents the background-corrected initial net count obtained in the absence of the absorber (x = 0); the quantity Nnet(x) represents the background-corrected net count obtained for an absorber material of thickness x.

ISBN NR.: 978-625-8795-56-1

The μ in the equation represents the effective linear attenuation coefficient (μ_{eff}) determined from experimental measurements under wide-beam geometry. In order to calculate this coefficient from the experimental data, the natural logarithm of both sides of Equation (2) has been taken, and the exponential relation has been transformed into a linear form.:

$$\ln[N_{net}(x)] = \ln[N_{net}(0)] - \mu_{eff}x \tag{3}$$

In this study, using this approach, the $\ln[N_{net}(x)]$ data for both absorbent materials were modelled graphically with respect to the absorbent thickness x. The experimental effective linear attenuation coefficient was determined as follows, using the absolute value of the slope of the line obtained from the linear fit applied to the data as a reference:

$$\mu_{eff} = -m \tag{4}$$

In this equation, the variable m represents the slope of the regression line fitted to the graph of $\ln[N_{net}(x)]=f(x)$. As the thickness of the absorbing material increases, this slope takes on a negative value due to the decrease in the net count. Since the linear attenuation coefficient is a positive scalar quantity, μ_{eff} has been defined as the absolute value of the slope.

In order to determine the accuracy of the experimental data's fit to the Beer–Lambert model, the coefficient of determination R^2 was also calculated. The R^2 value is a dimensionless parameter indicating the degree of fit to the linear model. This value was used to demonstrate the extent to which the system's attenuation behaviour is consistent with the exponential attenuation model employed. Furthermore, a high R^2 value indicates that the system meets the conditions for an ideal narrow beam or that the calculated coefficient approaches the theoretical linear attenuation coefficient.

2.4. Evaluation of Experimental Data

The mass attenuation coefficients were calculated using the effective linear attenuation coefficients previously calculated for aluminium and lead. Whilst the linear attenuation coefficient, which expresses attenuation per unit length, is influenced by the physical density of the material, the mass attenuation coefficient expresses the attenuation behaviour per unit mass. Therefore, the use of the mass attenuation coefficient provides a more appropriate assessment, particularly when comparing the photon attenuation properties of materials with different densities. The mass attenuation coefficient is determined by dividing the effective linear attenuation coefficient by the density of the relevant absorbing material, as follows;

$$\frac{\mu_{eff}}{\rho} = \mu_{\rho} \tag{5}$$

ISBN NR.: 978-625-8795-56-1

Here, μ_{eff} denotes the effective linear attenuation coefficient (cm^{-1}) determined in the wide-beam experimental geometry; ρ denotes the density of the absorbing material (g/cm^3); and μ_ρ denotes the experimental effective mass attenuation coefficient (cm^2/g).

The experimental μ_ρ parameter obtained was compared with the μ_ρ parameter taken from NIST XCOM [8]. NIST is an organisation that sets scientific and technological standards, its full name is the National Institute of Standards and Technology. XCOM, meanwhile, is a photon cross-section database defined by the institute's physics laboratory and widely accepted in the literature. Therefore, the fact that the experimental data obtained are consistent with the NIST XCOM data serves as an objective measure of the data's accuracy and is of great importance.

In order to evaluate the attenuation performance of the lead and aluminium used in the study, half-value thickness (HVL), one-tenth-value thickness (TVL) and mean free path (MFP) parameters were calculated. These parameters were determined using the effective linear attenuation coefficient (μ_{eff}) obtained experimentally from a wide-beam geometry.

The half-value thickness represents the thickness of the absorber required for the initial radiation intensity to be reduced to half. By applying the condition $N_{net}(x)/N_{net}(0)=1/2$ in the Beer-Lambert equation, the HVL was calculated using the equation,

$$HVL = \frac{\ln(2)}{\mu_{eff}} = \frac{0.693}{\mu_{eff}} \tag{6}$$

A lower HVL value indicates that, under the same experimental conditions, a thinner material is sufficient to reduce the initial radiation intensity by half, and therefore that the material exhibits a stronger attenuation behaviour per unit thickness. This definition of HVL is consistent with the standard photon attenuation approach.

Similarly, a thickness of one-tenth represents the thickness of the absorber required to reduce the initial radiation intensity to one-tenth. Applying the condition $N_{net}(x)/N_{net}(0)=1/10$ to the Beer-Lambert equation yields the following equation:

$$TVL = \frac{\ln(10)}{\mu_{eff}} = \frac{2.303}{\mu_{eff}} \tag{7}$$

When HVL and TVL are considered together, they enable a comparison of the physical thicknesses required by different absorber materials to achieve a specific attenuation level. The $\ln(10)/\mu_{eff}$ equation used for TVL is consistent with the standard definition of attenuation.

The mean free path is a characteristic length that defines the average distance travelled by a photon within an absorbing medium before an interaction occurs, in the ideal exponential attenuation model. In this study, however, the MFP has been evaluated as an effective

ISBN NR.: 978-625-8795-56-1

attenuation length using the experimental effective linear attenuation coefficient in a wide-beam geometry. Within the framework of the exponential attenuation model, the MFP is defined as the inverse of the attenuation coefficient as follows:

$$MFP = \frac{1}{\mu_{eff}} \tag{8}$$

A smaller MFP value corresponds to photons encountering interactions over shorter characteristic distances within the material in question. In a standard narrow beam, the value of $1/\mu$ related to the average free path of the photon between interactions.

In this study, the HVL, TVL and MFP values were derived not from the theoretical narrow-beam linear attenuation coefficient, but from the μ_{eff} value determined in the experimental wide-beam geometry. In particular, under wide-beam conditions, the fact that a portion of the photons scattered within the absorber can reach the detector may result in an experimental response that differs from the ideal narrow-beam attenuation; therefore, this distinction must be considered when comparing the results with theoretical reference data.

3. RESULTS

In extensive gamma transmission measurements carried out on lead and aluminium absorbers, it was found that the background-corrected net count values decreased in parallel with an increase in absorber thickness. The attenuation behaviour was measured quantitatively by applying linear regression to the variation in $\ln[N_{net}(x)]$ for both materials, and the effective linear attenuation coefficients μ_{eff} were determined from the slopes of the regression lines. The regression parameters obtained for Pb and Al (Figures 4 and 5) and the shielding parameters determined from the experimental results are summarised below (Table 1).

Table 1: The effective linear attenuation coefficient, mass attenuation coefficient and shielding parameters determined for Pb and Al.

Material	μ_{eff} (cm^{-1})	μ_ρ (cm^2/g)	HVL (cm)	TVL (cm)	MFP (cm)	μ_ρ(XCOM) (cm^2/g)	Relative difference (%) between μ_ρ and μ_ρ(XCOM)
Pb	1.2477	0.1100	0.5556	1.8455	0.8015	0.1101	0.0908
Al	0.2008	0.0744	3.4514	11.4655	4.9794	0.0747	0.4016

ISBN NR.: 978-625-8795-56-1

The data presented in Table 1 show that Pb exhibits a stronger gamma-attenuation behaviour than Al. This difference stems from the differing densities of Pb and Al and their distinct interaction properties with gamma photons. The higher μ_{eff} value obtained for Pb indicates that the attenuation per unit thickness is greater than that of Al. Similarly, the lower HVL and TVL values obtained for Pb indicate that a thinner Pb layer is sufficient to achieve the same level of attenuation as Al. The lower MFP value for Pb, meanwhile, indicates that gamma photons are attenuated over a shorter distance within the material before interacting with it.

The mass attenuation coefficients determined experimentally have shown results similar to the NIST XCOM reference values. The fact that the percentage difference is below the 1% limit for both materials demonstrates that the experimental findings are numerically consistent with the XCOM reference data. However, as the experimental coefficients were determined using a wide-beam geometry without a collimator, it should not be overlooked that a portion of the scattered photons may reach the detector and influence the measured count results. Therefore, when considering the closeness between the experimental data and the XCOM values, the effects of the experimental setup and the contribution of scattered photons must also be included.

Figures 4 and 5 show the count variations as a function of absorber thickness, obtained from the experimental data for Pb and Al.

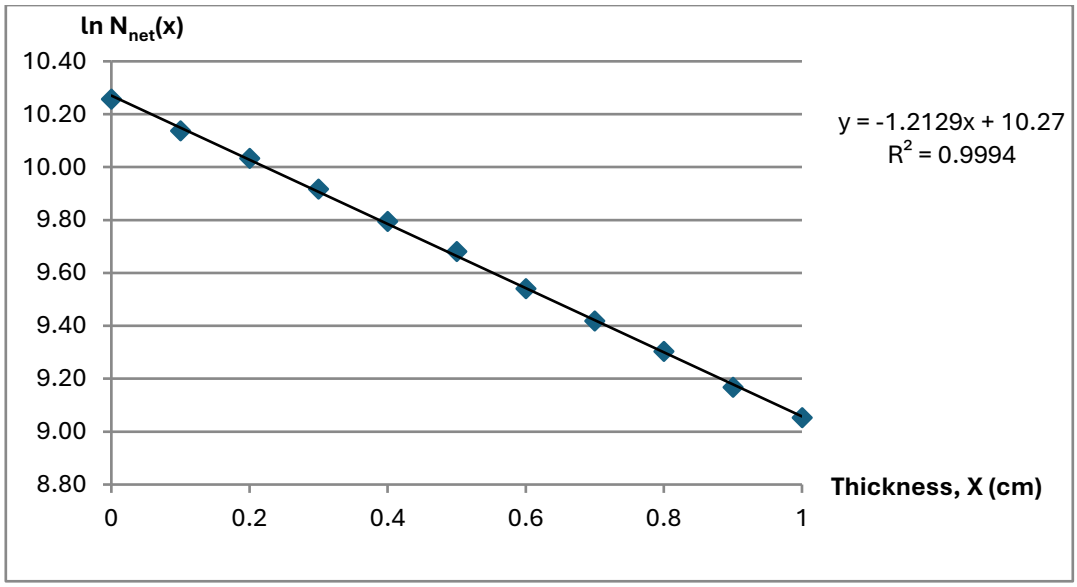


Figure 4: Variation of the ln[$N_{net}(x)$] values for Pb as a function of absorber thickness (x) and linear regression fit.

ISBN NR.: 978-625-8795-56-1

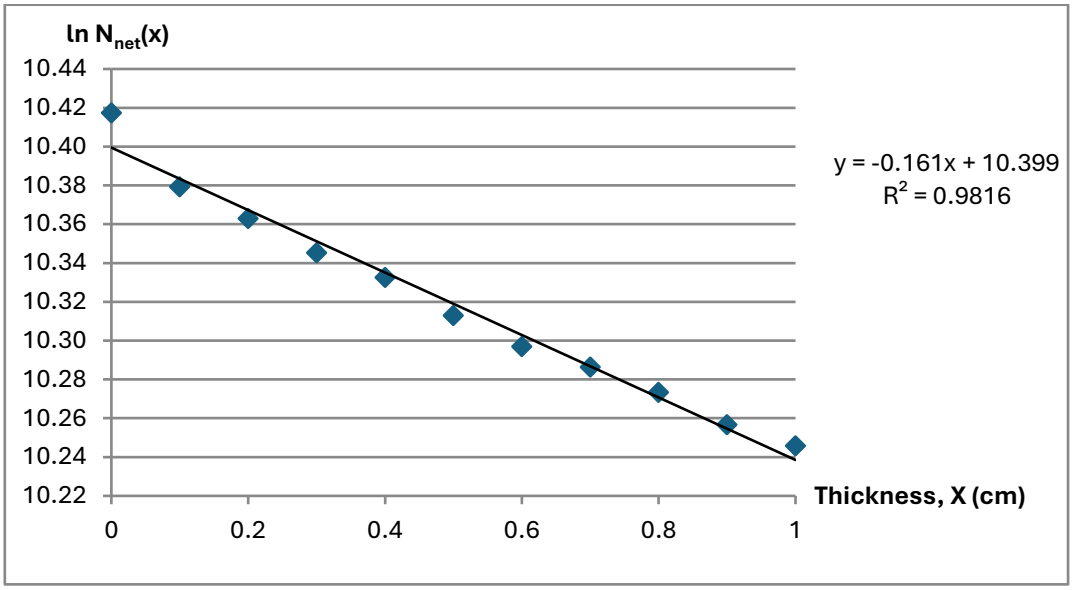


Figure 5: Variation of the ln[Nnet(x)] values for Al as a function of absorber thickness (x) and linear regression fit.

Figure 4 and Figure 5 show that, for both Pb and Al samples, the background-corrected net count values decrease logarithmically with increasing absorber thickness, as expected. In particular, the fact that the R^2 value determined for Pb is very close to 1 indicates that the relationship between the recorded counts and the absorber thicknesses is strongly represented by a linear model, and that the theoretical and experimental results show a high degree of agreement. The fact that this agreement is higher for Pb than for Al is related to the gamma-absorption properties of the materials. Consequently, the fact that scattered photons reach the detector and contribute to the count in the wide-beam geometry used has been assessed as one of the experimental factors contributing to these deviations. This is particularly evident for Al, which explains why the R^2 value is found to be smaller.

When the results obtained for Pb and Al materials are compared, it is clear that the Pb material exhibits a more significant gamma-ray attenuation effect than Al. The linear attenuation coefficients reported in the literature for 662 keV gamma rays show a high degree of agreement with the results obtained in our present study [1]

However, in many transmission studies in the literature, narrow-beam geometry configurations and collimation systems are preferred in order to minimise the detection of scattered photons by the detector. In the present study, however, as no collimator was used, it is likely that a portion of the photons scattered in the absorber layer reached the detector, thereby affecting the measured count results. It is known that in a wide-beam configuration, such scattering components can influence the measured transmission ratio. Thus, expressing the values calculated in this study as μ_{eff} and μ_{ρ} provides a more appropriate assessment that considers the effects arising from the experimental geometry [2]. The findings obtained for Pb and Al materials exhibit a consistent attenuation characteristic when compared with similar

ISBN NR.: 978-625-8795-56-1

studies in the literature. In another study investigating the gamma attenuation capabilities of Pb and Al samples, it was reported that Pb's linear and mass attenuation coefficients were larger than those of Al, whilst its HVL and MFP values were smaller [9]. This result is consistent with the higher attenuation coefficients and lower HVL and MFP values obtained for Pb in our study.

4. DISCUSSION

In this study, the transmission characteristics of Pb and Al absorbers in the presence of gamma photons with an energy of approximately 662 keV were investigated experimentally, and it was found that Pb exhibits a more pronounced attenuation tendency compared to Al. When the effective attenuation parameters obtained were considered together, it was observed that higher linear and mass attenuation coefficients were achieved for Pb, whilst the HVL, TVL and MFP values were lower than those for Al. This result demonstrates that a thinner layer of Pb material is sufficient to achieve an equivalent level of gamma intensity attenuation compared to Al.

It is seen in the literature that the investigation of the gamma-ray attenuation properties of lead and aluminium using a Cs-137 source is not a new phenomenon. The transmission behaviour of aluminium at different thicknesses has also been investigated using scintillation detectors and Cs-137 sources [10]. Similarly, studies in the literature have determined the attenuation coefficients of Al and Pb materials at an energy level of approximately 662 keV using various experimental set-ups [1, 4]. However, the present study does not merely reproduce the known narrow-beam coefficients; it also presents a comparative analysis of the effective gamma-ray attenuation behaviour of Pb and Al under a realistic geometry that accounts for the contribution of scattered photons, using an integrated counting system based on a plastic scintillator, a light guide and a PMT.

Whilst in narrow-beam configurations the collimation system limits the detection of scattered photons by the detector, in a wide-beam configuration some of the photons scattered within the absorber reach the detector and may influence the measured net count values. For this reason, the attenuation factors determined experimentally have been treated as effective parameters that incorporate the results of the experimental geometry and the possible scattering contributions and are expressed as μ_{eff} and μ_{ρ} [2].

As a result of this study, the transmission characteristics of Pb and Al absorbers in response to gamma photons with an energy of approximately 662 keV were experimentally analysed using a BC-400 plastic scintillator–light guide–PMT-based counting system, and the corresponding effective attenuation parameters were determined. Whilst NaI(Tl) is typically used in the literature for gamma attenuation coefficients, the BC-400 type plastic scintillator was used in this study instead. The fact that the gamma attenuation parameters obtained using this scintillator are consistent with the literature, and that results in line with the literature were

ISBN NR.: 978-625-8795-56-1

found using both the wide-beam method and the plastic scintillator, demonstrates the success of this study.

The findings have shown that future studies should compare measurement geometries with and without collimators, using different gamma-ray energies and absorbing materials, and should investigate in greater depth the effects of the experimental setup on the determined attenuation coefficients.

ACKNOWLEDGEMENTS

The authors thank to Prof. Dr Suat ÖZKORUCUKLU for his assistance in procuring the photomultiplier tube and its power supply.

REFERENCES

[1] Quyet, P. D., & Anh, T. T. T. (2025). Determination of the linear attenuation coefficients of aluminum, iron and lead for collimated 661.66 keV gamma rays using TCS-172 gamma scintillation survey meter. *Communications in Physics, 35(4),* 347–354. https://doi.org/10.15625/0868-3166/22766

[2] Knoll, G. F. (2000). *Radiation Detection and Measurement* (3rd ed.). John Wiley & Sons.

[3] Yıldırım, S., Tugrul, A. B., Buyuk, B., & Demir, E. (2016). Gamma attenuation properties of some aluminum alloys. *Acta Physica Polonica A, 129(4*), 813–815. https://doi.org/10.12693/APhysPolA.129.813

[4] Sheela, M., & Eshwarappa, K. M. (2024). Study of linear attenuation coefficient and buildup factor of some metals at 662 keV and 1332 keV. *The Nucleus, 61(2),* 63–68. https://doi.org/10.71330/thenucleus.2024.1396

[5] Akkaş, A., Tugrul, A. B., Buyuk, B., Addemir, A. O., Marsoglu, M., & Agacan, B. (2015). Shielding effect of boron carbide aluminium metal matrix composite against gamma and neutron radiation. *Acta Physica Polonica A, 128(2-B),* B-176–B-180. https://doi.org/10.12693/APhysPolA.128.B-176

ISBN NR.: 978-625-8795-56-1

[6] Wetzel, J., Tiras, E., Bilki, B., Onel, Y., & Winn, D. (2016). Radiation damage and recovery properties of common plastics PEN (polyethylene naphthalate) and PET (polyethylene terephthalate) using a 137Cs gamma ray source up to 1.4 Mrad and 14 Mrad. *Journal of Instrumentation, 11*(8), P08023. https://doi.org/10.1088/1748-0221/11/08/P08023

[7] Öztürk, S., & Akgün, B. (2026). Gadolinium loaded plastic scintillator production for nuclear reactor monitoring. *Nuclear Instruments and Methods in Physics Research Section A: Accelerators, Spectrometers, Detectors and Associated Equipment, 1083,* 171094. https://doi.org/10.1016/j.nima.2025.171094

[8] National Institute of Standards and Technology (NIST), *XCOM: Photon Cross Sections Database*, https://physics.nist.gov/PhysRefData/Xcom/html/xcom1.html (Access date: 28.09.2026)

[9] Elmzainy, A. S. A., Hazawi, A., & Basil, S. S. (2022). Determination of attenuation properties for gamma rays of some commercial materials used radiation shielding. *Journal of Humanitarian and Applied Sciences, 7(13),* 484–492. https://doi.org/10.65137/jhas.v7i13.263

[10] Turgay, M. E., Aras, B., Sezgin, N., & Şengül, M. (2022). Shielding effect of aluminum against Cs-137 source, according to gamma ray transmission technique. *Journal of Engineering Technology and Applied Sciences, 7(2),* 109–113. https://doi.org/10.30931/jetas.1027422

GLOBE 2ND INTERNATIONAL CONFERENCE ON ENGINEERING, ARCHITECTURE, MATHEMATICS and APPLIED SCIENCES
October 1 - 6, 2026 – BARSELONA
ISBN NR.: 978-625-8795-56-1

THE EFFECT OF IMAGE ENHANCEMENT TECHNIQUES ON DEEP LEARNING-BASED CLASSIFICATION PERFORMANCE IN BRAIN TUMOR MRI IMAGES

Asst. Prof. Dr. Olcay PALTA

Bitlis Eren University, Technical Sciences Vocational School, Electronics and Automation
ORCID: 0000-0002-7496-2101 | opalta@beu.edu.tr

Prof. Dr. Hanifi GÜLDEMIR

Firat University, Technology Faculty, Electrical-Electronics Engineering
ORCID: 0000-0003-0491-8348 | hguldemir@firat.edu.tr

Prof. Dr. Musa ÇIBUK

Bitlis Eren University, Engineering-Architecture Faculty, Computer Engineering
ORCID: 0000-0001-9028-2221 | mcibuk@beu.edu.tr

ABSTRACT

Image quality and preprocessing techniques can directly affect the performance of deep learning models in the automatic classification of brain tumors from magnetic resonance imaging (MRI). In this study, the effects of different image enhancement techniques on deep learning-based classification of brain tumor MRI images were comparatively investigated. A four-class dataset consisting of glioma, meningioma, pituitary tumor, and no-tumor images was used. In addition to the original images, CLAHE, gamma correction, histogram equalization, unsharp masking, and adaptive gamma correction were applied. To directly compare the effects of image enhancement methods, the classifier architecture was kept fixed in all experiments, and a transfer learning-based EfficientNet-B0 model was used under identical experimental conditions. Performance was evaluated using accuracy, precision, recall, F1-score, and ROC-AUC metrics. Experimental results showed that adaptive gamma achieved the highest overall performance, with 80.96% accuracy, 85.94% precision, 80.96% recall, 78.38% F1-score, and 95.80% ROC-AUC. Compared with the original images, which achieved 77.16% accuracy and a 73.16% F1-score, adaptive gamma improved these metrics by 3.80 and 5.22 percentage points, respectively. In contrast, unsharp masking reduced classification performance. The findings indicate that selecting an appropriate image enhancement method can improve deep learning-based classification of brain tumor MRI images and that image-adaptive gamma correction is an effective preprocessing approach.

Keywords: Brain tumor, MRI, image enhancement, adaptive gamma, EfficientNet-B0, deep learning

1. INTRODUCTION

Magnetic resonance imaging (MRI) provides high soft tissue contrast and is central to the non-invasive assessment of intracranial lesions. Automated interpretation remains challenging because tumor appearance varies with morphology, location, intensity distribution, acquisition

ISBN NR.: 978-625-8795-56-1

conditions, and surrounding anatomy. Recent four-class brain-tumor studies continue to show that deep neural networks can achieve strong classification performance, while class-level errors remain sensitive to dataset composition and evaluation design [1].

Transfer learning is particularly useful when medical imaging datasets are smaller than general-purpose computer-vision corpora. Rasheed et al. evaluated DenseNet121 for multiclass brain-tumor MRI classification [2], whereas Khan et al. compared AlexNet, MobileNetV2, and GoogleNet under a transfer-learning framework [3]. These studies demonstrate the value of pretrained representations, but classifier choice alone does not eliminate variability introduced before feature extraction.

Preprocessing is therefore an experimental variable rather than a neutral preliminary step. Solak systematically examined increasing preprocessing depth through denoising, contrast enhancement, edge sharpening, gamma correction, and normalization, showing that the composition of the preprocessing pipeline can alter downstream behavior across convolutional and transformer architectures [4]. Hekmat et al. likewise placed contrast enhancement within a brain MRI classification pipeline by combining CLAHE with discrete wavelet transform-based image fusion before deep feature extraction [5].

Whether an enhanced image looks clearer to a human reader is not the point. What matters is whether the transformation keeps, or even sharpens, the information the classifier actually relies on. In MRI this is far from obvious, since local contrast, global intensity distribution and texture can each influence the learned features in different ways.

Work on brain tumors keeps moving toward efficient feature learning and attention. EfficientNet-based classification and segmentation are still widely used [6] [7], and designs such as Ghost-ResNet and hierarchical local attention encoders try to separate similar classes by focusing the network on more informative regions [8] [9]. EfficientNet [10] scales depth, width and input resolution with one compound coefficient, which keeps the model small for the accuracy it delivers.

The question we address is a narrow one. With the classifier held constant, how much does the enhancement method alone change the outcome? We compared six versions of the input: the original images, CLAHE, fixed gamma correction, histogram equalization, unsharp masking and adaptive gamma correction. Each was classified by the same EfficientNet-B0 model. Since nothing else varies, a difference in the scores comes from the input.

Accuracy alone can hide class-specific failures, especially when one class is much harder than the rest, so we also report precision, recall, F1-score and ROC-AUC, together with confusion matrices and class-wise ROC curves. Adaptive gamma gave the best overall test result, but glioma remained the main source of error. For this reason we treat enhancement here as something that changes what the feature extractor receives, rather than as a cosmetic step.

ISBN NR.: 978-625-8795-56-1

2. MATERIALS AND METHODS

2.1. Dataset

We used a four-class brain MRI dataset of glioma, meningioma, pituitary tumor and no-tumor images. It has 3,264 images: 2,870 in the original training partition and 394 in a separate test partition (100 glioma, 115 meningioma, 105 no-tumor and 74 pituitary-tumor images). Table 1 gives the class distribution. The no-tumor class has noticeably fewer training images (395) than each of the three tumor classes [11].

Table 1. Distribution of brain MRI images in the dataset.

Class	Training	Testing	Total
Glioma	826	100	926
Meningioma	822	115	937
No tumor	395	105	500
Pituitary tumor	827	74	901
Total	2870	394	3264

2.2. Experimental Design

We split the original training partition into training and validation subsets with a stratified 80/20 split (random seed 42). The supplied test partition played no part in model selection and was used only for the final evaluation. Each enhancement method was applied as a separate input condition, with the classifier and training protocol unchanged, which gave six experiments: Original, CLAHE, Gamma Correction, Histogram Equalization, Unsharp Masking and Adaptive Gamma Correction.

We fixed everything except the input so that differences on the test set could be linked to preprocessing and not to the network. The classifier, data split and training settings were identical in all six runs. This matters because earlier work has already shown that the depth of the preprocessing pipeline alone can shift brain MRI classification results [4].

2.3. Image Enhancement Methods

2.3.1. Contrast Limited Adaptive Histogram Equalization

CLAHE was applied to the luminance component with a clip limit of 2.0 and an 8 × 8 tile grid. Local contrast is raised tile by tile, and clipping the histograms limits how much noise gets amplified. Hekmat et al. [5] used CLAHE in a similar way, as one step of an enhancement and image-fusion pipeline placed before deep feature extraction.

2.3.2. Gamma Correction

Fixed gamma correction used $\gamma = 0.7$ for every image. We wanted to see whether one global brightness adjustment, applied identically everywhere, already gives a measurable gain over the original images.

ISBN NR.: 978-625-8795-56-1

2.3.3. Histogram Equalization

For histogram equalization we worked on the luminance channel, so the color channels were not equalized separately. Intensities are redistributed over the whole image, which makes this the global counterpart of the tile-wise CLAHE above.

2.3.4. Unsharp Masking

Unsharp masking emphasizes high-frequency structure. Each image was smoothed with a Gaussian filter ($\sigma = 2.0$), and the result was combined with the original at weights of 1.5 and -0.5. Stronger edges and finer detail might help EfficientNet-B0; they might equally amplify structure that says nothing about tumor type. This condition was meant to show which of the two happens.

2.3.5. Adaptive Gamma Correction

In adaptive gamma correction the exponent depends on the image. Gamma was computed from the mean grayscale intensity, aiming at a target of 0.5 and restricted to the range [0.5, 2.0], so a dark scan and a bright scan are corrected by different amounts. Fixed gamma cannot do this. We included the method to check whether per-image adjustment copes better with heterogeneous inputs than a single global value.

Table 2 lists the operations and parameters. Each setting was used unchanged within its condition, and the classifier and training protocol stayed the same.

Table 2. Image enhancement settings used in the experiments.

Condition	Implementation
Original	No enhancement; baseline input
CLAHE	Luminance-channel CLAHE; clip limit 2.0; tile grid 8 × 8
Gamma correction	Fixed $\gamma = 0.7$
Histogram equalization	Equalization of luminance component
Unsharp masking	Gaussian $\sigma = 2.0$; weighted combination 1.5 × image − 0.5 × blurred image
Adaptive gamma	Image-dependent gamma from mean grayscale intensity; target 0.5; γ clipped to [0.5, 2.0]

2.4. EfficientNet-B0 and Transfer Learning

EfficientNet-B0 was the common classifier for all six conditions. The EfficientNet family scales depth, width and input resolution together instead of enlarging only one of them [10]. The small B0 baseline suits a study like this one, where the classifier has to stay the same across experiments.

The network started from pretrained ImageNet weights, and its last layer was replaced with a four-class output. EfficientNet variants are still common in recent brain-tumor classification and combined classification–segmentation work [6] [7], which is a further reason to use this family here.

ISBN NR.: 978-625-8795-56-1

2.5. Training Protocol

All images were resized to 224 × 224 pixels and normalized using ImageNet statistics. Training-time augmentation consisted of random horizontal flipping with probability 0.5 and random rotation up to 10°. A batch size of 32 was used. Optimization was performed with AdamW using an initial learning rate of 1×10^{-4} and weight decay of 1×10^{-4}. Training was limited to 30 epochs, with early stopping patience of five epochs. ReduceLROnPlateau reduced the learning rate by a factor of 0.5 after two epochs without validation improvement. The same protocol was used for every preprocessing condition.

The common training configuration is given in Table 3. An input size of 224 × 224 pixels, a batch size of 32, and an initial learning rate of 1×10^{-4} were retained for every enhancement condition to preserve experimental comparability.

Table 3. Common training configuration.

Parameter	Value
Architecture	EfficientNet-B0
Initialization	Pretrained ImageNet weights
Input size	224 × 224
Classes	4
Batch size	32
Maximum epochs	30
Optimizer	AdamW
Initial learning rate	1×10^{-4}
Weight decay	1×10^{-4}
Train/validation split	80/20, stratified, seed 42
Augmentation	Horizontal flip (p = 0.5), rotation ±10°
Early stopping	Patience = 5
Learning-rate scheduler	ReduceLROnPlateau, factor = 0.5, patience = 2

2.6. Evaluation Metrics

Final performance was calculated on the 394-image test partition. Accuracy measures the proportion of correct predictions, whereas precision and recall characterize prediction quality from complementary perspectives. The F1-score provides a harmonic balance between precision and recall. For multiclass discrimination, ROC-AUC was computed using a one-vs-rest strategy with weighted aggregation. We also kept the confusion matrices and class-wise ROC curves, since aggregate scores do not show which tumor classes produce the errors.

ISBN NR.: 978-625-8795-56-1

3. RESULTS

3.1. Overall Classification Performance

Table 4 compares the six input conditions on the test set. Adaptive gamma had the highest value on all five aggregate metrics, and unsharp masking had the lowest accuracy and F1-score.

Table 4. Overall test performance of the six input conditions (%).

Method	Accuracy	Precision	Recall	F1	ROC-AUC
Original	77.16	83.50	77.16	73.16	94.59
CLAHE	77.92	83.95	77.92	75.15	93.78
Gamma Correction	77.16	81.43	77.16	73.59	95.27
Histogram Equalization	77.41	81.38	77.41	73.91	94.12
Unsharp Masking	76.40	82.75	76.40	72.26	93.70
Adaptive Gamma	80.96	85.94	80.96	78.38	95.80

The enhancement methods did not affect the classifier in the same way. Adaptive gamma was the only condition to reach the highest value on every metric: 80.96% accuracy, 85.94% precision, 80.96% recall, 78.38% F1-score and 95.80% ROC-AUC. Compared with the original images, accuracy rose by 3.81 percentage points and F1-score by 5.22 points. F1 improving more than accuracy suggests that the gain is not just a larger number of correct predictions overall.

CLAHE gave a small accuracy gain (77.16% to 77.92%) and raised F1 from 73.16% to 75.15%, but ROC-AUC fell from 94.59% to 93.78%. Fixed gamma left accuracy at 77.16% and pushed ROC-AUC up to 95.27%. Histogram equalization changed accuracy and F1 only slightly, and unsharp masking lowered both. A method that makes images look better is therefore not guaranteed to help the classifier.

The magnitude and direction of change relative to the original-image baseline are shown in Table 5. Adaptive gamma increased accuracy by 3.81 percentage points and F1-score by 5.22 points; by contrast, the modest accuracy gain obtained with CLAHE was accompanied by a reduction in ROC-AUC.

ISBN NR.: 978-625-8795-56-1

Table 5. Change relative to the original-image baseline (percentage points).

Method	Accuracy	F1	ROC-AUC
CLAHE	+0.76	+1.99	−0.81
Gamma Correction	+0.00	+0.44	+0.68
Histogram Equalization	+0.25	+0.76	−0.47
Unsharp Masking	−0.76	−0.89	−0.90
Adaptive Gamma	+3.81	+5.22	+1.21

3.2. Class-Specific Error Patterns

Class-wise recall values derived from the confusion matrices are presented in Table 6. Glioma was the weakest class under every condition, although its recall increased from 25.00% with the original images to 35.00% with adaptive gamma.

Table 6. Class-wise recall derived from the confusion matrices (%).

Method	Glioma	Meningioma	No tumor	Pituitary
Original	25.00	100.00	100.00	79.73
CLAHE	33.00	98.26	100.00	75.68
Gamma	26.00	98.26	97.14	85.14
Histogram Equalization	27.00	97.39	97.14	86.49
Unsharp	24.00	97.39	100.00	81.08
Adaptive Gamma	35.00	99.13	100.00	87.84

Glioma was the dominant source of error under every condition. Baseline recall was only 25.00%; CLAHE raised it to 33.00% and adaptive gamma to 35.00%, the best value we obtained. Even so, with adaptive gamma 46 of the 100 glioma images were still labelled meningioma and 19 no tumor. The main limitation of the model clearly sits in this class.

Meningioma and no-tumor images were much easier. With adaptive gamma, 114 of 115 meningioma images and all 105 no-tumor images were classified correctly, and pituitary recall rose from 79.73% (original) to 87.84%. So the overall gain came from better glioma and pituitary recognition, while the already strong results for meningioma and no-tumor were kept.

Other studies point the same way: the tumor classes rarely contribute equally to the error. On the same 3,264-image dataset, for instance, lower category-wise performance was reported for glioma than for no-tumor images despite high overall accuracy [3]. We would not compare numbers directly, since architectures and protocols differ, but glioma's recurring difficulty is a good reason to look at class-level results.

3.3. ROC Analysis

ROC-AUC stayed high in all six experiments, between 93.70% and 95.80%, but its ranking did not match the accuracy ranking. Fixed gamma shows this most clearly: accuracy was identical

ISBN NR.: 978-625-8795-56-1

to the baseline, yet ROC-AUC went up by 0.68 percentage points. CLAHE did the opposite, improving accuracy and F1 while AUC dropped. Preprocessing evidently affected probability ranking and final class decisions in different ways.

For adaptive gamma, the class-wise AUC values were 0.9098 for glioma, 0.9806 for meningioma, 0.9783 for no tumor and 0.9589 for pituitary tumor. Glioma has the weakest curve again, matching what the confusion matrix shows. A high overall AUC can hide this: the four classes are not equally well separated.

Figure 1 shows the baseline. Of the 100 glioma images only 25 were correct, with 48 sent to meningioma, 24 to no tumor and three to pituitary tumor. Every meningioma and no-tumor image was classified correctly, and so were 59 of 74 pituitary images. Good probability-level separation in the ROC curves does not remove these glioma errors, so the two plots need to be read side by side.

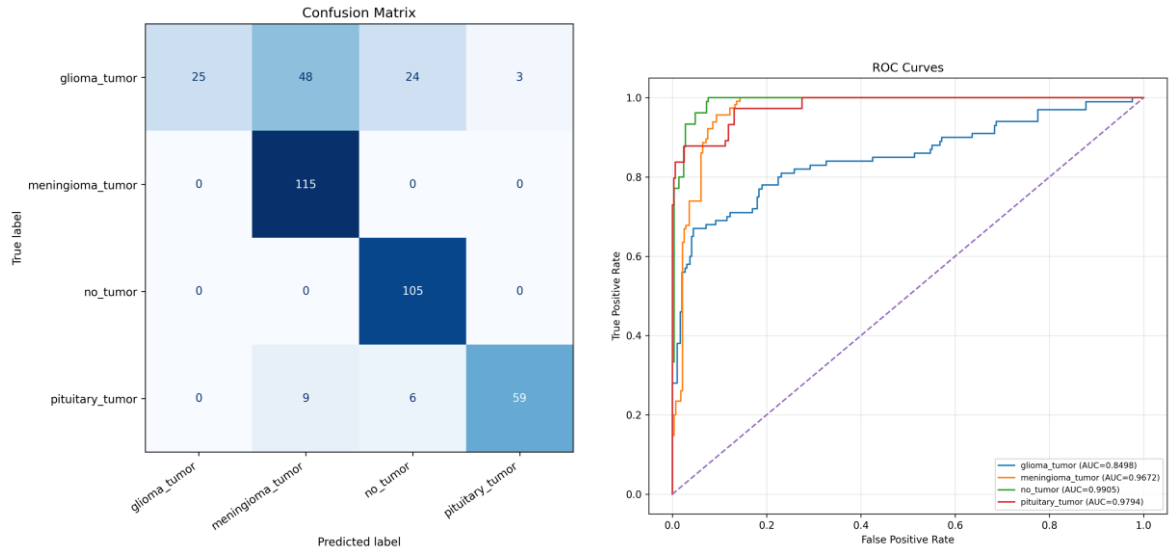


Figure 1. Original images. Confusion matrix (left), class-wise ROC curves (right).

Figure 2 shows CLAHE. Glioma gained eight correct predictions (25 to 33), yet 46 glioma images were still called meningioma. Meningioma and no-tumor stayed strong, while pituitary fell to 56 correct out of 74. A rise in F1 together with a fall in ROC-AUC fits this picture.

ISBN NR.: 978-625-8795-56-1

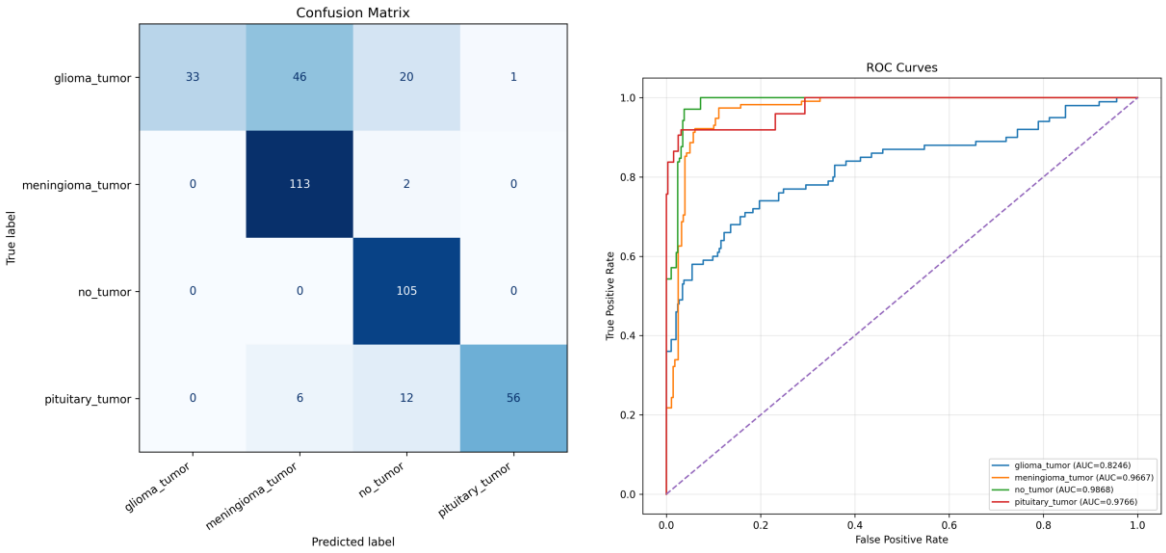


Figure 2. CLAHE. Confusion matrix (left), class-wise ROC curves (right).

Figure 3 shows fixed gamma. Glioma remained hard: only 26 of 100 images were correct and 55 were predicted as meningioma. Pituitary recognition improved to 63 of 74, but overall accuracy equals that of the original images. The higher ROC-AUC therefore reflects better probability ranking, not more correct test predictions.

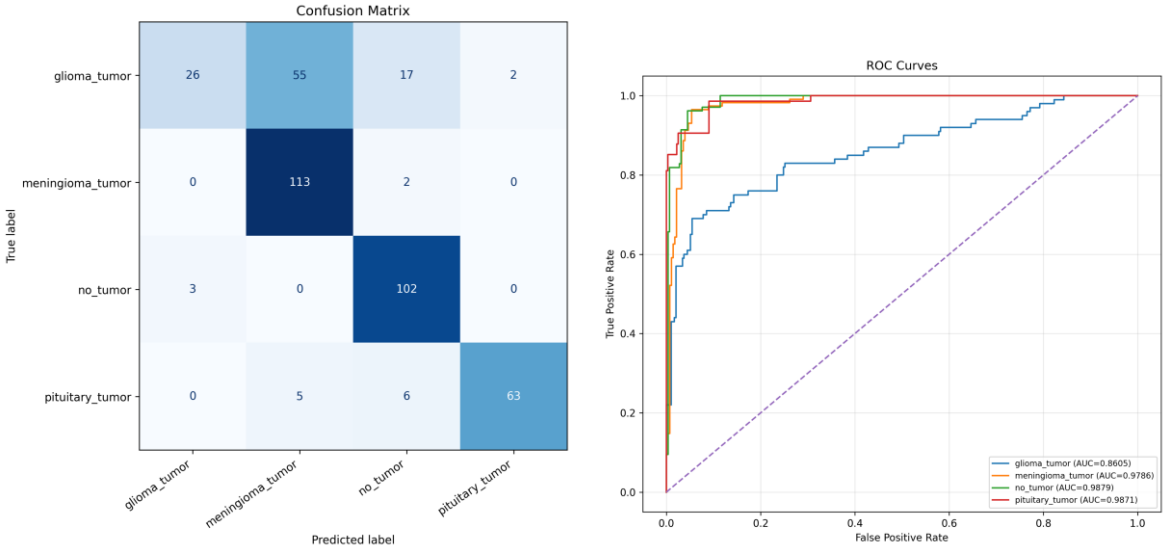


Figure 3. Fixed gamma correction. Confusion matrix (left), class-wise ROC curves (right).

The class-level effect of histogram equalization is visible in Figure 4. Of the 100 glioma images, 27 were classified correctly, 50 were assigned to meningioma, 22 to no tumor, and one to pituitary tumor. By contrast, 64 of 74 pituitary images were correctly identified. The ROC

ISBN NR.: 978-625-8795-56-1

curves indicate useful probability-level separation, but the confusion matrix shows that this separation did not translate into equally strong hard decisions for glioma.

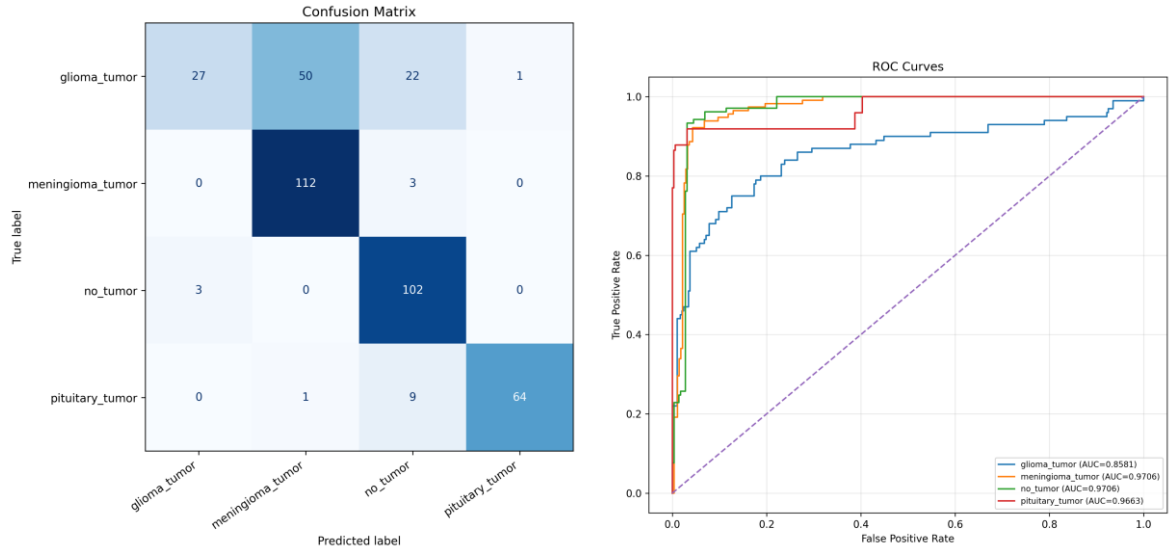


Figure 4. Histogram Equalization: confusion matrix (left) and class-wise ROC curves (right).

Figure 5 presents the results obtained with unsharp masking. Correct glioma predictions decreased to 24, while 45 images were assigned to meningioma and 28 to no tumor. Together with the reductions in overall accuracy and F1-score, this distribution indicates that stronger edge emphasis did not produce a more discriminative representation for this dataset.

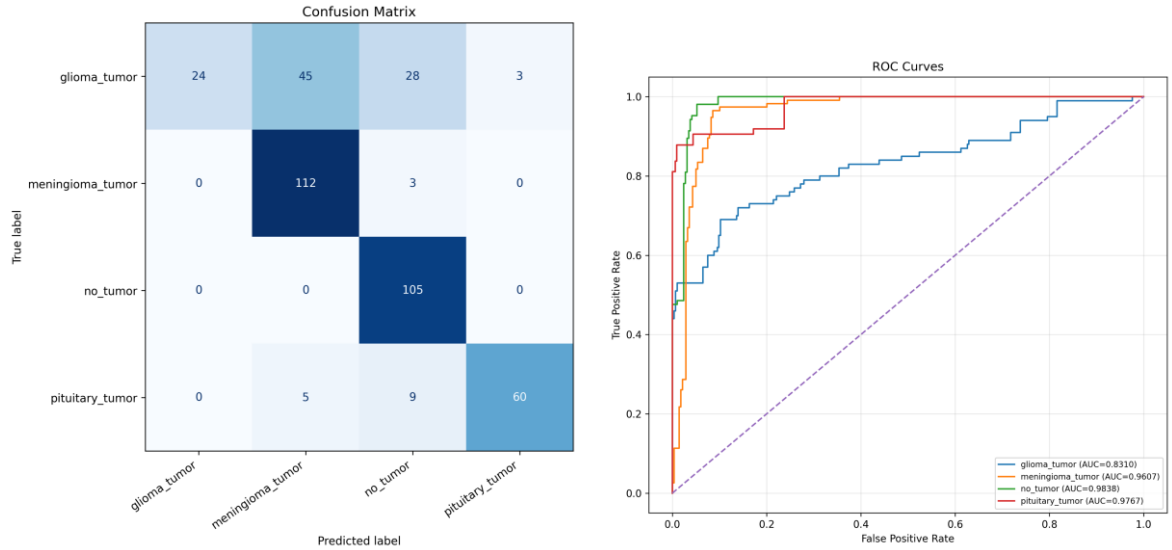


Figure 5. Unsharp Masking: confusion matrix (left) and class-wise ROC curves (right).

The adaptive-gamma confusion matrix and ROC curves are presented in Figure 6. Thirty-five of 100 glioma images were classified correctly, while 46 were assigned to meningioma and 19 to no tumor. Correct predictions reached 114/115 for meningioma, 105/105 for no tumor, and 65/74 for pituitary tumor. Class-wise AUC values were 0.9098, 0.9806, 0.9783, and 0.9589 for

ISBN NR.: 978-625-8795-56-1

glioma, meningioma, no tumor, and pituitary tumor, respectively. Thus, the best aggregate performance was achieved without eliminating the main glioma-related limitation.

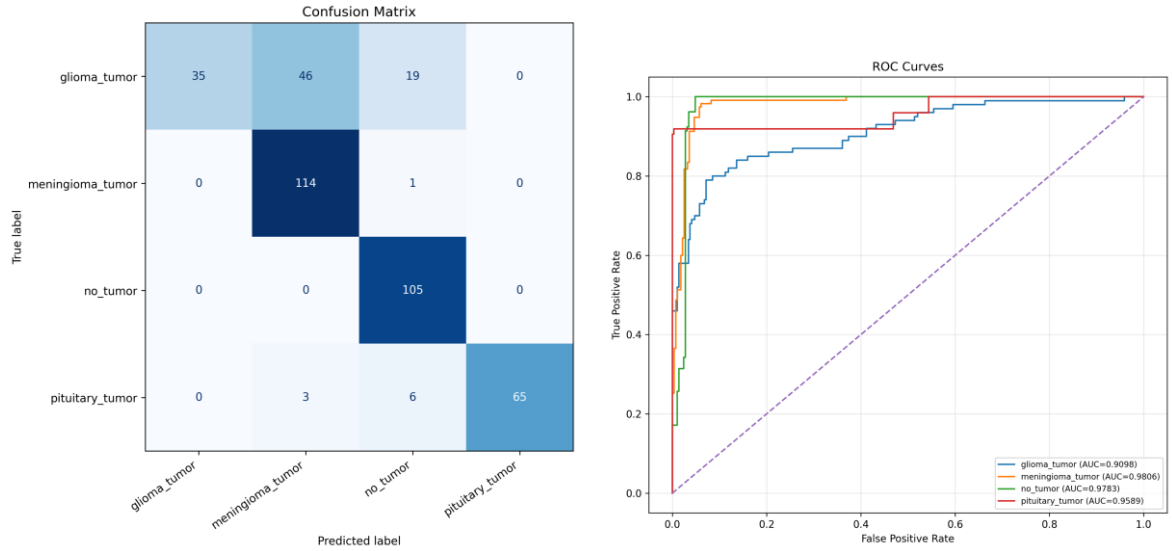


Figure 6. Adaptive Gamma: confusion matrix (left) and class-wise ROC curves (right).

3.4. Training and Validation Behavior

In all six experiments training accuracy rose rapidly to roughly 99–100%, and validation accuracy mostly stayed in the high 90% range. Losses fell steeply at first and then levelled off. Some conditions showed a small gap opening between training and validation loss toward the end, a sign of mild overfitting. Methods were compared on the independent test partition only.

Validation accuracy was high and test accuracy was lower, which is a reason for caution when choosing an enhancement method from training curves. All six conditions seemed to converge without trouble, yet only adaptive gamma gave a clearly better test result. How well a model converges and how well it generalizes are separate questions.

4. DISCUSSION

How much the fixed EfficientNet-B0 classifier changed, and in which direction, depended on the preprocessing method. Adaptive gamma was the most consistent, improving accuracy, precision, recall, F1-score and ROC-AUC together. One possible reason is that brightness varies across the dataset. A fixed mapping treats all images alike, whereas adaptive gamma adjusts its strength to each image's intensity.

This agrees with recent work that treats preprocessing as a factor able to change model behavior. Solak found that different preprocessing depths gave different outcomes in CNN and transformer models [4], and Hekmat et al. placed CLAHE-based enhancement inside an MRI image-fusion framework before classification [5]. Preprocessing should therefore be reported and evaluated as part of the experimental design, not handled as an interchangeable first step.

Our results do not support the idea that stronger contrast or sharper edges automatically help. Unsharp masking gave the lowest accuracy and F1-score. Sharpening can emphasize boundaries, but it can also amplify high-frequency structure unrelated to tumor identity, or change texture cues that the pretrained filters depend on. Histogram equalization changed little,

ISBN NR.: 978-625-8795-56-1

which suggests that for this dataset a global redistribution of intensities works less well than a brightness correction tailored to each image.

CLAHE shows the same dependence on the metric. It improved accuracy and F1-score over the originals but lowered ROC-AUC. This does not make CLAHE a poor choice in general; Hekmat et al. used it inside a wider enhancement and fusion framework [5]. What the result shows is that the effect of a preprocessing method depends on the dataset, the downstream architecture, the parameters and the metric.

The class-level picture matters as much. Adaptive gamma raised glioma recall from 25% to 35%, but glioma stayed far behind the other classes, so preprocessing alone did not resolve the visual overlap behind the main misclassification pattern. Attention mechanisms and local-context modeling have been used on such difficult class boundaries [8] [9]. We deliberately did not add them, because that would have blurred the effect of image enhancement, which is what this experiment is meant to isolate.

Recent brain-tumor studies often report accuracies above 90% [1] [2] [3] [6]. We do not use these as benchmarks for our 80.96%, because datasets, train–test organization, augmentation, preprocessing and model complexity all differ. Our aim is to measure the relative change caused by six input conditions with the classifier and test set held fixed.

Table 7 lists selected recent studies to place our findings in the current MRI classification literature. They deal with preprocessing, transfer learning, EfficientNet-based modeling or attention mechanisms, whereas our experiment isolates preprocessing under a single EfficientNet-B0 classifier.

Table 7. Selected recent studies relevant to MRI brain-tumor classification and preprocessing.

Study	Year	Relevant aspect	Reported setting/result
Hekmat et al.	2025	CLAHE + DWT image fusion; deep feature fusion	Kaggle and Figshare MRI datasets; enhancement integrated before classification
Rasheed et al.	2025	DenseNet121 transfer learning	Multiclass brain-tumor MRI classification; 96.90% average accuracy reported
Khan et al.	2025	Transfer-learning comparison	AlexNet, MobileNetV2, GoogleNet; GoogleNet 99.2% reported
Solak	2026	Progressive preprocessing depth	Denoising, contrast enhancement, sharpening, gamma correction, and normalization across CNN/ViT models
Anand et al.	2026	Four-class brain-tumor classification	Optimized CNN and transfer-learning comparison on a four-class MRI dataset
Alkharaan et al.	2026	EfficientNet-based MRI analysis	EfficientNet classification combined with U-Net++ segmentation
Shatnawi et al.	2026	Efficient attention model	Ghost modules and Efficient Channel Attention for MRI brain-tumor classification

ISBN NR.: 978-625-8795-56-1

Table 7 is meant to position the experiment, not to rank studies. Data and protocols differ too much for the reported accuracies to be compared with our 80.96%. The useful comparison is methodological: preprocessing, transfer learning, EfficientNet-family models and attention mechanisms are all still being studied as separate factors in MRI classification.

5. LIMITATIONS

Several caveats apply. We used one public dataset with its existing train–test split and did no external validation on data from another institution or scanner. The images are 2D rather than complete volumetric examinations, so correlations between slices and patient-level clinical context are not captured. The enhancement settings were fixed in advance, and a broader parameter search might reorder the methods.

Only EfficientNet-B0 was evaluated, and the ranking of the enhancement methods could look different with other architectures. The glioma result is the most serious weakness, and it should be stated plainly instead of being hidden behind aggregate AUC values. Future work could test patient-wise datasets, external validation, lesion-aware processing or class-sensitive learning to reduce this error pattern while keeping the preprocessing comparison controlled.

6. CONCLUSION

We compared five image-enhancement techniques with the original brain MRI images under a fixed EfficientNet-B0 transfer-learning framework. Because the classifier and training protocol did not change, the differences in performance can be attributed to the input transformation. Preprocessing did not affect all metrics or classes in the same way.

Adaptive gamma gave the strongest aggregate result: 80.96% accuracy, 85.94% precision, 80.96% recall, 78.38% F1-score and 95.80% ROC-AUC. Compared with the original images, accuracy rose by 3.80 percentage points and F1-score by 5.22 points. CLAHE gave modest gains in accuracy and F1-score but a lower AUC, fixed gamma raised AUC without changing accuracy, histogram equalization brought only small improvements, and unsharp masking reduced performance. More contrast or sharpness therefore does not necessarily mean better classification.

The class-level analysis adds a qualification. Adaptive gamma lifted correct glioma predictions from 25 to 35, but 46 glioma images were still classified as meningioma and 19 as no tumor. In the same condition 114 of 115 meningioma, all 105 no-tumor and 65 of 74 pituitary images were correct. Glioma remained the main source of error, and the gain was not spread evenly over the classes.

Under our protocol, adaptive gamma was the best preprocessing method on this dataset. That statement holds only for the present data split and the EfficientNet-B0 configuration. External datasets, repeated runs or cross-validation, and class-sensitive strategies for the glioma–meningioma boundary would show how stable the advantage really is.

REFERENCES

[1] V. Anand, A. Khajuria, R. K. Pachauri, and V. Gupta, "Multi-class classification of brain tumors using optimized CNN and transfer learning techniques," Scientific Reports, vol. 16, art. 4709, 2026. doi: 10.1038/s41598-025-34806-6.

[2] M. Rasheed, M. A. Jaffar, A. Akram, J. Rashid, T. A. N. Alshalali, A. Irshad, and N. Sarwar, "Improved brain tumor classification through DenseNet121 based transfer learning," Discover Oncology, vol. 16, art. 1645, 2025. doi: 10.1007/s12672-025-03501-3.

[3] M. A. Khan, M. Z. Hussain, S. Mehmood, M. F. Khan, M. Ahmad, T. Mazhar, T. Shahzad, and M. M. Saeed, "Transfer learning for accurate brain tumor classification in MRI: a step forward in medical diagnostics," Discover Oncology, vol. 16, art. 1040, 2025. doi: 10.1007/s12672-025-02671-4.

[4] F. Z. Solak, "Comprehensive evaluation of preprocessing pipeline depth in deep learning-based brain tumor classification using CNN and vision transformer architectures," Cluster Computing, vol. 29, art. 155, 2026. doi: 10.1007/s10586-026-05999-w.

[5] A. Hekmat, Z. Zhang, S. U. R. Khan, and O. Bilal, "Brain tumor diagnosis redefined: Leveraging image fusion for MRI enhancement classification," Biomedical Signal Processing and Control, vol. 109, art. 108040, 2025. doi: 10.1016/j.bspc.2025.108040.

[6] R. Alkharaan, J. Alobaidi, J. Bakarman, and H. Alshamlan, "Brain Tumor Classification and Segmentation in MR Images Using EfficientNet and U-Net++ Models," Diagnostics, vol. 16, no. 11, art. 1745, 2026. doi: 10.3390/diagnostics16111745.

[7] P. Sambandham, S. Perla, R. Majji, and P. Datta, "Brain tumor classification using hybrid spinal-EfficientNet using MRI images," Journal of Neuroimmunology, vol. 417, art. 578948, 2026. doi: 10.1016/j.jneuroim.2026.578948.

[8] N. Shatnawi, K. M. O. Nahar, R. E. Al Mamlook, A. S. Almuflih, A. M. Al Fatais, S. Alhatamleh, A. Alishwait, and M. Amin, "Efficient attention-based Ghost-ResNet for brain tumor classification in magnetic resonance imaging (MRI)," Frontiers in Neuroscience, vol. 20, art. 1778376, 2026. doi: 10.3389/fnins.2026.1778376.

[9] C. Dong, D. Sun, and B. Luo, "HLAE: Hierarchical Local Attention Encoder for MRI Brain Tumor Image Classification," Cognitive Computation, vol. 17, art. 54, 2025. doi: 10.1007/s12559-025-10419-z.

[10] M. Tan and Q. V. Le, "EfficientNet: Rethinking Model Scaling for Convolutional Neural Networks," Proceedings of the 36th International Conference on Machine Learning, PMLR, vol. 97, pp. 6105–6114, 2019.

[11] Spanhol, F., Oliveira, L. S., Petitjean, C., Heutte, L., A Dataset for Breast Cancer Histopathological Image Classification, IEEE Transactions on Biomedical Engineering (TBME), 63(7):1455-1462, 2016.

GLOBE 2ND INTERNATIONAL CONFERENCE ON ENGINEERING, ARCHITECTURE, MATHEMATICS and APPLIED SCIENCES
October 1 - 6, 2026 – BARSELONA
ISBN NR.: 978-625-8795-56-1

EXPLAINABLE ARTIFICIAL INTELLIGENCE IN BRAIN TUMOR MRI CLASSIFICATION: A COMPARATIVE ANALYSIS BASED ON GRAD-CAM AND GRAD-CAM++

Asst. Prof. Dr. Olcay PALTA
Bitlis Eren University, Technical Sciences Vocational School, Electronics
ORCID: 0000-0002-7496-2101 opalta@beu.edu.tr
Prof. Dr. Musa ÇIBUK
Bitlis Eren University, Engineering-Architecture Faculty, Computer Engineering
ORCID: 0000-0001-9028-2221 mcibuk@beu.edu.tr
Prof. Dr. Hanifi GÜLDEMIR
Firat University, Technology Faculty, Electrical-Electronics Engineering
ORCID: 0000-0003-0491-8348 hguldemir@firat.edu.tr

ABSTRACT

With the increasing use of deep learning methods in automated medical image analysis, the explainability of model decisions has become an important research topic. In this study, Grad-CAM and Grad-CAM++ explainable artificial intelligence methods were comparatively investigated to visually and quantitatively analyze model decisions in brain tumor MRI classification. A total of 394 test images from a four-class dataset consisting of glioma, meningioma, pituitary tumor, and no-tumor images were analyzed. Raw activation maps generated by both methods were evaluated in terms of activation intensity, focus area, entropy, center distance, and spatial similarity between the explanation maps.

Quantitative analysis yielded a mean correlation of 0.9645, a Dice overlap of 0.9296, and a Jaccard overlap of 0.8857 between Grad-CAM and Grad-CAM++. For correctly classified images, the correlation and Dice overlap reached 0.9893 and 0.9515, respectively, whereas these values decreased to 0.8808 and 0.8555 for incorrectly classified images. Differences in the agreement of explanation maps were also observed among the individual classes.

The findings demonstrate that Grad-CAM and Grad-CAM++ generally produce highly similar explanations, while the agreement between their activation maps decreases noticeably in misclassified cases. These results suggest that consistency between explainable artificial intelligence methods may serve as a complementary indicator for examining model decisions and erroneous classifications.

Keywords: Brain tumor, MRI, explainable artificial intelligence, Grad-CAM, Grad-CAM++, activation map

1. INTRODUCTION

High classification performance does not, by itself, explain how a neural network reached a decision. In medical imaging, that gap is important: a predicted label and its confidence score describe the output, but not the image evidence that influenced it [1], [2]. Explanation methods

ISBN NR.: 978-625-8795-56-1

are therefore useful when the aim is to inspect the behavior of a trained model rather than simply report its accuracy.

MRI of brain tumors is a useful test case, because findings that look alike can turn up in different tumor categories. Glioma, meningioma and pituitary tumors usually differ in location and appearance, but single images can still share intensity or shape patterns. Correctness is therefore only part of the question. It also matters whether two explanation methods, given the same prediction, point to the same regions of the image.

Explainability has already been applied to brain MRI in several ways. Mahesh et al. paired Grad-CAM with EfficientNetB0 [3], Islam et al. built explainability into a tumor-detection framework [4], and Sánchez-Moreno et al. combined Grad-CAM++ with Integrated Gradients inside an ensemble model [5]. Others studied Grad-CAM next to LIME [6] or within federated learning [7], and a recent systematic review surveys XAI techniques, applications and challenges in medical imaging more broadly [8]. Most of this work shows selected examples; image-by-image agreement between two CAM methods is not what it reports.

We took a different route and treated the agreement between Grad-CAM and Grad-CAM++ as something to measure on every image of the test set. A handful of convincing heatmaps can mislead. Measuring all 394 pairs lets us ask whether the two methods stay consistent when the classifier is right, when it is wrong, and for each tumor class separately.

The classifier itself was not touched. One stored EfficientNet-B0 model processed all 394 test images, and both CAM methods were computed from exactly the same predictions. No training took place during the XAI analysis.

The comparison used the raw activation arrays. For each map we computed activation magnitude, spatial spread, entropy and distance from the image center; for each pair we computed pixel-wise differences, Pearson correlation and overlap after thresholding. One caveat applies to the Dice and Jaccard values reported below: they measure how much the two CAM maps overlap each other. Without lesion masks they say nothing about how well a tumor is localized.

2. MATERIALS AND METHODS

2.1. Dataset and Test Group

We used the independent test portion of the four-class Brain Tumor Classification (MRI) dataset released by Bhuvaji et al. [9]. The classes were glioma, meningioma, no tumor, and pituitary tumor. Only test images were included in the XAI stage; the training partition was not reused.

There were 394 test images in total: 100 glioma, 115 meningioma, 105 no-tumor, and 74 pituitary-tumor images. Each image was passed through the fixed classifier once. The predicted class was then explained twice, first with Grad-CAM and then with Grad-CAM++, so that the resulting maps formed a paired observation for that image.

The class counts and classification outcomes are given in Table 1. Errors were concentrated in glioma, whereas all meningioma and no-tumor images in the test set were classified correctly.

ISBN NR.: 978-625-8795-56-1

Table 1. Test-set distribution and class-wise classification results.

Class	Test n	Correct	Incorrect	Class accuracy (%)
Glioma	100	25	75	25.00
Meningioma	115	115	0	100.00
No tumor	105	105	0	100.00
Pituitary tumor	74	59	15	79.73
Total	394	304	90	77.16

2.2. Classification Model and Fixed Experimental Setting

The classifier was EfficientNet-B0, using weights saved from an earlier transfer-learning experiment. EfficientNet scales network depth, width, and input resolution jointly [10]. In the present analysis, the architecture and the stored parameters were left unchanged.

Before inference, images were resized to 224×224 pixels and normalized with ImageNet statistics. The network output contained four classes. For both XAI methods, the target convolutional layer was the final feature block, model.features[-1]. Using the same layer was necessary for a direct comparison of the two activation maps.

Explanations were generated for the predicted class, not the true label: in the implementation both methods received ClassifierOutputTarget(predicted_label). This choice matters for the errors. When the network picked the wrong class, the map shows what supported that wrong decision, and not what would have supported the correct one.

2.3. Grad-CAM and Grad-CAM++

Grad-CAM builds a class-specific map by weighting the convolutional feature maps with gradients of the target class score [11]. Being post hoc, it can be applied to a trained network as it is, with no retraining or architectural change.

Grad-CAM++ follows the same general idea but uses a finer weighting of the positive gradients [12]. As a result, the two methods do not have to highlight exactly the same pixels, even when model, image, layer and target class are identical.

All numbers in this paper come from grayscale CAM arrays; color overlays appear only in the visual examples. Before analysis, non-finite values were replaced, each map was rescaled independently to the [0,1] range, and the normalized array was saved.

2.4. Raw CAM Metrics

Table 2 lists the descriptors computed for each CAM map. Some capture how strong the activation is, others how concentrated or dispersed it is. None of them measures lesion localization, because no ground-truth tumor contour was available.

ISBN NR.: 978-625-8795-56-1

Table 2. Metrics computed from the raw activation maps.

Metric	Definition / interpretation
Mean Activation	Mean activation intensity in the normalized CAM matrix.
Std Activation	Standard deviation of activation values.
Focus Area ≥0.50 / ≥0.75	Proportion of pixels above the specified activation threshold.
Mass Area 50% / 75%	Smallest pixel proportion accounting for 50%/75% of total activation mass; a smaller value indicates a more compact focus.
Normalized Entropy	Spatial spread of activation; values closer to 1 indicate a more diffuse distribution.
Center Distance	Distance between the activation center of mass and image center, normalized by the maximum center-to-corner distance.
Pearson r	Linear similarity between intensity patterns in the two CAM matrices.
MAE / MSE	Mean absolute and squared pixel-level differences between the two normalized CAM matrices.
Dice / Jaccard	Spatial overlap between the two active regions obtained with CAM≥0.50.

2.5. Grad-CAM / Grad-CAM++ Similarity

For each image we computed the Pearson correlation between the flattened Grad-CAM and Grad-CAM++ arrays. MAE and MSE, taken from the same normalized arrays, describe the average pixel-wise difference. To look at spatial overlap, both maps were also binarized at a threshold of 0.50.

With A as the set of active Grad-CAM pixels and B as the set of active Grad-CAM++ pixels, Dice is $2|A \cap B|/(|A|+|B|)$ and Jaccard is $|A \cap B|/|A \cup B|$. Both quantify agreement between two explanation maps; neither is a segmentation score against a reference tumor mask.

2.6. Levels of Analysis

Results were summarized at three levels: all 394 images, each true class separately, and correct versus incorrect predictions. We also correlated model confidence with entropy and with Focus Area≥0.50, to see whether a confident prediction goes together with a more concentrated activation pattern.

3. RESULTS

3.1. Verification of Classification Results

We first checked the classification outcome attached to each CAM pair. The model classified 304 of the 394 test images correctly and 90 incorrectly. Accuracy was 0.771574, and weighted precision, recall and F1-score were 0.834963, 0.771574 and 0.731577.

Figure 1 shows how unevenly the errors are spread. Glioma accounts for 75 of the 90 mistakes: 48 images were predicted as meningioma, 24 as no tumor and 3 as pituitary tumor. Meningioma (115/115) and no tumor (105/105) were classified without error, and 59 of 74 pituitary-tumor images were correct.

ISBN NR.: 978-625-8795-56-1

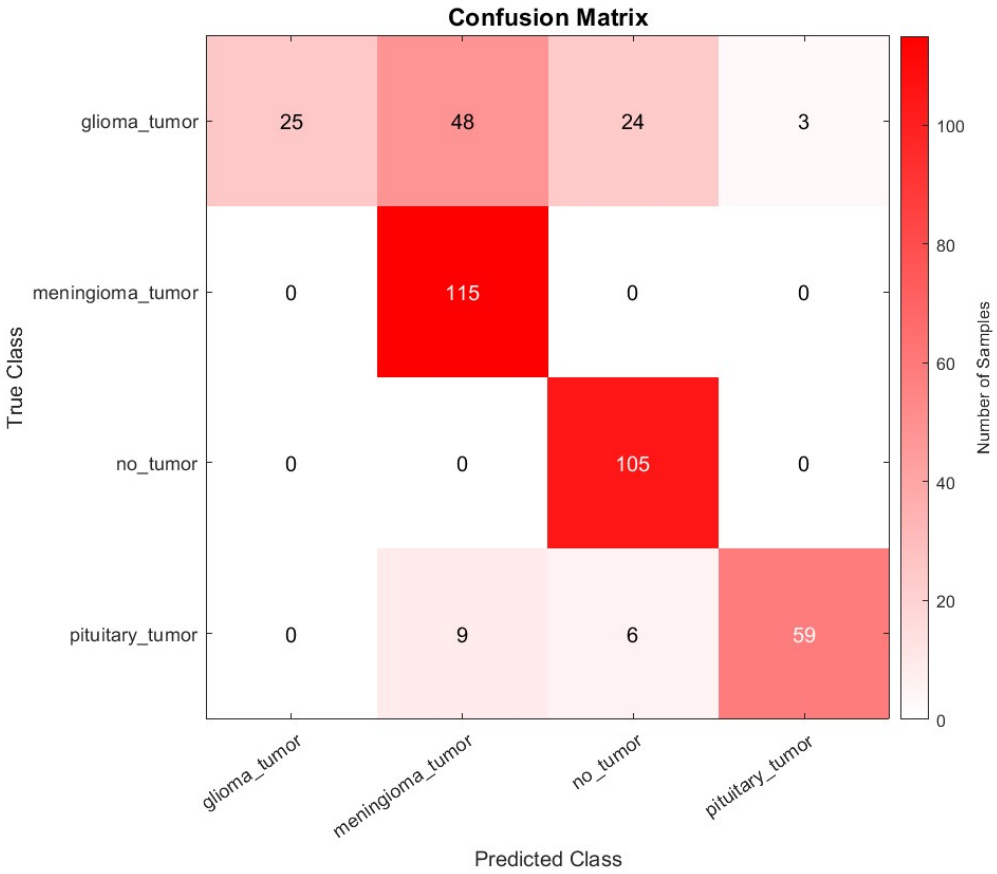


Figure 1. Confusion matrix of the EfficientNet-B0 model on the 394-image test set

3.2. Overall Comparison of Grad-CAM and Grad-CAM++

Table 3 reports the descriptive CAM measurements. Mean activation was slightly higher for Grad-CAM (0.2223) than for Grad-CAM++ (0.2065). The proportion of pixels above 0.50 showed the same direction, 0.1669 versus 0.1579. Both maps were spatially diffuse according to normalized entropy (0.9342 and 0.9266), and their mean center distances were nearly the same (0.1863 and 0.1866).

Table 3. Raw Grad-CAM and Grad-CAM++ metrics across the test set (n=394).

Metric	Grad-CAM Mean	Grad-CAM SD	Grad-CAM++ Mean	Grad-CAM++ SD
Mean Activation	0.2223	0.1097	0.2065	0.1003
Std Activation	0.2290	0.0313	0.2319	0.0328
Focus Area ≥0.50	0.1669	0.1051	0.1579	0.0958
Focus Area ≥0.75	0.0583	0.0397	0.0556	0.0396
Mass Area 50%	0.1600	0.0773	0.1473	0.0688
Mass Area 75%	0.3004	0.1333	0.2755	0.1184
Normalized Entropy	0.9342	0.0365	0.9266	0.0354
Center Distance	0.1863	0.1244	0.1866	0.1234

ISBN NR.: 978-625-8795-56-1

Table 4 gives the direct comparison of the two maps: mean Pearson correlation 0.9645, Dice 0.9296 and Jaccard 0.8857, with mean MAE and MSE of 0.0314 and 0.00485. On average the two methods are close. The correlation SD of 0.1383 shows, though, that individual images vary considerably.

Table 4. Overall similarity between Grad-CAM and Grad-CAM++ maps

Metric	Mean
Pearson correlation	0.9645
Correlation SD	0.1383
MAE	0.0314
MSE	0.00485
Dice (threshold≥0.50)	0.9296
Jaccard (threshold≥0.50)	0.8857

3.3. Class-Wise XAI Behavior

Table 5 shows where agreement is weakest. Glioma has the lowest mean correlation (0.8955), followed by no tumor (0.9755), pituitary tumor (0.9885) and meningioma (0.9989). Dice and Jaccard follow the same ordering.

Table 5. Class-wise classification performance and Grad-CAM/Grad-CAM++ agreement.

Class	n	Accuracy	Confidence	CAM r	Dice	Jaccard
Glioma	100	0.2500	0.8723	0.8955	0.8701	0.8075
Meningioma	115	1.0000	0.9966	0.9989	0.9793	0.9598
No tumor	105	1.0000	0.9803	0.9755	0.9234	0.8742
Pituitary tumor	74	0.7973	0.9644	0.9885	0.9414	0.8926

Figure 2 makes the class difference easy to see. Glioma is the only group with both very low classification accuracy and noticeably lower CAM agreement. This is a descriptive association in these data; it does not show that disagreement between XAI methods is the cause of the classification errors.

ISBN NR.: 978-625-8795-56-1

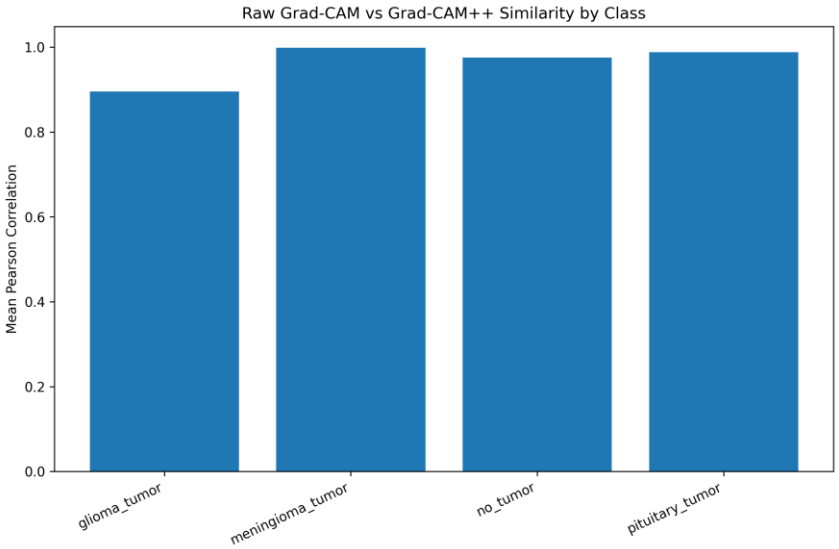


Figure 2. Mean Grad-CAM / Grad-CAM++ Pearson correlation by true class.

The overlap results in Figure 3 tell a similar story. Mean Dice was 0.8701 for glioma and 0.9793 for meningioma, with no tumor at 0.9234 and pituitary tumor at 0.9414. Jaccard followed the same ordering.

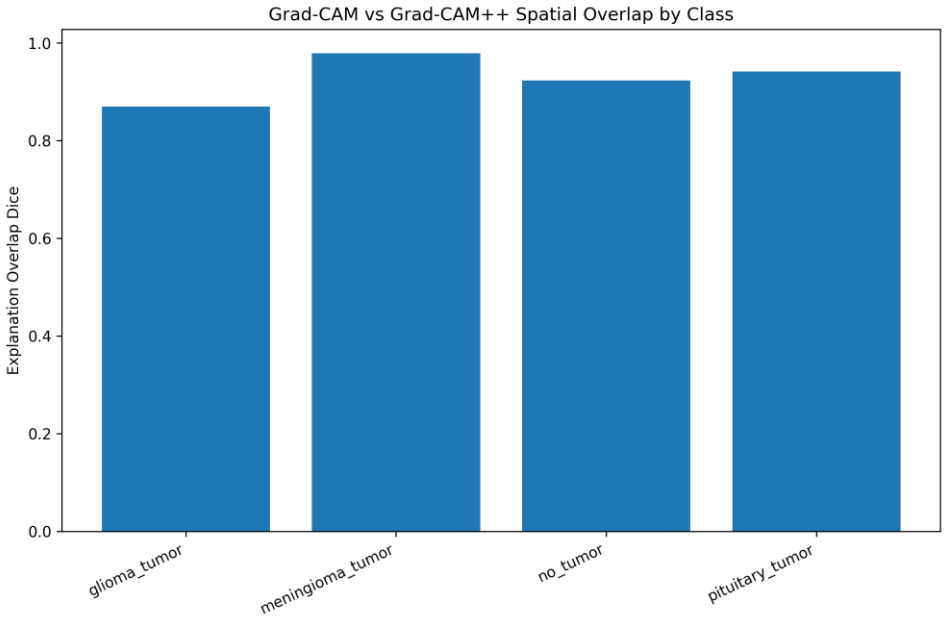


Figure 3. Class-wise Dice overlap between active Grad-CAM and Grad-CAM++ regions (threshold≥0.50).

3.4. Explanation Agreement in Correct and Incorrect Predictions

Table 6 separates correct from incorrect predictions. The 304 correct predictions have a mean confidence of 0.9863, CAM correlation of 0.9893, Dice of 0.9515 and Jaccard of 0.9153; the 90 errors have 0.8476, 0.8808, 0.8555 and 0.7856.

ISBN NR.: 978-625-8795-56-1

Table 6. Confidence and XAI agreement for correct and incorrect predictions

Group	n	Confidence	GC Mean Act.	GCPP Mean Act.	CAM r	Dice	Jaccard
Incorrect	90	0.8476	0.1999	0.1829	0.8808	0.8555	0.7856
Correct	304	0.9863	0.2289	0.2135	0.9893	0.9515	0.9153

Figure 4 shows the difference in mean correlation, but averages hide a lot here. The error group is less consistent overall, yet some wrong predictions came with Grad-CAM and Grad-CAM++ maps that were almost identical. High agreement alone cannot tell us whether the classifier was right.

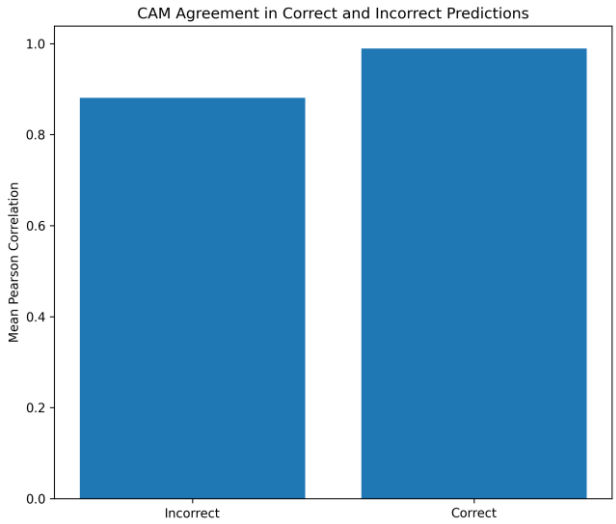


Figure 4. Mean CAM correlation for correct and incorrect predictions.

3.5. Visual Examples and Extreme Cases

A representative correct prediction is shown in Figure 5. The image was classified as meningioma with 99.98% confidence, and the main activated regions in Grad-CAM and Grad-CAM++ largely overlap. This example is consistent with the high average agreement measured in the correct-prediction group.

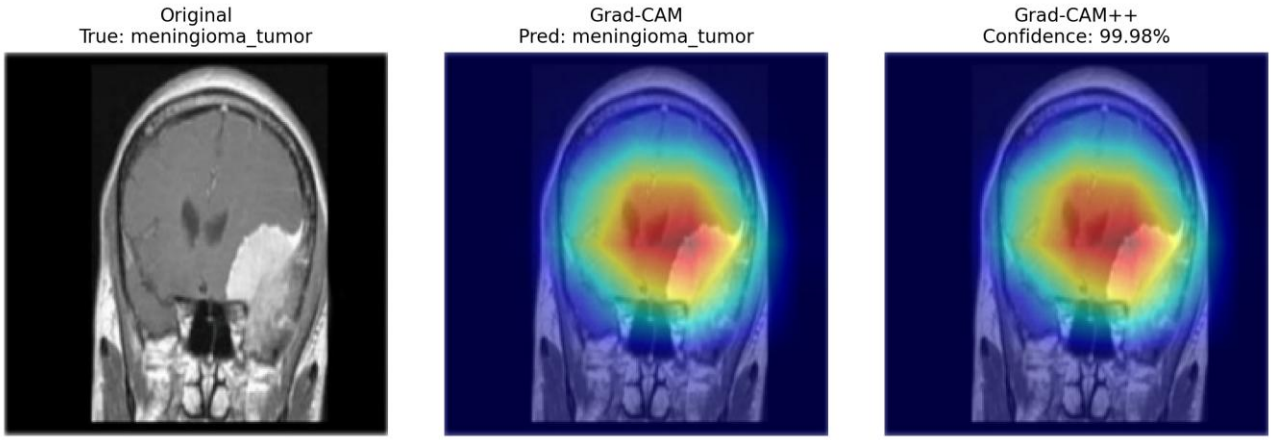


Figure 5. Grad-CAM and Grad-CAM++ explanations for a correctly classified meningioma image.

ISBN NR.: 978-625-8795-56-1

Figure 6 is more informative because the prediction is wrong despite almost perfect agreement between the two XAI methods. A glioma image was classified as meningioma with 99.998% confidence. The correlation between the maps was 0.9998, and the Dice overlap was also very high. The two methods were therefore consistent with each other, but the classifier decision itself was incorrect.

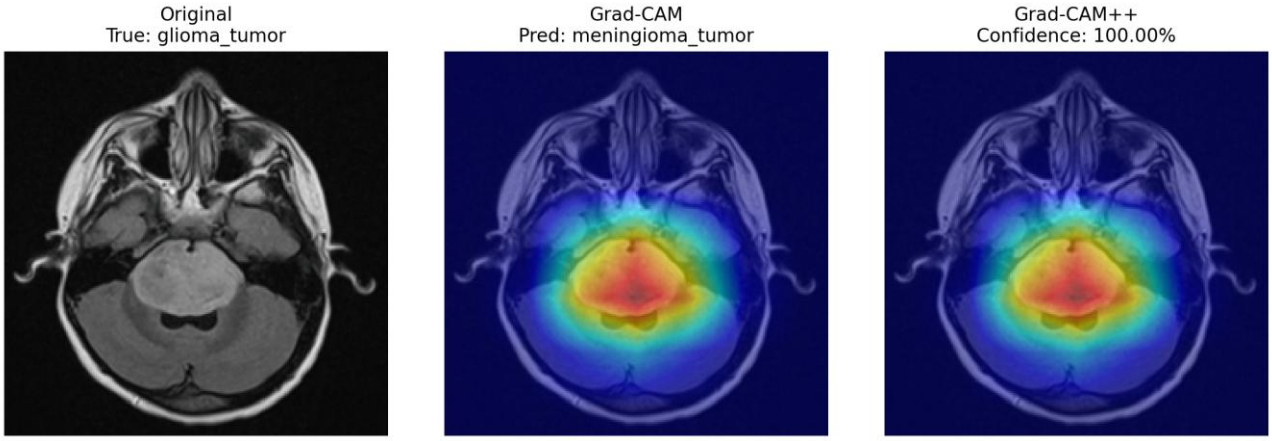


Figure 6. High XAI agreement in a high-confidence glioma→meningioma misclassification.

The case in Figure 7 shows the other extreme. The model assigned a glioma image to the no-tumor class with 56.08% confidence. Here, Grad-CAM and Grad-CAM++ differed sharply: Pearson correlation was -0.5097, Dice was 0.00036, and Jaccard was close to zero. The example shows that two CAM methods can respond very differently even when they explain the same prediction.

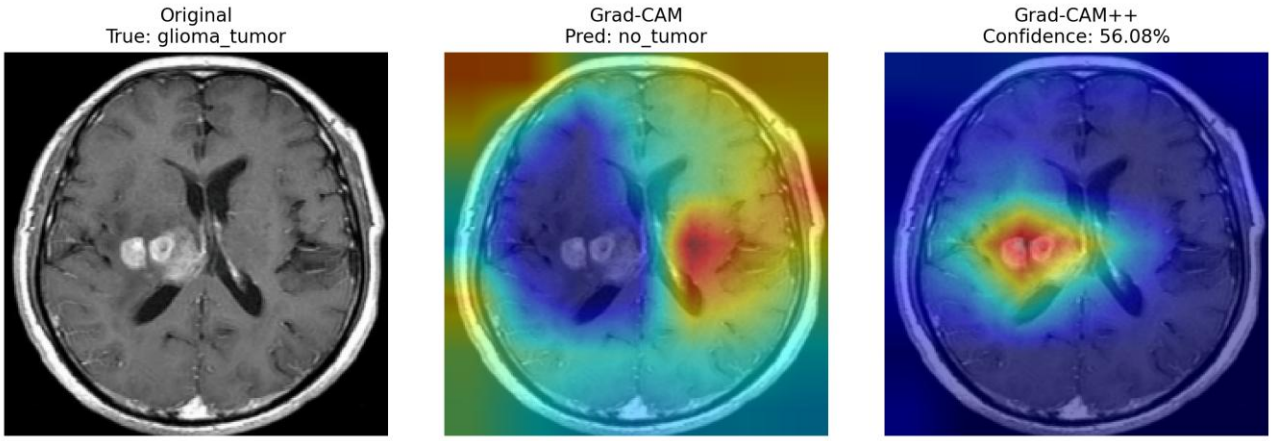


Figure 7. Glioma→no-tumor error with marked divergence between Grad-CAM and Grad-CAM++ maps.

3.6. Relationship Between Model Confidence and XAI Distribution

The confidence analysis produced only weak correlations. Confidence versus entropy was 0.0356 for Grad-CAM and 0.0711 for Grad-CAM++. Confidence versus Focus Area≥0.50 was 0.1383 and 0.1360. In this dataset, a high softmax score was therefore not accompanied consistently by a smaller or less entropic activated region.

ISBN NR.: 978-625-8795-56-1

Table 7. Correlations between model confidence and selected XAI-map characteristics

Relationship	Correlation
Grad-CAM: Confidence–Entropy	0.0356
Grad-CAM++: Confidence–Entropy	0.0711
Grad-CAM: Confidence–Focus50	0.1383
Grad-CAM++: Confidence–Focus50	0.1360

4. DISCUSSION

The most direct result is the overall agreement between the two CAM methods. Across 394 images, the mean correlation was 0.9645 and the mean Dice overlap was 0.9296. Those values were calculated from the raw normalized maps for every test image, rather than from a small set of hand-picked heatmaps. This gives a dataset-level view of how similarly Grad-CAM and Grad-CAM++ describe the same EfficientNet-B0 decisions.

The literature cited in this work has largely used explanation maps as a visual aid. For example, Mahesh et al. presented Grad-CAM with EfficientNetB0 [3]; Sánchez-Moreno et al. combined Grad-CAM++ with Integrated Gradients [5]; Mastoi et al. used Grad-CAM in a federated framework [7]; and Srinivas and Parvathi examined Grad-CAM alongside LIME [6]. Our analysis adds a different type of evidence by measuring pairwise agreement for every test image.

The comparison of correct and incorrect predictions is interesting because the separation is not clean. Correct predictions have higher correlation and Dice (0.9893 and 0.9515) than incorrect ones (0.8808 and 0.8555). Agreement therefore tends to be lower among errors, but the distributions overlap, and turning the difference in means into a rule for detecting errors would be misleading.

Figure 6 shows why. The classifier was almost fully confident in a wrong meningioma label, and the two CAM maps were nearly identical. Seen as an explanation, the result is stable; seen as a classification, it is wrong. The two properties are separate and should not be mixed up.

Figure 7 shows a different kind of failure: here the two methods disagreed strongly. Cases like this could help when reviewing a model by hand, since the explanation clearly depends on which XAI method is chosen. We did not define or validate a disagreement threshold, so this remains an exploratory observation.

Glioma needs its own comment. It produced most of the errors and also had the lowest mean CAM agreement: only 25% of glioma images were classified correctly, with a mean correlation of 0.8955 and a mean Dice of 0.8701. Many were confused with meningioma or no tumor. The class is hard for the classifier and, on average, also for agreement between the two explanation methods.

Confidence told us little about the geometry of the CAM maps; its correlations with entropy and Focus Area were small. The near-100% confidence error in Figure 6 makes the same point: confidence, explanation consistency and correctness are different quantities.

ISBN NR.: 978-625-8795-56-1

Comparisons with other XAI studies need care. Grad-CAM, Grad-CAM++, LIME and Integrated Gradients have been used with different architectures and pipelines [3]-[7], and the maps they produce depend on network structure, target layer, preprocessing and even software implementation. Numerical XAI descriptors are therefore only meaningful when the experimental settings are reported in full.

Table 8 is included for this methodological context. It summarizes how selected recent studies used XAI in brain-tumor MRI and shows where the present pairwise CAM analysis differs from them.

Table 8. Selected recent studies and the methodological position of the present work.

Study	Year	Model / XAI	Relevant aspect for the present study
Mahesh et al. [3]	2024	EfficientNetB0 + Grad-CAM	Visual explanation with Grad-CAM in four-class MRI classification.
Islam et al. [4]	2025	CNN-based XAI	Explainable deep-learning framework for brain-tumor detection.
Sánchez-Moreno et al. [5]	2025	Ensemble + Grad-CAM++ + Integrated Gradients	Use of multiple explanation methods for interpretability.
Mastoi et al. [7]	2025	Federated GoogLeNet + Grad-CAM	Heatmap-based explanation of predictions in federated learning.
Srinivas & Parvathi [6]	2026	CNN + Grad-CAM + LIME	Visual analysis of model decisions using Grad-CAM and LIME.
Present study	2026	EfficientNet-B0 + Grad-CAM + Grad-CAM++	Quantitative consistency analysis of two raw CAM methods across 394 test images, including correct/incorrect and class-wise comparisons.

5. LIMITATIONS

The study has no tumor-segmentation masks. Consequently, we cannot determine whether either CAM method identifies the true lesion more accurately. The reported Dice and Jaccard values only quantify overlap between Grad-CAM and Grad-CAM++.

The findings also come from one EfficientNet-B0 model, one test partition, and one target layer (model.features[-1]). A different architecture, training run, preprocessing pipeline, or target layer may produce different activation maps and a different level of agreement.

Finally, the comparison between correct and incorrect predictions is descriptive. Some errors retained almost perfect agreement between Grad-CAM and Grad-CAM++, so explanation consistency cannot be treated as an error detector in its present form. That question would require repeated runs, prespecified statistical tests, and validation on independent data.

6. CONCLUSION

We evaluated Grad-CAM and Grad-CAM++ on the predictions of a fixed EfficientNet-B0 classifier for 394 brain MRI test images. The network was not retrained, and the two explanation methods were applied to the same predicted class for each image. Their raw normalized activation maps were then compared numerically.

ISBN NR.: 978-625-8795-56-1

Across the test set, the two methods showed high agreement (r=0.9645; Dice=0.9296; Jaccard=0.8857). Agreement was higher on average for correct predictions than for incorrect ones. Glioma was the most difficult class for the classifier and also had the lowest mean CAM agreement.

The image-level results are important because they prevent an overly simple interpretation of the averages. Some wrong predictions still had almost identical explanation maps, whereas a few cases showed very strong divergence. Inter-method agreement can therefore add context when reviewing a model, but it does not establish that a decision is correct and it does not measure lesion localization.

INFORMATION NOTE

The EfficientNet-B0 weights used in this analysis were taken, without additional training, from the original-MRI condition reported in "The Effect of Image Enhancement Techniques on Deep Learning-Based Classification Performance in Brain Tumor MRI Images." The two works are independent in purpose and evaluation. The earlier work compares image-enhancement methods through classification metrics; the present work uses the fixed classifier only as a basis for comparing Grad-CAM and Grad-CAM++ explanations.

REFERENCES

[1] E. H. Houssein, A. M. Gamal, E. M. G. Younis, and E. Mohamed, "Explainable artificial intelligence for medical imaging systems using deep learning: a comprehensive review," Cluster Computing, vol. 28, art. 469, 2025. doi: 10.1007/s10586-025-05281-5.

[2] K. M. Hosny and M. A. Mohammed, "Explainable AI and vision transformers for detection and classification of brain tumor: a comprehensive survey," Artificial Intelligence Review, vol. 58, art. 259, 2025. doi: 10.1007/s10462-025-11221-x.

[3] Mahesh T. R., M. Gupta, Anupama T. A., V. Kumar, O. Geman, and D. Kumar, "An XAI-enhanced EfficientNetB0 framework for precision brain tumor detection in MRI imaging," Journal of Neuroscience Methods, vol. 410, art. 110227, 2024. doi: 10.1016/j.jneumeth.2024.110227.

[4] M. A. Islam, M. F. Mridha, M. Safran, S. Alfarhood, and M. M. Kabir, "Revolutionizing Brain Tumor Detection Using Explainable AI in MRI Images," NMR in Biomedicine, vol. 38, no. 3, e70001, 2025. doi: 10.1002/nbm.70001.

[5] L. Sánchez-Moreno, A. Perez-Peña, L. Duran-Lopez, and J. P. Dominguez-Morales, "Ensemble-based Convolutional Neural Networks for brain tumor classification in MRI: Enhancing accuracy and interpretability using explainable AI," Computers in Biology and Medicine, vol. 195, art. 110555, 2025. doi: 10.1016/j.compbiomed.2025.110555.

[6] V. R. Srinivas and R. Parvathi, "Explainable AI-driven MRI-based brain tumor classification: a novel deep learning approach," Frontiers in Artificial Intelligence, vol. 8, art. 1700214, 2026. doi: 10.3389/frai.2025.1700214.

[7] Q. Mastoi, S. Latif, S. Brohi, J. Ahmad, A. Alqhatani, M. S. Alshehri, A. Al Mazroa, and R. Ullah, "Explainable AI in medical imaging: an interpretable and collaborative federated learning model for brain tumor classification," Frontiers in Oncology, vol. 15, art. 1535478, 2025. doi: 10.3389/fonc.2025.1535478.

[8] F. Ahmed, N. S. Naz, S. Khan, A. U. Rehman, W. M. Ismael, et al., "Explainable artificial intelligence (XAI) in medical imaging: a systematic review of techniques, applications, and challenges," BMC Medical Imaging, vol. 26, art. 37, 2026. doi: 10.1186/s12880-025-02118-w.

[9] S. Bhuvaji, A. Kadam, P. Bhumkar, and S. Dedge, "Brain Tumor Classification (MRI)," Kaggle, 2020. doi: 10.34740/KAGGLE/DSV/1183165.

[10] M. Tan and Q. V. Le, "EfficientNet: Rethinking Model Scaling for Convolutional Neural Networks," in Proceedings of the 36th International Conference on Machine Learning, PMLR, vol. 97, pp. 6105–6114, 2019.

[11] R. R. Selvaraju, M. Cogswell, A. Das, R. Vedantam, D. Parikh, and D. Batra, "Grad-CAM: Visual Explanations From Deep Networks via Gradient-Based Localization," in Proceedings of the IEEE International Conference on Computer Vision (ICCV), pp. 618–626, 2017. doi: 10.1109/ICCV.2017.74.

[12] A. Chattopadhyay, A. Sarkar, P. Howlader, and V. N. Balasubramanian, "Grad-CAM++: Generalized Gradient-Based Visual Explanations for Deep Convolutional Networks," in 2018 IEEE Winter Conference on Applications of Computer Vision (WACV), pp. 839–847, 2018. doi: 10.1109/WACV.2018.00097.

GLOBE 2ND INTERNATIONAL CONFERENCE ON ENGINEERING, ARCHITECTURE, MATHEMATICS and APPLIED SCIENCES
October 1 - 6, 2026 – BARSELONA
ISBN NR.: 978-625-8795-56-1

THE ENVIRONMENTAL IMPACT OF INPUT USE IN AGRICULTURAL ENTERPRISES ENGAGED IN CROP PRODUCTION

Kardelen UĞUR **Zuhal KARAKAYACI**

0009-0006-2825-1399 0000-0003-2933-5608.

Selcuk University Agricultural Faculty Department of Agricultural Economics, Konya Türkiye

zuhalunal@selcuk.edu.tr

ABSTRACT

This study was conducted to determine the environmental impacts of input use and the levels of environmental awareness among operators at agricultural enterprises engaged in crop production in the Akşehir district of Konya Province. The intensive and indiscriminate use of chemical fertilizers and pesticides in agricultural production can lead to significant environmental problems such as soil and water pollution, a decline in biodiversity, and disruption of ecosystem balance. Therefore, identifying the environmental impacts of inputs used in agricultural production and determining the extent to which producers' environmental awareness is reflected in their practices is crucial for sustainable agriculture. In the study, face-to-face surveys were conducted with 98 agricultural enterprises, and the enterprises' levels of environmental awareness were determined using the Environmental Awareness Index (EAI) based on a Likert scale. According to the findings, 71.43% of the farms prefer chemical methods for controlling diseases and pests, while 52.04% dispose of empty pesticide containers by burning them after use. While 37% of the farms wish to transition to organic farming, 63% intend to continue with conventional agricultural production. The farms' Environmental Awareness Index (EAI) was calculated at 81.73%, indicating that producers have a high level of environmental awareness. However, it was determined that this high level of environmental awareness is not reflected in their practices to the same extent. Consequently, it is important to develop training and advisory services for producers to translate environmental sensitivity into action, to promote environmentally friendly production techniques, and to disseminate sustainable agriculture strategies.

Keywords: Crop production, Agricultural inputs, Environmental awareness index, Awareness

1. INTRODUCTION

Ever since it first came into existence, humankind has been interacting with the environment. In line with their needs, people have continuously altered their surroundings using

ISBN NR.: 978-625-8795-56-1

advancing technology in order to improve their standard of living. However, this has also led to environmental problems.

Throughout civilisation's history, humans have sought to shape the environment using their intellect. After they began using tools, humans transitioned to a settled lifestyle and learned to shape their environment according to their needs. The impact of humanity on nature is driven by its level of knowledge, the state of its technology, and the tools it has developed. The desire to control nature has developed rapidly within the technology-raw materials-energy triangle. The excessive pressure placed on natural resources and the drive for development marked the beginning of major environmental problems. Environmental problems first emerged after World War II. Initially, people believed that pollution was a result of industrialisation and that it affected only their immediate regions. Consequently, they thought that solutions to these problems were regional in nature. In reality, however, these problems threaten not only the people and environment of a specific region, but all of humanity and the world (Alagoz, 2007). Pollution — the waste generated by humans and discharged into land, air and water — poses a threat to human and global health, regardless of the associated costs and consequences. This jeopardises the sustainability of modern societies (Fuller et al., 2022). The process of environmental degradation poses a risk to global sustainability and takes on a more concrete and significant dimension through agricultural practices, one of the fundamental dynamics of human existence, and the methods used in these practices.

Since the beginning of humankind, agriculture has formed the foundation of social, economic and cultural life. It is a vital sector for ensuring food security, supporting rural development and sustainably managing natural resources. The inputs used in crop production, such as seeds, fertilisers, pesticides, water and fuel, are the cornerstones of the production process in agricultural enterprises, and the manner and intensity of their consumption directly shape the magnitude of environmental impacts. Indiscriminate or excessive use of these inputs can disrupt the balance of ecosystems by increasing water, air and soil pollution, thereby threatening long-term economic and environmental sustainability (Aydoğdu, 2014). Pesticides used in agricultural activities migrate into the air, water, soil and living organisms, and those released into the air return to the earth’s surface through various pathways. When pesticides are applied to plants, a large proportion leaches into the soil. Even very small amounts of pesticide residues can harm the environment (Altıkat et al., 2009). Consequently, while agricultural inputs such as fertilisers, pesticides and irrigation water increase productivity, they also create

ISBN NR.: 978-625-8795-56-1

serious environmental problems. These problems lead to soil, water and air pollution, as well as a loss of biodiversity. This necessitates the conscious and controlled use of agricultural inputs for sustainable agriculture. The growing global hunger problem, the nutritional challenges faced by Turkey's rapidly growing population and the need to boost agriculture's contribution to the economy are prompting agricultural experts to prioritise increasing production. As it is not possible to create new agricultural land, the only way to boost yields and increase production is to use agricultural inputs more efficiently. The efficient use of agricultural inputs is the most important factor in increasing yield, production volume and product quality, playing a key role in this process. Inputs such as fertilisers, seeds, pesticides, tools/machinery and irrigation systems make the most of land, labour and capital. Excessive use of these inputs indicates intensive agricultural activity. However, incorrect or excessive use can lead to negative consequences such as reduced product quality, as well as soil and water pollution (Çelik, 2000). A lack of knowledge about agricultural pest control can lead to improper application of control methods. When carried out conscientiously, agricultural pest control reduces production losses and associated costs while significantly impacting environmental pollution and human health. For this reason, a flow of information from universities and research institutions is necessary (Erkuş et al., 1992). The techniques used by agricultural enterprises when applying these inputs are very important for the environment. Indeed, the improper use of these inputs can cause environmental harm. To prevent this, it is necessary to improve producers' knowledge, attitudes and behaviours with regard to the environment, as well as their environmental awareness

The aim of this study is to determine the levels of knowledge, attitudes, and behaviors regarding input use in agricultural enterprises, to identify misapplications and misconceptions in this regard, and to assess their environmental awareness.

2. MATERIALS AND METHODS

This study was conducted on agricultural enterprises operating in the Akşehir district of Konya province. The data in this study were collected through face-to-face interviews with the enterprises and consist of information obtained from previous studies on the subject. In the study area, Akşehir District, 4,480 farms registered in the Farm Registration System (ÇKS) were identified. Stratified sampling was used to determine the number of producers to be

ISBN NR.: 978-625-8795-56-1

surveyed among these farms. A confidence interval of 90% and a margin of error of 5% were assumed in the calculations, and the sample size was determined to be 98.

In the survey used as the data collection tool for this study, a Likert-type scale (Likert, 1932) was chosen to assess participants' environmental awareness. An environmental awareness index was calculated to measure producers' sensitivity toward the environment. This calculation was based on the responses to the Likert-type questions in the survey. A 5-point Likert scale was used in the study, and the statements were rated as follows: (1) Strongly Disagree, (2) Disagree, (3) Undecided, (4) Agree, (5) Strongly Agree.

This scaling method aims to measure not only the direction of attitudes but also their intensity. In the data analysis, arithmetic means were calculated based on the numerical values assigned to each option to determine the participants' general tendencies. Thus, the maximum score producers could achieve on the prepared Likert scale was determined. Out of the 28 statements sent to the businesses, the maximum score producers could achieve was set at 140 points.

Table 1. Likert Scale Questions Used in the Environmental Sensitivity Analysis

Agricultural Inputs
Efficient irrigation systems, such as drip irrigation, conserve water.
The use of appropriate irrigation systems increases agricultural productivity.
Regular maintenance of irrigation systems improves water efficiency.
I do not apply pesticides or fertilizers unless there are visible signs of disease, pests, or weeds.
I do not apply pesticides or fertilizer directly by hand.
I observe the required waiting period between the last application of pesticides and harvest.
I keep a record of the timing and amount of the pesticides and fertilizers I use.
When purchasing pesticides and fertilizers, I check the expiration dates.
I read the instructions for using pesticides and fertilizers.
I review the label information before applying pesticides or fertilizers.
I take the necessary safety precautions during spraying and fertilizing.
I check whether the pesticides and fertilizers I use are registered.
Environmental Pollution
I am sufficiently aware of environmental pollution.
I take personal responsibility for reducing environmental pollution.
I actively work to promote recycling and waste management.
To protect the environment, I prefer to use public transportation instead of private vehicles.
I prefer to buy eco-friendly products.
I believe governments should implement stricter environmental protection policies.
I take measures at home and at work to conserve energy.
I believe that conserving water is important for environmental protection.
I believe green spaces should be protected and expanded.
I think there should be more education on environmental protection.

ISBN NR.: 978-625-8795-56-1

To protect the environment, I use pesticides and fertilizers at the recommended doses.
I think pesticides and fertilizers harm the environment.
Organic Farming
Organic farming is an environmentally friendly and sustainable farming method.
Organic agricultural products are safer for your health.
Organic farming practices help preserve soil health.
Organic agricultural products contribute to environmental sustainability.

An environmental sensitivity analysis was conducted by calculating an index based on the data obtained. The formula for the environmental sensitivity index is shown below.

Environmental Sensitivity Index = (TSP/MPS) * 100

TSP: Total score earned by producers

Maximum Possible Score: The maximum score producers can achieve (Yener, 2017).

3. RESEARCH FINDINGS AND DISCUSSION

In the enterprises surveyed, the population was found to be 8.42% for those aged 0–6; 8.34% for those aged 7–14; 34.55% for those aged 15–49; and 48.69% for those aged 50 and older. The age group of 50 and older accounts for the largest share of the enterprise population, at 48.69%. This percentage appears to indicate the importance of the elderly population in agricultural activities and the participation of individuals of retirement age in the family workforce. In contrast, the 15–49 age group—considered the active working-age population—accounts for 34.55% of the average workforce across these enterprises. This suggests that these enterprises have a moderate level of young and productive labor. On average across enterprises, the largest segment of the workforce—40.94 percent—consists of elementary school graduates. This concentration indicates that the workforce possesses basic literacy skills, but that the overall level of education remains low. On average, 25.82% of employees in these enterprises are high school graduates; 18.16% have completed secondary education; and 6.96% hold a bachelor's degree.

3.1. Awareness and Behavioral Patterns of the Studied Enterprises

People's behaviors and attitudes toward the environment are crucial in terms of environmental awareness. Unconscious behaviors ultimately lead to environmental pollution, which harms both people and nature. To prevent this harm, people must develop their environmental awareness. The study identified the knowledge, attitudes, and behaviors of

ISBN NR.: 978-625-8795-56-1

agricultural businesses in the research area regarding input use, as well as any misconceptions and incorrect practices in this regard. Accordingly, the study determined the extent of these businesses' uninformed behaviors before, during, and after input use; what factors they considered; and how they utilized these inputs, thereby revealing their environmental impact and the enterprises level of environmental awareness.

As the negative effects caused by synthetic chemicals and agricultural inputs have been recognized globally by informed producers and consumers, the practice of organic farming has rapidly gained widespread adoption (Aydın, 2023). In organic farming, the use of synthetic inputs is eliminated entirely or as much as possible during production; this system aims to improve soil health and productivity. To this end, crop rotation, animal manure, green manure, and organic waste are utilized. Additionally, biological control methods are employed to manage diseases, pests, and weeds (Ağızan, 2022).

It was found that 37% of the farms surveyed wished to transition to organic farming, while 63% preferred conventional farming. The reason for this was determined to be that the farms generally struggled with pest control and were unable to achieve satisfactory yields. Table 2 presents the farms' views on organic farming.

Table 2: Farms' Views on Organic Farming

Statements	**1**	**2**	**3**	**4**	**5**	**Total**	**Overall Average**
Organic farming is an environmentally friendly and sustainable farming method.	10	4	6	51	27	98	3.83
Organic agricultural products are safer for your health.	9	4	3	51	31	98	3.93
Organic farming practices help preserve soil health.	9	4	4	53	28	98	3.89
Organic agricultural products contribute to environmental sustainability.	9	4	3	50	32	98	3.94

*1=Strongly disagree 2=Disagree 3=Undecided 4=Agree 5=Strongly agree

According to the results in Table 2, it was determined that businesses hold positive views regarding the environmental and health benefits of organic farming. The highest average score, 3.94, was obtained for the statement "Organic agricultural products contribute to environmental sustainability", followed by the statement "Organic agricultural products are safer for health," with an average of 3.93. The averages for the statements "Organic farming practices protect soil health" and "Organic farming is an environmentally conscious and sustainable farming method" were calculated as 3.89 and 3.83, respectively. The findings

ISBN NR.: 978-625-8795-56-1

indicate that businesses hold a positive view regarding the significant contributions organic farming makes to environmental sustainability, human health, and the protection of soil health.

The attitudes and behaviors of producers in the study area regarding water sources, irrigation methods, water-related problems, and appropriate irrigation systems were examined. The most commonly used water source in the region is private wells owned by farms, accounting for 71.96%. The second most common water source is wells operated by the State Water Works, accounting for 22.43%. It was determined that 3.74% of the farms do not have an irrigation water source. The high dependence of the farms examined on groundwater resources poses a risk to sustainability due to the potential for water levels to drop as a result of drought or over-irrigation. Half of the farms use sprinkler irrigation, while 23.47% use a combination of sprinkler and drip irrigation. Farms that use only drip irrigation account for 22.45%. 4.08% of the farms do not use any irrigation method.

Table 3: Perceptions of the Studied Farms Regarding Irrigation Systems

Statements	**1**	**2**	**3**	**4**	**5**	**Total**	**Overall Average**
Efficient irrigation systems, such as drip irrigation, conserve water.	1	0	1	35	61	98	4.58
The use of appropriate irrigation systems increases agricultural productivity.	0	0	0	35	63	98	4.64
Regular maintenance of irrigation systems improves water efficiency.	0	1	4	37	56	98	4.51

*1=Strongly disagree 2=Disagree 3=Undecided 4=Agree 5=Strongly agree

Table 3 presents the perceptions of the farms examined regarding irrigation systems. Looking at the overall averages for the farms, the statement “Efficient irrigation systems, such as drip irrigation, conserve water” received a score of 4.58; the statement “The use of appropriate irrigation systems increases agricultural productivity” received a score of 4.64; and “Regular maintenance of irrigation systems increases water efficiency” scored 4.51, indicating a high level of awareness.

This indicates that the farms possess a high level of awareness regarding the efficiency and water-saving potential of irrigation systems. However, there is a gap between this awareness and actual implementation; in fact, only 22.45% of the farms use drip irrigation , which is the most efficient method. In summary, while producers in the region are mentally

ISBN NR.: 978-625-8795-56-1

prepared for modern practices, dependence on groundwater and economic conditions are the primary factors determining the pace of this transition.

The primary goal of agricultural production is to increase output in terms of both quality and quantity. Since expanding existing farmland is difficult, increasing the yield per unit area is the solution. This is achieved through the use of certified seeds and modern agricultural inputs such as pesticides (Akar, 2017).

The study reveals that the farms examined rely heavily on chemical control methods for pest management in agricultural production, with a very high rate of 71.43%. This preference is followed, in order, by a combination of chemical, cultural, and biological methods (17.35%), chemical and biological control (8.16%), and a combination of chemical and cultural control (3.06%). Notably, all alternative methods are still supported by chemical methods, and it is evident that chemical-free pest control methods have not become widespread. This situation indicates that, despite modern agricultural techniques, producers prefer traditional methods focused on quick results, while sustainable and environmentally friendly integrated pest management approaches remain secondary.

Table 4: Pesticide and Fertilizer Practices of the Studied Farms

Statements	**1**	**2**	**3**	**4**	**5**	**Total**	**Overall Average**
I do not apply pesticides or fertilizer unless there is a visible disease, pest, or weed .	12	8	5	57	16	98	3.58
I do not apply pesticides or fertilizer directly by hand.	2	2	1	65	28	98	4.17
I pay attention to the waiting period between the last application and harvest.	0	0	2	62	34	98	4.33
I keep track of the timing and amount of the pesticides and fertilizers I use.	2	9	3	45	39	98	4.12
When purchasing agricultural pesticides and fertilizers, I pay attention to the expiration date.	3	9	1	54	31	98	4.03
I am reading the instructions for using pesticides and fertilizers.	2	5	2	53	36	98	4.18
I review the label information before applying pesticides or fertilizer.	4	5	2	56	31	98	4.07
I take the necessary safety precautions during spraying and fertilizing.	4	4	7	49	34	98	4.07
I check whether the pesticides and fertilizers I use are registered.	4	8	6	56	24	98	3.90

*1=Strongly disagree 2=Disagree 3=Undecided 4=Agree 5=Strongly agree

ISBN NR.: 978-625-8795-56-1

Table 4 presents the pesticide and fertilizer-related practices of the farms examined. Looking at the overall averages, farms that indicated they pay attention to the waiting period between the last application and harvest have the highest overall average at 4.33. Farms that stated they do not apply pesticides and fertilizers directly by hand demonstrate a high level of awareness regarding occupational health and safety, with an average score of 4.17. Farms that stated they read the instructions regarding pesticide and fertilizer use have an overall average of 4.18, indicating that they use these products as intended, which is considered a sign of high environmental sensitivity. Enterprises that pay attention to the expiration date when purchasing agricultural pesticides and fertilizers scored 4.03; those that record the timing and quantity of the pesticides and fertilizers they use scored 4.12; and enterprises that stated they take the necessary safety precautions during spraying and fertilization had an average score of 4.07. The overall average for enterprises that take the necessary safety precautions during spraying and fertilization is 4.07. When compared to the overall average (4.18) for enterprises that read the instructions, label review scores were lower. Farms that reported checking whether the pesticides and fertilizers they used were licensed showed a moderate level of awareness, with an average score of 3.90. Finally, the overall average for farms that stated they did not apply pesticides or fertilizers in the absence of visible diseases, pests, or weeds was 3.58. This behavior on the part of farms should be improved in terms of environmentally friendly practices.

It was observed that 6.12% of producers bury the packaging of used pesticides and fertilizers in the ground, 12.24% recycle them, 29.59% throw them in the trash, and 52.04% dispose of the packaging by burning it. The careless incineration of agricultural pesticide and fertilizer packaging releases toxic gases into the air, posing a risk to human and environmental health.

ISBN NR.: 978-625-8795-56-1

Table 5: Attitudes and Behaviors of the Studied Enterprises Toward Environmental Pollution

Statements	**1**	**2**	**3**	**4**	**5**	**Total**	**Overall Average**
I am sufficiently aware of environmental pollution.	0	5	8	72	13	98	3.95
I take personal responsibility for reducing environmental pollution.	1	3	7	49	38	98	4.22
I am actively working on recycling and waste management.	3	9	9	49	28	98	3.92
To protect the environment, I prefer to use public transportation instead of a private vehicle.	23	26	13	31	5	98	2.68
I prefer to buy eco-friendly products.	0	7	11	63	17	98	3.92
I think governments should tighten their environmental protection policies.	7	0	4	33	54	98	4.30
I'm taking steps to save energy at home and at work.	0	2	2	65	29	98	4.23
I think saving water is important for environmental protection	0	2	1	42	53	98	4.49
I believe that green spaces should be protected and expanded.	0	0	0	47	51	98	4.52
I think there should be more education on environmental protection	3	0	0	53	42	98	4.34
To protect the environment, I use pesticides and fertilizers at the recommended dosage.	2	0	2	66	28	98	4.20
I think pesticides and fertilizers harm the environment.	8	8	6	42	34	98	3.88

*1=Strongly disagree 2=Disagree 3=Undecided 4=Agree 5=Strongly agree

Looking at the overall averages for businesses, those with sufficient awareness of environmental pollution scored 3.95; those actively striving for recycling and waste management and preferring to purchase eco-friendly products scored 3.92; and businesses that believe pesticides and fertilizers harm the environment had an overall average of 3.88, while businesses that prefer to use public transportation instead of private vehicles to protect the environment had an overall average of 2.68. It is evident that businesses possess a high level of theoretical knowledge and awareness. However, the data indicates that this awareness has not been translated into action.

3.2. Awareness and Behavioral Status of the Studied Businesses

Environmental sensitivity is no longer merely a preference but also a major responsibility toward future generations. The level of environmental awareness among agricultural businesses must be on par with the extent to which this awareness is put into

ISBN NR.: 978-625-8795-56-1

practice. Otherwise, if the level of implementation falls below the level of awareness, it may lead to problems regarding the sustainability of natural resources.

Table 6: Average Environmental Awareness Index of the Studied Farms

Maximum Score Producers Can Achieve	140.00
Average Score Achieved by Producers	114.43
Environmental Awareness Index	81.73

Table 6 presents the average environmental awareness index values for the agricultural enterprises examined. The average environmental awareness index for the enterprises studied in this research was calculated as **81.73**%. This value indicates that, in general, the enterprises have a high level of environmental awareness and that their awareness of environmental issues is above a certain level. In determining the enterprises' levels of environmental sensitivity, various criteria were taken into account, such as their approaches to environmental pollution, the forms and levels of agricultural input use, their attitudes toward the conservation of natural resources, and their approaches to organic farming practices. The average index value obtained indicates that the enterprises in the study area generally exhibit a positive attitude toward environmental protection and sustainable agricultural production.

Table 7: Environmental Sensitivity Index Levels of the Studied Farms

Standard Deviation		8.03	
Mean		81.73	
Minimum Threshold		73.70	
Maximum Limit		89.77	
Environmental Sensitivity Index Level		**Number**	**% Distribution**
Low	0–73.7	16	16.33
Medium	73.8–89.7	66	67.35
High	89.8–100	16	16.33

Table 7 shows the distribution of the businesses examined in the study according to their environmental sensitivity index levels. Accordingly, of the 98 businesses examined in the study**,**

ISBN NR.: 978-625-8795-56-1

66 (67.35%) have a moderate level**,** 16 (16.33%) have a low level, and 16 (16.33%) have a high level of environmental sensitivity index. The fact that approximately two-thirds of the enterprises have a moderate level of environmental sensitivity indicates that while the majority of enterprises in the study area possess a certain level of awareness regarding environmental issues, this sensitivity has not yet translated into a widespread, high-level behavioral pattern. Indeed, the research findings reveal that the necessary care is not being exercised in practices requiring environmental sensitivity, such as fertilizer use, irrigation methods, and the disposal of waste from production inputs.

4. CONCLUSIONS AND RECOMMENDATIONS

This study examined the level of awareness among producers regarding the environmental impact of input use in agricultural operations engaged in crop production in the Akşehir district of Konya province. According to the results, it was observed that producers have a high level of environmental awareness. However, it was determined that their performance in practice falls short of this level of awareness. The burning of chemical pesticide and fertilizer packaging, as well as a lack of sufficient care in the use of modern irrigation techniques, poses risks to environmental sustainability. At the same time, it was determined that producers use chemical inputs at a high rate, while their knowledge and behaviors regarding organic farming are at a moderate level.

In light of these findings, it is evident that while a significant portion of agricultural operations demonstrate environmental awareness, they continue to rely on traditional practices due to a lack of knowledge on how to implement sustainable practices. In this context, recommendations have been developed regarding the environmental impacts of input use by agricultural operations:

Education and Outreach Activities: Continuous education and outreach activities should be conducted to improve farms' knowledge regarding the proper and effective use of fertilizers, chemical pesticides, and irrigation systems. Practical training programs for producers should be organized through collaboration among universities, provincial and district directorates of the Ministry of Agriculture and Forestry, and agricultural cooperatives. To make educational activities more effective and engaging, practical events such as field days, demonstrations, technical tours, and agricultural fairs should be utilized. This will facilitate agricultural

ISBN NR.: 978-625-8795-56-1

businesses' access to up-to-date information and technologies, thereby raising their level of knowledge and promoting the widespread adoption of environmentally friendly production practices.

Promotion of Sustainable Irrigation Systems: To promote the widespread adoption of modern, water-saving irrigation methods, financial incentives for producers should be increased, and credit and grant support should be provided under appropriate conditions. The economic and environmental benefits that modern irrigation systems offer to farm owners—in terms of water conservation, efficiency, production costs, and environmental protection—should be highlighted through outreach activities. In addition, technical advisory services regarding the installation and effective use of irrigation systems should be strengthened.

Promotion of Environmentally Friendly Agricultural Practices: To minimize the negative environmental impacts of agricultural production and develop sustainable production systems, farm owners should be encouraged to adopt environmentally friendly production methods such as green agriculture and organic farming. Certification and bureaucratic procedures encountered during the transition to organic farming should be streamlined, and technical and financial support should be provided to producers. Furthermore, cooperative and organizational activities aimed at marketing organic products should be supported to improve producers' access to markets.

Waste Management and Raising Environmental Awareness: Appropriate waste collection points should be established in residential areas to ensure that packaging waste from chemical fertilizers and plant protection products is collected and disposed of in accordance with regulations and in a manner that does not harm the environment. Business owners should be provided with information and awareness training regarding the risks posed by the disposal of chemical fertilizer and plant protection product packaging into the environment. Additionally, ongoing training and outreach activities aimed at raising environmental awareness should be conducted to increase businesses' awareness of natural resource conservation, proper waste management, and sustainable agricultural production.

ISBN NR.: 978-625-8795-56-1

REFERENCES

- *Ağızan, K. (2022). Organik Tarım Ürünlerinde Değer Zinciri Analizi Ve Girişimcilik Fırsatları. Konya: Selçuk Üniversitesi Fen Bilimleri Enstitüsü.*
- *Akar, Ö. (2017). Antalya İlinde Üreticilerin Pestisit Kullanımı Ve Seçimindeki Eğitim Ve Bilgi Düzeyi İle Çevresel Duyarlılıklarının Araştırılması. Kayseri: Erciyes Üniversitesi Fen Bilimleri Enstitüsü.*
- *Alagöz, B. (2007). Çevre Sorunları, Teknoloji Ve Değişen Öncelikler., (s. 43-52).*
- *Altikat, A., Turan, T., & Torun, F. E. (2009). Türkiye'de Pestisit Kullanımı ve Çevreye Olan Etkileri. Atatürk Üniv. Ziraat Fak.Derg. , s. 87-92.*
- *Aydin, Ö. Ç. (2023). Kayseri İlinde Organik Tarım Yapan Üreticilerin Organik Tarıma Bakışlarının Değerlendirilmesi. Kayseri: Erciyes Üniversitesi Fen Bilimleri Enstitüsü.*
- *Aydoğdu, İ. B. (2014). Yerel Ve Bölgesel Düzeyde Çevre Kirliliği Sorunları: Elazığ İli Örneği. Fırat Üniversitesi Harput Araştırmaları Dergisi , s. 133-148.*
- *Çelik, N. (2000). Tarımda Girdi Kullanımı ve Verimliliğe Etkileri. Devlet Planlama Teşkilatı.*
- *Erkuş, A., Toros, S., & Yalçın, Ö. F. (1992). Sincan İlçesi Sebze Üreticilerinin Zararlı Ve Hastalıklara Karşı İlaç Kullanım Durumu Ve İlaç Kullanımının Ekonomik Analizi Üzerine Bir Araştırma. Ankara Üniversitesi Ziraat Fakültesi Yayınları, s. 59-66.*
- Likert, R. (1932). *A technique for the measurement of attitudes*. Archives of Psychology, 140, 1–55.
- *Richard Fuller, P. J.-O. (2022). Pollution and health: a progress update. Lancet Planet Health , s. 535-547.*
- *Yener, A. (2017). Konya İlinde Süt Sığırcılığı Yapan Aile İşletmelerinde Yeniliklerin Benimsenmesi Ve Yayılmasına Etki Eden Faktörler. Konya: Selçuk Üniversitesi Fen Bilimleri Enstitüsü.*

GLOBE 2ND INTERNATIONAL CONFERENCE ON ENGINEERING, ARCHITECTURE, MATHEMATICS and APPLIED SCIENCES
October 1 - 6, 2026 – BARSELONA
ISBN NR.: 978-625-8795-56-1

IMPACTS OF OPEN-PIT COPPER AND GOLD MINING ON SOIL HEAVY METAL ACCUMULATION AND NATURAL FOREST VEGETATION IN THE ALMALYK MINING REGION OF UZBEKISTAN

Prof. Dr. Bakhtiyor Rakhimov, Dilnoza Karimova, Sherzod Tursunov
National University of Uzbekistan named after Mirzo Ulugbek, Faculty of Biology, Department of Ecology, Tashkent, Uzbekistan
Tashkent State Technical University named after Islam Karimov, Faculty of Geology and Mining, Department of Mining, Tashkent, Uzbekistan
Tashkent State Agrarian University, Faculty of Forestry and Landscape Design, Department of Forestry, Tashkent, Uzbekistan

ABSTRACT

The Almalyk mining region, located on the slopes of the Kurama and Chatkal ranges in eastern Uzbekistan, hosts one of the largest copper and gold mining and metallurgical complexes in Central Asia. Decades of open-pit extraction, ore processing, smelting and the disposal of overburden and tailings have profoundly transformed the surrounding landscape and raised serious concerns about soil contamination and the condition of natural vegetation. The foothill and mountain forests of the region, dominated by juniper, walnut, maple, wild fruit trees and shrub communities, are of considerable ecological value, as they protect slopes from erosion, regulate water flow and preserve genetic resources of wild relatives of cultivated plants. This study assesses the impacts of open-pit copper and gold mining on heavy metal accumulation in soils and on the structure and health of natural forest vegetation in the Almalyk region. Soil samples were collected along transects at increasing distances from open pits, waste dumps and tailing ponds, and analysed for copper, zinc, lead, cadmium, arsenic and other elements using atomic absorption spectrometry. Contamination factors, the geoaccumulation index and the potential ecological risk index were calculated. Vegetation surveys recorded species composition, tree density, crown condition and regeneration, while leaf samples were analysed to evaluate metal uptake. The results reveal strong enrichment of copper, zinc, lead and cadmium in soils near mining and processing sites, with contamination decreasing gradually with distance and following prevailing wind directions. Forest stands close to the mines show reduced species richness, crown defoliation, chlorosis and poor natural regeneration, while some shrub species display notable tolerance and metal accumulation capacity. The study concludes that systematic environmental monitoring, dust control, progressive reclamation of waste dumps and phytoremediation using tolerant native species are essential for mitigating mining impacts and conserving mountain forest ecosystems.

Keywords: Open-pit mining, Heavy metals, Soil contamination, Forest vegetation, Phytoremediation, Almalyk, Uzbekistan

GLOBE 2ND INTERNATIONAL CONFERENCE ON ENGINEERING, ARCHITECTURE, MATHEMATICS and APPLIED SCIENCES
October 1 - 6, 2026 – BARSELONA
ISBN NR.: 978-625-8795-56-1

CARBON SEQUESTRATION POTENTIAL AND ECOSYSTEM SERVICES OF AVICENNIA MARINA MANGROVE FORESTS ALONG THE QATARI COASTLINE: A FIELD-BASED AND SATELLITE MONITORING STUDY

Assoc. Prof. Dr. Jassim Al-Hajri, Aisha Al-Muhannadi, Mohammed Al-Kaabi
Qatar University, College of Arts and Sciences, Department of Biological and Environmental Sciences, Doha, Qatar
Qatar University, Environmental Science Center, Doha, Qatar
Hamad Bin Khalifa University, College of Science and Engineering, Division of Sustainable Development, Doha, Qatar

ABSTRACT

Mangrove forests are among the most carbon-rich ecosystems on Earth, storing large quantities of organic carbon in their biomass and, above all, in their waterlogged sediments. Along the coastline of Qatar, mangroves are represented by a single species, Avicennia marina, which forms stands in sheltered bays and lagoons such as Al Thakhira, Al Khor and Fuwairit. Despite growing under extreme conditions of high salinity, intense heat and low rainfall, these forests provide valuable ecosystem services, including coastal protection, nursery habitats for fish and crustaceans, feeding grounds for migratory birds and opportunities for recreation and environmental education. However, coastal development, land reclamation, pollution and climate change pose increasing threats to their extent and functioning. This study evaluates the carbon sequestration potential and ecosystem services of Avicennia marina mangrove forests along the Qatari coastline by combining field-based measurements with satellite monitoring. Field plots were established in the main mangrove sites to measure tree height, stem diameter and density, and allometric equations were used to estimate above-ground and below-ground biomass. Sediment cores were collected to determine bulk density and organic carbon content at different depths. Multitemporal satellite imagery was analysed using vegetation indices and supervised classification to map changes in mangrove cover and canopy condition over time. Ecosystem services were further assessed through interviews with fishers, environmental managers and visitors. The results indicate that, although tree biomass is relatively low compared with tropical mangroves, sediment carbon stocks are substantial and represent the largest share of total ecosystem carbon. Satellite analysis reveals overall expansion of mangrove cover in protected areas, alongside localized losses near development zones. The study concludes that Qatari mangroves represent an important blue carbon resource and that their protection and restoration should be incorporated into national climate and coastal management strategies.

Keywords: Avicennia marina, Blue carbon, Mangrove forests, Ecosystem services, Remote sensing, Qatar

GLOBE 2ND INTERNATIONAL CONFERENCE ON ENGINEERING, ARCHITECTURE, MATHEMATICS and APPLIED SCIENCES
October 1 - 6, 2026 – BARSELONA
ISBN NR.: 978-625-8795-56-1

LIMESTONE AND GABBRO QUARRYING IN ARID ENVIRONMENTS OF QATAR: DUST EMISSIONS, DESERT VEGETATION LOSS AND POST-MINING LAND REHABILITATION APPROACHES

Dr. Khalid Al-Mannai, Maryam Al-Kuwari, Prof. Dr. Abdulrahman Al-Sulaiti, Noora Al-Marri, Assist. Prof. Dr. Hamad Al-Naimi
Qatar University, College of Engineering, Department of Civil and Environmental Engineering, Doha, Qatar

ABSTRACT

Rapid urban growth and large-scale infrastructure development in Qatar have generated a strong demand for construction aggregates, which has been met largely through limestone quarrying within the country and imports of gabbro from neighbouring regions, along with associated crushing and stockpiling operations. Quarrying in arid environments creates distinctive environmental pressures, as fragile desert soils, sparse vegetation and slow natural recovery make ecosystems highly vulnerable to disturbance. The removal of topsoil and vegetation, the creation of deep pits and waste heaps, and the movement of heavy vehicles damage the biological soil crusts and perennial plants that stabilize the desert surface. In addition, blasting, crushing, screening and transport generate considerable amounts of fugitive dust, which affects air quality, the health of workers and nearby residents, and the physiological functioning of surrounding vegetation. This study examines dust emissions, desert vegetation loss and post-mining land rehabilitation approaches associated with limestone and gabbro quarrying in arid environments of Qatar. The research combined air quality monitoring of particulate matter around active quarries and crushers, measurements of dust deposition on plant leaves, vegetation surveys in disturbed and undisturbed areas and the analysis of satellite imagery to map changes in land cover over time. Interviews with quarry operators, regulators and environmental specialists provided insights into current management practices. The findings show elevated particulate concentrations near crushing and loading areas, particularly during periods of strong northwesterly winds, and substantial dust accumulation on native shrubs such as Ziziphus nummularia and Lycium shawii, which reduces photosynthetic activity. Quarried sites show near-complete loss of perennial vegetation and very limited spontaneous recovery. The study concludes that dust suppression technologies, topsoil conservation, landform reshaping and revegetation with drought-tolerant native species, supported by stronger rehabilitation regulations, are essential for sustainable quarrying in desert environments.

Keywords: Quarrying, Dust emissions, Desert vegetation, Land rehabilitation, Arid ecosystems, Qatar

GLOBE 2ND INTERNATIONAL CONFERENCE ON ENGINEERING, ARCHITECTURE, MATHEMATICS and APPLIED SCIENCES
October 1 - 6, 2026 – BARSELONA
ISBN NR.: 978-625-8795-56-1

RIVERBED SAND AND STONE MINING IN THE SYLHET REGION OF BANGLADESH: EFFECTS ON RIPARIAN FOREST ECOSYSTEMS, RIVERBANK EROSION AND LOCAL LIVELIHOODS

Asst. Prof. Dr. Kamrul Hasan Talukder
Shahjalal University of Science and Technology, School of Agriculture and Mineral Sciences, Department of Forestry and Environmental Science, Sylhet, Bangladesh

ABSTRACT

The rivers of the Sylhet region in northeastern Bangladesh, including the Piyain, Dhalai, Jadukata and Sari, carry large quantities of sand, gravel and boulders from the Meghalaya hills, making the region a major source of construction materials for the rapidly expanding national economy. Riverbed sand and stone extraction, carried out both by mechanized dredgers and by thousands of manual labourers, has grown in recent decades, often exceeding legally permitted levels and taking place in ecologically sensitive areas such as Jaflong, Bholaganj and Lovachara. These activities raised serious concerns about their effects on river morphology, riparian forests and the communities that depend on rivers for their livelihoods. This study examines the effects of riverbed sand and stone mining in the Sylhet region on riparian forest ecosystems, riverbank erosion and local livelihoods. A mixed-methods approach was adopted, combining analysis of multitemporal satellite imagery to detect changes in river channels and riparian vegetation, field surveys of riparian forest structure and species composition at mined and less disturbed sites, and household surveys and focus group discussions with miners, farmers, fishers and local officials. The findings reveal that intensive extraction has caused channel deepening, bank instability and accelerated riverbank erosion, resulting in the loss of agricultural land, homesteads and riparian forest patches. Riparian vegetation near mining sites shows reduced tree density, lower species diversity and limited regeneration. Although mining provides important income opportunities for poor households, workers face hazardous working conditions, frequent accidents and health problems, and benefits are unequally distributed in favour of influential intermediaries. Fishing and farming livelihoods have declined in heavily mined stretches. The study concludes that scientifically determined extraction limits, strict enforcement, riparian reforestation and alternative livelihood programmes are necessary for balancing resource use with ecosystem conservation.

Keywords: Sand mining, Stone extraction, Riparian forests, Riverbank erosion, Livelihoods, Sylhet, Bangladesh

GLOBE 2ND INTERNATIONAL CONFERENCE ON ENGINEERING, ARCHITECTURE, MATHEMATICS and APPLIED SCIENCES
October 1 - 6, 2026 – BARSELONA
ISBN NR.: 978-625-8795-56-1

MANGROVE FOREST DEGRADATION IN THE SUNDARBANS: A GIS-BASED ANALYSIS OF SALINITY INTRUSION, ILLEGAL LOGGING AND COMMUNITY-BASED CONSERVATION STRATEGIES IN BANGLADESH

Prof. Dr. Abul Kalam Chowdhury, Sabrina Haque, Md. Imran Hossain, Dr. Rumana Sultana

Khulna University, Life Science School, Forestry and Wood Technology Discipline, Khulna, Bangladesh

University of Dhaka, Faculty of Earth and Environmental Sciences, Department of Geography and Environment, Dhaka, Bangladesh

Khulna University, Life Science School, Environmental Science Discipline, Khulna, Bangladesh

University of Chittagong, Institute of Forestry and Environmental Sciences, Chattogram, Bangladesh

ABSTRACT

The Sundarbans, the largest contiguous mangrove forest in the world, extends across the delta of the Ganges, Brahmaputra and Meghna rivers and is shared by Bangladesh and India. Recognized as a World Heritage Site and a Ramsar wetland, it supports exceptional biodiversity, including the Bengal tiger, and provides millions of people with timber, fish, honey and protection from cyclones and storm surges. However, the Sundarbans is experiencing progressive degradation driven by both natural and human factors. Reduced freshwater flow from upstream, partly due to river diversion, combined with sea level rise has intensified salinity intrusion, which is associated with top-dying disease of the dominant species Heritiera fomes and shifts toward more salt-tolerant species. At the same time, illegal logging, overharvesting of non-timber forest products and pollution from shipping and industrial development place additional pressures on the forest. This study applies a GIS-based analysis to examine mangrove forest degradation in the Bangladeshi Sundarbans in relation to salinity intrusion and illegal logging, and evaluates community-based conservation strategies. Multitemporal satellite imagery was classified to assess changes in forest cover and canopy density, while spatial data on soil and water salinity, distance to settlements, waterways and forest stations were integrated through overlay and regression analysis. Field verification and interviews with forest-dependent communities, co-management committees and forest officials complemented the spatial analysis. The results indicate that canopy degradation is most pronounced in high-salinity western and southwestern zones and in areas close to settlements and navigable channels, where illegal felling is concentrated. Community-based co-management initiatives, alternative income generation and community patrolling were associated with reduced illegal extraction in some areas, although weak institutional support and benefit-sharing problems limited their effectiveness. The study concludes that restoring freshwater flows, strengthening law enforcement and empowering local communities are essential for conserving the Sundarbans.

ISBN NR.: 978-625-8795-56-1

Keywords: Sundarbans, Mangrove degradation, Salinity intrusion, Illegal logging, GIS, Community-based conservation

GLOBE 2ND INTERNATIONAL CONFERENCE ON ENGINEERING, ARCHITECTURE, MATHEMATICS and APPLIED SCIENCES
October 1 - 6, 2026 – BARSELONA
ISBN NR.: 978-625-8795-56-1

ASSESSING THE ENVIRONMENTAL AND SOCIOECONOMIC CONSEQUENCES OF THE BARAPUKURIA UNDERGROUND COAL MINE ON SURROUNDING AGRICULTURAL LAND, GROUNDWATER LEVELS AND FOREST RESOURCES IN NORTHWESTERN BANGLADESH

Md. Rafiqul Islam, Dr. Nusrat Jahan, Tanvir Ahmed, Assoc. Prof. Dr. Shahida Akter, Mahmudul Hasan, Farzana Rahman
Hajee Mohammad Danesh Science and Technology University, Faculty of Agriculture, Department of Soil Science, Dinajpur, Bangladesh

ABSTRACT

The Barapukuria coal mine in the Dinajpur district of northwestern Bangladesh is the country's only operating underground coal mine and supplies fuel to an adjacent thermal power plant, playing an important role in national energy security. However, the mine is located in a densely populated and highly productive agricultural area, where rice, wheat and vegetables are cultivated and homestead forests, roadside plantations and village groves provide timber, fuelwood and fruit. Since production began, local communities have reported land subsidence, cracks in houses, waterlogging, declining groundwater levels and contamination of water and soils, leading to protests and demands for compensation. This study assesses the environmental and socioeconomic consequences of the Barapukuria underground coal mine on surrounding agricultural land, groundwater levels and forest resources. The research integrated analysis of satellite imagery and land use maps to detect changes in cropland, water bodies and tree cover, monitoring data from observation wells to evaluate groundwater fluctuations, and laboratory analysis of soil and water samples for heavy metals and acidity. Household surveys, key informant interviews and focus group discussions were conducted in affected and control villages to capture changes in livelihoods, income, health and compensation experiences. The findings reveal substantial land subsidence above the mined panels, resulting in the formation of permanent water bodies, the loss of cultivable land and damage to homes, roads and trees. Mine dewatering has contributed to a marked lowering of groundwater levels in surrounding areas, affecting irrigation and drinking water supplies, particularly during the dry season. Elevated concentrations of certain heavy metals were found in soils and water near coal handling and waste disposal sites. Many households experienced declining agricultural income, while compensation was often perceived as inadequate. The study concludes that improved mining methods, continuous environmental monitoring, fair compensation and land rehabilitation are urgently required.

Keywords: Underground coal mining, Land subsidence, Groundwater depletion, Agricultural land, Forest resources, Barapukuria, Bangladesh

GLOBE 2ND INTERNATIONAL CONFERENCE ON ENGINEERING, ARCHITECTURE, MATHEMATICS and APPLIED SCIENCES
October 1 - 6, 2026 – BARSELONA
ISBN NR.: 978-625-8795-56-1

CLIMATE CHANGE, DROUGHT STRESS AND TIMBER PRODUCTION IN HUNGARIAN BEECH AND OAK FORESTS: IMPLICATIONS FOR SUSTAINABLE FOREST MANAGEMENT POLICIES UNDER EUROPEAN UNION REGULATIONS

Prof. Dr. Péter Molnár, Anikó Farkas
University of Sopron, Faculty of Forestry, Institute of Silviculture and Forest Protection, Sopron, Hungary
Hungarian University of Agriculture and Life Sciences, Institute of Environmental Sciences, Gödöllő, Hungary

ABSTRACT

Hungary lies at the dry, low-elevation limit of the natural distribution of European beech and sessile oak, two of the most important tree species for the country's forestry sector and biodiversity. Climate change is increasing the frequency, duration and intensity of droughts and heatwaves in the Carpathian Basin, exposing these forests to growing physiological stress. In recent years, extensive canopy dieback, reduced growth and increased mortality have been observed, particularly in beech stands at lower elevations and in oak forests on shallow or sandy soils. Drought-weakened trees are also more susceptible to secondary pests and pathogens, which further threatens timber production, carbon storage and other ecosystem services. At the same time, Hungarian forest management must adapt to European Union regulations and strategies, including the forest strategy, biodiversity strategy, deforestation-free products regulation and the land use, land-use change and forestry framework, which emphasize climate resilience, close-to-nature management and carbon sinks. This study examines the effects of climate change and drought stress on timber production in Hungarian beech and oak forests and discusses implications for sustainable forest management policies under European Union regulations. Tree-ring analysis was applied to selected stands along a climatic gradient to assess growth responses to drought, while national forest inventory data were used to evaluate changes in increment, mortality and harvested volumes. Climate projections and a drought index were combined to identify areas at increasing risk. Interviews with forest managers and policymakers provided insights into adaptation measures and regulatory challenges. The results show strong growth declines during and after severe drought years, with beech exhibiting greater sensitivity than oak, and a shift of climatically suitable zones toward higher elevations. The study concludes that species diversification, assisted migration, continuous cover forestry and coherent national implementation of European Union policies are essential for maintaining productive and resilient forests.

Keywords: Climate change, Drought stress, Beech forests, Oak forests, Timber production, Forest policy, Hungary

GLOBE 2ND INTERNATIONAL CONFERENCE ON ENGINEERING, ARCHITECTURE, MATHEMATICS and APPLIED SCIENCES
October 1 - 6, 2026 – BARSELONA
ISBN NR.: 978-625-8795-56-1

SYNTHESIS AND CHARACTERIZATION OF ZEOLITE-BASED ADSORBENTS FROM NATURAL CLINOPTILOLITE FOR THE REMOVAL OF HEAVY METAL IONS FROM INDUSTRIAL WASTEWATER

Prof. Dr. Ivan Georgiev Petrov
University of Chemical Technology and Metallurgy, Faculty of Chemical Technologies, Department of Inorganic Chemical Technology, Sofia, Bulgaria

ABSTRACT

Industrial activities such as mining, metallurgy, electroplating and leather tanning discharge wastewater containing toxic heavy metal ions, including lead, cadmium, copper, zinc, nickel and chromium. Because these metals are persistent, non-biodegradable and capable of accumulating in living organisms, their removal from effluents is a major environmental priority. Conventional treatment methods such as chemical precipitation, ion exchange with synthetic resins and membrane separation are costly or generate large volumes of sludge, which has stimulated interest in low-cost natural adsorbents. Clinoptilolite, the most abundant natural zeolite, is widely available in Bulgaria and possesses a three-dimensional aluminosilicate framework with exchangeable cations, high cation exchange capacity and good thermal and chemical stability. This study focuses on the synthesis and characterization of zeolite-based adsorbents prepared from natural clinoptilolite and evaluates their effectiveness for removing heavy metal ions from industrial wastewater. The raw tuff was purified and modified through acid activation, conversion into the sodium form and surface functionalization with iron oxide, to enhance exchange capacity and selectivity. The materials were characterized by X-ray diffraction, X-ray fluorescence, scanning electron microscopy, Fourier transform infrared spectroscopy and nitrogen adsorption. Batch adsorption experiments investigated the effects of pH, contact time, adsorbent dosage, initial metal concentration and temperature, and the data were analysed using kinetic and isotherm models. The results show that modification preserved the crystalline framework while increasing specific surface area and exchange capacity. The sodium and iron-modified forms exhibited markedly higher uptake, following the selectivity sequence lead, copper, cadmium, zinc and nickel. Adsorption followed pseudo-second-order kinetics and was well described by the Langmuir model, indicating monolayer chemisorption and ion exchange. Regeneration tests demonstrated good reusability. The study concludes that modified clinoptilolite is a promising, economical adsorbent for industrial wastewater treatment.

Keywords: Clinoptilolite, Natural zeolite, Adsorption, Heavy metal removal, Ion exchange, Wastewater treatment

GLOBE 2ND INTERNATIONAL CONFERENCE ON ENGINEERING, ARCHITECTURE, MATHEMATICS and APPLIED SCIENCES
October 1 - 6, 2026 – BARSELONA
ISBN NR.: 978-625-8795-56-1

EFFECT OF SOL-GEL PROCESSING PARAMETERS ON THE MICROSTRUCTURE, PHASE COMPOSITION AND PHOTOCATALYTIC ACTIVITY OF NITROGEN-DOPED TITANIUM DIOXIDE THIN FILMS

Assoc. Prof. Dr. Maria Dimitrova, Stoyan Kolev, Dr. Elena Todorova, Nikolay Ivanov, Desislava Angelova
Sofia University St. Kliment Ohridski, Faculty of Chemistry and Pharmacy, Department of Applied Inorganic Chemistry, Sofia, Bulgaria

ABSTRACT

Titanium dioxide is one of the most extensively studied semiconductor photocatalysts because of its chemical stability, non-toxicity, low cost and strong oxidizing power under illumination. It is widely applied in self-cleaning surfaces, air purification and the degradation of organic pollutants in water. However, its relatively wide band gap restricts photoactivity mainly to ultraviolet light, which represents only a small fraction of the solar spectrum. Doping with nitrogen has emerged as an effective strategy for narrowing the band gap and extending light absorption into the visible region, while the sol-gel method offers a versatile, low-temperature route for preparing homogeneous thin films with controlled composition. Nevertheless, the properties of the resulting films depend strongly on processing conditions. This study investigates the effect of sol-gel processing parameters on the microstructure, phase composition and photocatalytic activity of nitrogen-doped titanium dioxide thin films. Films were prepared from titanium alkoxide precursors with urea as the nitrogen source and deposited on glass substrates by dip coating. The influence of precursor concentration, nitrogen-to-titanium ratio, number of coating layers, withdrawal speed and annealing temperature was systematically examined. The films were characterized by X-ray diffraction, Raman spectroscopy, X-ray photoelectron spectroscopy, scanning electron and atomic force microscopy, and ultraviolet-visible spectroscopy. Photocatalytic activity was evaluated through the degradation of methylene blue and methyl orange under ultraviolet and visible light irradiation. The results show that annealing temperature is the key factor controlling crystallization, with anatase predominating at moderate temperatures and rutile appearing at higher temperatures, accompanied by grain growth and partial loss of nitrogen. Moderate nitrogen content produced substitutional and interstitial nitrogen species, a red shift in the absorption edge and the highest visible-light activity, while excessive doping created recombination centres. Film thickness and porosity also influenced performance. The study concludes that careful optimization of sol-gel parameters enables efficient visible-light-active photocatalytic coatings.

Keywords: Titanium dioxide, Nitrogen doping, Sol-gel method, Thin films, Photocatalysis, Visible light

GLOBE 2ND INTERNATIONAL CONFERENCE ON ENGINEERING, ARCHITECTURE, MATHEMATICS and APPLIED SCIENCES
October 1 - 6, 2026 – BARSELONA
ISBN NR.: 978-625-8795-56-1

INVESTIGATION OF THE THERMODYNAMIC PROPERTIES AND CORROSION BEHAVIOR OF ALUMINIUM–ZINC ALLOYS MODIFIED WITH RARE-EARTH ELEMENTS IN NEUTRAL CHLORIDE MEDIA

Prof. Dr. Rustam Nazarov, Farrukh Saidov, Dilnoza Rahimova
Tajik Technical University named after Academician M. S. Osimi, Faculty of Chemical Technology and Metallurgy, Dushanbe, Tajikistan
National Academy of Sciences of Tajikistan, V. I. Nikitin Institute of Chemistry, Dushanbe, Tajikistan
Tajik National University, Faculty of Chemistry, Department of Physical and Colloid Chemistry, Dushanbe, Tajikistan

ABSTRACT

Aluminium–zinc alloys are widely used as protective coatings and sacrificial anodes for the cathodic protection of steel structures in marine and chloride-containing environments, including pipelines, ship hulls, offshore platforms and storage tanks. Their effectiveness depends on a favourable combination of electrochemical activity, uniform dissolution and resistance to self-corrosion. However, aluminium alloys tend to form a dense passive oxide film that may reduce their protective efficiency, while localized corrosion such as pitting can shorten their service life. Alloying with small additions of rare-earth elements, including lanthanum, cerium, praseodymium and neodymium, has attracted increasing attention as a means of refining the microstructure, modifying intermetallic phases and improving corrosion behaviour. This study investigates the thermodynamic properties and corrosion behaviour of aluminium–zinc alloys modified with rare-earth elements in neutral chloride media. Alloys with varying rare-earth contents were prepared by melting high-purity metals in an electric furnace under a protective flux. The temperature dependence of heat capacity was determined using the cooling method, and thermodynamic functions, including enthalpy, entropy and Gibbs energy, were calculated. The kinetics of high-temperature oxidation in air was studied by thermogravimetry, and oxidation products were identified using X-ray diffraction and infrared spectroscopy. Electrochemical behaviour was examined in sodium chloride solutions of different concentrations by potentiostatic and potentiodynamic polarization methods, and the corroded surfaces were analysed by optical and scanning electron microscopy. The results show that heat capacity and thermodynamic functions increase with temperature, while rare-earth additions slightly decrease enthalpy and entropy and increase Gibbs energy. Small rare-earth additions reduced the oxidation rate and shifted the corrosion, pitting and repassivation potentials toward more positive values, lowering the corrosion rate. Increasing chloride concentration accelerated corrosion for all alloys. The study concludes that rare-earth-modified aluminium–zinc alloys are promising materials for anodic protection of steel structures.

Keywords: Aluminium–zinc alloys, Rare-earth elements, Thermodynamic properties, Corrosion behaviour, Chloride media, Anodic protection

GLOBE 2ND INTERNATIONAL CONFERENCE ON ENGINEERING, ARCHITECTURE, MATHEMATICS and APPLIED SCIENCES
October 1 - 6, 2026 – BARSELONA
ISBN NR.: 978-625-8795-56-1

PHYSICOCHEMICAL PROCESSING OF LOCAL KAOLIN CLAYS FOR THE PRODUCTION OF ALUMINA-CONTAINING COAGULANTS BY ACID LEACHING AND THERMAL ACTIVATION

Assist. Prof. Dr. Firuz Qodirov, Shahlo Mirzoeva
Tajik National University, Faculty of Chemistry, Department of Inorganic Chemistry, Dushanbe, Tajikistan
National Academy of Sciences of Tajikistan, V. I. Nikitin Institute of Chemistry, Dushanbe, Tajikistan

ABSTRACT

Coagulants containing aluminium, such as aluminium sulphate, aluminium chloride and polyaluminium chloride, are essential reagents in drinking water purification, industrial wastewater treatment and paper production. Many countries, including Tajikistan, depend heavily on imported coagulants or on bauxite, which is scarce and costly, and therefore the use of local aluminosilicate raw materials represents an attractive alternative. Tajikistan possesses considerable deposits of kaolin clays, which consist mainly of kaolinite together with quartz, feldspar, mica and iron-bearing impurities. Kaolinite has a stable layered structure and is poorly soluble in acids in its natural state, so effective extraction of aluminium requires activation that disrupts its crystal lattice. This study investigates the physicochemical processing of local kaolin clays for the production of alumina-containing coagulants through acid leaching and thermal activation. Representative clay samples were characterized by chemical analysis, X-ray diffraction, differential thermal analysis and infrared spectroscopy. Thermal activation was carried out by calcining the clays over a range of temperatures to transform kaolinite into reactive metakaolin. The activated materials were then leached with sulphuric and hydrochloric acids, and the effects of calcination temperature and duration, acid concentration, leaching temperature, solid-to-liquid ratio and reaction time on the extraction of aluminium oxide and iron oxide were examined. The kinetics of leaching was analysed using shrinking core models, and apparent activation energies were determined. The results show that calcination converts kaolinite into an amorphous metakaolin phase, dramatically increasing its reactivity, while excessive temperatures lead to the formation of less soluble mullite-like phases. Optimal conditions produced high extraction of aluminium oxide, with the process controlled mainly by chemical reaction at the particle surface. The resulting coagulant solutions effectively reduced turbidity and colour in model water samples. The study concludes that local kaolin clays are a viable raw material for producing efficient coagulants.

Keywords: Kaolin clay, Metakaolin, Acid leaching, Thermal activation, Aluminium coagulants, Water treatment, Tajikistan

GLOBE 2ND INTERNATIONAL CONFERENCE ON ENGINEERING, ARCHITECTURE, MATHEMATICS and APPLIED SCIENCES
October 1 - 6, 2026 – BARSELONA
ISBN NR.: 978-625-8795-56-1

GREEN SYNTHESIS OF SILVER NANOPARTICLES USING JUTE LEAF EXTRACT AND THEIR INCORPORATION INTO CHITOSAN-BASED FILMS FOR ANTIBACTERIAL FOOD PACKAGING APPLICATIONS

Prof. Dr. Mohammad Rafiqul Islam, Nusrat Jahan, Dr. Tanvir Ahmed, Sadia Afrin, Md. Kamrul Hasan, Farhana Akter

University of Dhaka, Faculty of Engineering and Technology, Department of Applied Chemistry and Chemical Engineering, Dhaka, Bangladesh
Bangladesh Council of Scientific and Industrial Research, Institute of Food Science and Technology, Dhaka, Bangladesh
Bangladesh Jute Research Institute, Chemistry Division, Dhaka, Bangladesh
Bangladesh Agricultural University, Faculty of Agricultural Engineering and Technology, Department of Food Technology and Rural Industries, Mymensingh, Bangladesh
Jahangirnagar University, Faculty of Mathematical and Physical Sciences, Department of Chemistry, Savar, Dhaka, Bangladesh
University of Dhaka, Faculty of Biological Sciences, Department of Microbiology, Dhaka, Bangladesh

ABSTRACT

Microbial contamination is a major cause of food spoilage and foodborne illness, and growing concern about the environmental impact of petroleum-based plastics has stimulated the development of biodegradable active packaging materials. Silver nanoparticles are known for their broad-spectrum antimicrobial activity, but conventional chemical synthesis often relies on toxic reducing agents and stabilizers. Green synthesis using plant extracts offers an environmentally friendly alternative, as phytochemicals such as polyphenols, flavonoids and proteins can act simultaneously as reducing and capping agents. Jute, a major crop in Bangladesh, produces leaves rich in antioxidants and bioactive compounds that remain underutilized. Chitosan, a biodegradable polysaccharide derived from crustacean shells, possesses good film-forming ability and intrinsic antimicrobial properties, making it a suitable matrix for nanocomposite packaging. This study reports the green synthesis of silver nanoparticles using jute leaf extract and their incorporation into chitosan-based films for antibacterial food packaging applications. Aqueous extracts of Corchorus olitorius leaves were used to reduce silver nitrate under controlled pH, temperature and reaction time. The nanoparticles were characterized by ultraviolet-visible spectroscopy, Fourier transform infrared spectroscopy, X-ray diffraction, transmission electron microscopy and dynamic light scattering. Chitosan films containing different nanoparticle loadings were prepared by solution casting with glycerol as a plasticizer and evaluated for tensile strength, elongation, water vapour permeability, transparency and antibacterial activity against Escherichia coli, Staphylococcus aureus and Salmonella species. The results confirmed the formation of spherical, crystalline and stable silver nanoparticles capped by phenolic compounds from the extract. Their incorporation improved the mechanical strength and barrier properties of the films and

ISBN NR.: 978-625-8795-56-1

produced strong antibacterial activity. Packaging trials showed delayed microbial growth in minced meat and fresh cheese during refrigerated storage, with limited silver migration. The study concludes that jute leaf-mediated nanocomposite films are promising sustainable active packaging materials.

Keywords: Green synthesis, Silver nanoparticles, Jute leaf extract, Chitosan films, Antibacterial packaging,

GLOBE 2ND INTERNATIONAL CONFERENCE ON ENGINEERING, ARCHITECTURE, MATHEMATICS and APPLIED SCIENCES
October 1 - 6, 2026 – BARSELONA
ISBN NR.: 978-625-8795-56-1

CATALYTIC PYROLYSIS OF WASTE POLYETHYLENE AND POLYPROPYLENE OVER MODIFIED HZSM-5 CATALYSTS FOR LIQUID FUEL PRODUCTION: KINETIC AND PRODUCT DISTRIBUTION ANALYSIS

Assoc. Prof. Dr. Shahidul Alam, Rumana Chowdhury, Md. Arifur Rahman, Dr. Tahmina Sultana

Bangladesh University of Engineering and Technology, Faculty of Chemical and Materials Engineering, Department of Chemical Engineering, Dhaka, Bangladesh
Chittagong University of Engineering and Technology, Faculty of Mechanical Engineering, Department of Petroleum and Mining Engineering, Chattogram, Bangladesh
Shahjalal University of Science and Technology, School of Applied Sciences and Technology, Department of Chemical Engineering and Polymer Science, Sylhet, Bangladesh
Rajshahi University of Engineering and Technology, Faculty of Mechanical Engineering, Department of Chemical and Food Process Engineering, Rajshahi, Bangladesh

ABSTRACT

The rapid growth of plastic consumption has generated enormous quantities of waste, much of which ends up in landfills and natural environments, causing serious environmental and public health problems. Polyethylene and polypropylene, which dominate packaging and household products, are particularly persistent because of their chemical stability. Pyrolysis, the thermal decomposition of polymers in the absence of oxygen, offers a promising route for converting plastic waste into valuable liquid fuels and chemicals, supporting waste management and energy recovery. However, purely thermal pyrolysis requires high temperatures and produces waxy products with a broad distribution of hydrocarbons. The use of acidic zeolite catalysts, particularly shape-selective MFI-type zeolites, can lower reaction temperatures and improve the quality of liquid products, although strong acidity may also promote excessive cracking, gas formation and coke deposition. This study investigates the catalytic pyrolysis of waste polyethylene and polypropylene over modified zeolite catalysts for liquid fuel production, with particular attention to reaction kinetics and product distribution. The parent zeolite was modified by desilication to introduce mesoporosity and by impregnation with nickel and zinc to tune acidity and hydrogen transfer. The catalysts were characterized by X-ray diffraction, nitrogen physisorption, ammonia temperature-programmed desorption and pyridine infrared spectroscopy. Kinetic parameters were determined by thermogravimetric analysis at different heating rates using isoconversional methods, while pyrolysis experiments were carried out in a semi-batch reactor. Liquid products were analysed by gas chromatography–mass spectrometry. The results show that the modified catalysts substantially reduced apparent activation energies compared with thermal pyrolysis. Hierarchical and metal-modified catalysts increased liquid yields and selectivity toward gasoline-range hydrocarbons and aromatics while reducing coke formation. The resulting oils resembled conventional fuels. The study concludes that modified zeolite catalysts offer an effective pathway for converting plastic waste into liquid fuels.

ISBN NR.: 978-625-8795-56-1

Keywords: Catalytic pyrolysis, Plastic waste, Polyethylene, Polypropylene, Zeolite catalysts, Liquid fuels, Kinetics

GLOBE 2ND INTERNATIONAL CONFERENCE ON ENGINEERING, ARCHITECTURE, MATHEMATICS and APPLIED SCIENCES
October 1 - 6, 2026 – BARSELONA
ISBN NR.: 978-625-8795-56-1

DEVELOPMENT OF RICE HUSK ASH-DERIVED MESOPOROUS SILICA AS A LOW-COST SUPPORT FOR NICKEL CATALYSTS IN THE HYDROGENATION OF VEGETABLE OILS

Mahmudul Hasan Chowdhury
University of Chittagong, Faculty of Science, Department of Chemistry, Chattogram, Bangladesh

ABSTRACT

Rice husk is one of the most abundant agricultural residues in rice-producing countries such as Bangladesh, and its combustion for energy generates large quantities of ash rich in amorphous silica. Improper disposal of rice husk ash causes air and land pollution, yet its high silica content makes it a valuable and inexpensive precursor for advanced materials. Mesoporous silica materials, characterized by high surface area, ordered pore structures and tunable pore sizes, are widely used as catalyst supports because they allow good dispersion of active metals and efficient diffusion of reactants. Conventional mesoporous silicas are usually synthesized from costly silicon alkoxides, limiting industrial application. At the same time, the hydrogenation of vegetable oils remains an important process in the food and oleochemical industries, where nickel catalysts are used to produce fats with desired melting properties and improved oxidative stability. This study develops rice husk ash-derived mesoporous silica as a low-cost support for nickel catalysts in the hydrogenation of vegetable oils. Silica was extracted from rice husk ash by alkaline dissolution to produce sodium silicate, which was then used to synthesize mesoporous silica through a surfactant-templated sol-gel route. Nickel was loaded by impregnation and deposition-precipitation methods, followed by calcination and reduction. The supports and catalysts were characterized by X-ray fluorescence, X-ray diffraction, nitrogen physisorption, transmission electron microscopy and temperature-programmed reduction. Catalytic performance was evaluated in the hydrogenation of soybean and palm oils in a stirred reactor, monitoring iodine value, fatty acid composition and trans isomers. The results show that the synthesized silica possessed a high surface area and uniform mesopores comparable to commercial materials. Deposition-precipitation produced smaller, well-dispersed nickel particles and stronger metal-support interaction, resulting in higher activity and lower trans fatty acid formation. The study concludes that rice husk ash is a sustainable source for efficient catalyst supports.

Keywords: Rice husk ash, Mesoporous silica, Nickel catalyst, Vegetable oil hydrogenation, Catalyst support, Waste valorization

GLOBE 2ND INTERNATIONAL CONFERENCE ON ENGINEERING, ARCHITECTURE, MATHEMATICS and APPLIED SCIENCES
October 1 - 6, 2026 – BARSELONA
ISBN NR.: 978-625-8795-56-1

OPTIMIZATION OF BIODIESEL PRODUCTION FROM WASTE PALM COOKING OIL USING CALCIUM OXIDE CATALYST DERIVED FROM EGGSHELL WASTE VIA RESPONSE SURFACE METHODOLOGY

Prof. Dr. Nor Azlina Abdullah, Lim Wei Keat, Dr. Muhammad Hafiz Ramli, Siti Aisyah Kamaruddin, Rajesh Kumar Subramaniam
Universiti Teknologi Malaysia, Faculty of Chemical and Energy Engineering, Johor Bahru, Johor, Malaysia

ABSTRACT

Malaysia is one of the world's leading producers of palm oil, and large quantities of used palm cooking oil are generated daily by households and restaurants. Improper disposal of this waste oil into drains and landfills causes blockages, water pollution and environmental damage, while its conversion into biodiesel offers an opportunity to produce renewable fuel and support national biofuel policies. However, the high cost of feedstock and catalysts remains a major barrier to commercial biodiesel production. Heterogeneous catalysts such as calcium oxide offer easier separation and reusability than homogeneous bases, and eggshell waste, which consists mainly of calcium carbonate, represents an abundant and inexpensive source of this catalyst. This study optimizes biodiesel production from waste palm cooking oil using a calcium oxide catalyst derived from eggshell waste through response surface methodology. Eggshells were cleaned, dried, ground and calcined to convert calcium carbonate into active calcium oxide. The catalyst was characterized by X-ray diffraction, X-ray fluorescence, Fourier transform infrared spectroscopy, scanning electron microscopy and basicity measurements. The waste oil was pretreated to reduce moisture and free fatty acid content before transesterification with methanol. A central composite design was applied to examine the effects of methanol-to-oil molar ratio, catalyst loading, reaction temperature and reaction time on biodiesel yield, and analysis of variance was used to evaluate model significance. The results show that calcination produced a highly crystalline calcium oxide with strong basic sites. The quadratic model showed excellent agreement with experimental data, identifying the methanol-to-oil ratio and catalyst loading as the most influential factors. Under optimum conditions, a high methyl ester yield was obtained, and the biodiesel properties met international standards. The catalyst retained good activity over several cycles. The study concludes that eggshell-derived calcium oxide is an effective, sustainable catalyst for valorizing waste palm cooking oil.

Keywords: Biodiesel, Waste cooking oil, Eggshell, Calcium oxide catalyst, Response surface methodology, Malaysia